

Katharina RENNER

Flip Operations in Pointed Pseudo-Triangulations

MASTERARBEIT

zur Erlangung des akademischen Grades einer
Diplom-Ingenieurin

Masterstudium Mathematische Computerwissenschaften



Graz University of Technology

Technische Universität Graz

Betreuer:

Assoc. Prof. Dipl.-Ing. Dr. techn. Oswin AICHHOLZER

Dipl.-Ing. Dr. techn. Thomas HACKL

Institut für Softwaretechnologie

Graz, Juni 2013

EIDESSTATTLICHE ERKLÄRUNG

Ich erkläre an Eides statt, dass ich die vorliegende Arbeit selbständig verfasst, andere als die angegebenen Quellen/Hilfsmittel nicht benutzt, und die den benutzten Quellen wörtlich und inhaltlich entnommenen Stellen als solche kenntlich gemacht habe.

Graz, am
(Unterschrift)

STATUTORY DECLARATION

I declare that I have authored this thesis independently, that I have not used other than the declared sources/resources, and that I have explicitly marked all material which has been quoted either literally or by content from the used sources.

.....
date (signature)

Abstract

In this thesis we consider pointed pseudo-triangulations of point sets in the plane in certain degree-bounded settings. The main focus lies on pointed pseudo-triangulations with face degree four (4-PPT) in combination with so called edge flip operations that allow to locally transform a 4-PPT into a different one. We investigate the flip graphs of all 4-PPTs of special point sets like the single chain, the reverse single chain, and the double circle and show that their flip graphs of 4-PPTs are connected. We introduce a new special set of points, the muffin set, and prove the connectivity of its flip graph of 4-PPTs. To investigate flip graphs of 4-PPTs for arbitrary point sets we introduce the concept of a dual graph. Applied to 4-PPTs of point sets with three points on the convex hull this concept aims to move the single triangle in such a pseudo-triangulation. The dual approach was also implemented to extend a flip software tool. Experiments with this software have been performed and are discussed.

Zusammenfassung

In dieser Arbeit betrachten wir pointed Pseudotriangulierungen von Punktemengen in der Ebene unter gewissen Gradrestriktionen. Das Hauptaugenmerk liegt hierbei auf sogenannten 4-PPTs, pointed Pseudotriangulierungen deren geschlossene Flächen durch maximal vier Kanten begrenzt werden. Eine lokale Operation, Kantenflip, erlaubt es, eine Pseudotriangulierung in eine andere zu transformieren. Wir untersuchen Flipgraphen von 4-PPTs von verschiedenen speziellen Punktemengen, wie das *single chain set*, *reverse single chain set* oder auch den *double circle* und beweisen, dass diese Flipgraphen zusammenhängend sind. Weiters führen wir eine neue spezielle Punktemenge, das *muffin set*, ein und beweisen auch hier den Zusammenhang des Flipgraphen aller 4-PPTs dieser Menge. Für die Untersuchung von Flipgraphen von 4-PPTs beliebiger Punktemengen wird das Konzept eines dualen Flipgraphen eingeführt. Dieser Ansatz vereinfacht das Verschieben eines Dreiecks in einer 4-PPT einer Punktemenge. Der Ansatz wurde implementiert um ein bereits existierendes Flip-Software Tool zu erweitern. Versuche mit dieser Software wurden durchgeführt und Ergebnisse werden in dieser Arbeit diskutiert.

Danksagung

Diese Arbeit bildet den Abschluss meiner Studienzeit, welche ohne die wertvolle Unterstützung meiner Familie so nicht möglich gewesen wäre. Daher danke ich in erster Linie meinen Eltern für die Ermöglichung dieses Bildungsweges und für die Begleitung auf selbigem. Bedanken möchte ich mich besonders bei Prof. O. Aichholzer für die gute Unterstützung und Betreuung dieser Arbeit. Sehr gefreut und motiviert hat mich die Teilnahme an der PT Research Week, wodurch ich auch einen Einblick in das internationale Forschungsgeschehen bekam. Mein Dank geht außerdem an T. Hackl, A. Pilz und B. Vogtenhuber für die vielen Anregungen und das konstruktive Feedback. Dankbar bin ich ebenso meinen lieben Freunden und Kollegen, die mich selbst in schwierigeren Phasen des Studium zum Strahlen bringen konnten.

Contents

1	Introduction	8
1.1	Thesis Overview	8
2	Background on Pseudo-Triangulations	10
2.1	Basic Definitions	10
2.2	Pointed Pseudo-Triangulation	13
2.2.1	Counting Vertices, Edges and Faces	14
2.2.2	Constructing Pointed Pseudo-Triangulations	16
2.3	Flip Graphs of Pseudo-Triangulations	18
2.4	Degree Limitation	20
2.5	Application of Pseudo-Triangulations	21
3	Overview on related research results	25
3.1	Connectivity and Counting	25
3.2	Degree Limitation	27
3.2.1	Constructing 4-PPTs	27
3.3	Abstract Pseudo-Triangulations	30
3.3.1	Flips in Abstract Pointed Pseudo-Triangulations	31
3.3.2	Coloring of 4-PPTs	33
3.3.3	Recent research results on CPPTs	33
3.4	Research Question	35
4	Special Point Sets And Their Flip Graph	36
4.1	Simple Polygons	36
4.2	Flip graph of ≥ 5 -PPTs	37
4.3	The Single Chain	38
4.3.1	Connectivity of the Flip Graph	38
4.3.2	Counting 4-PPTs of The Single Chain	43
4.3.3	Counting 4-PPTs of The Reverse Single Chain	46

4.4	The Double Circle	48
4.5	The Muffin Set	53
4.5.1	Counting 4-PPTs of $M_{1,m}$	60
5	A Dual Approach	63
5.1	Introduction and Definitions	63
5.1.1	The Dual Graph	63
5.1.2	Definition and Classification of Flip Operations	66
5.2	Implementation of the Dual Graph	71
5.3	Moving the Triangle in 4-PPTs	73
5.3.1	Moving the Triangle along Alternating Paths	74
5.3.2	Implementation of the Alternating Path Idea and Experimental Results	77
5.3.3	Describing Special Geometric Gadgets	79
6	Conclusion	86
6.1	Summary	86
6.2	Future Research	87
	Glossary	88
	List of Figures	91
	Bibliography	94

1 Introduction

The first records of humans studying geometry aims back to 3000BC in ancient India and Babylonia. Since then a tremendous amount of research has made geometry to a well-studied branch of mathematics. In the 3rd century BC Euclid set standards that define the branch of Euclidean Geometry. Especially triangles are geometric objects that have been studied from early time on. Compared to that, the field of pseudo-triangulations is a young branch of computational geometry. In 1993 the terms pseudo-triangle and pseudo-triangulation were first stated by Pocchiola and Vegter [29]. Back then a pseudo-triangle was defined as : “... *a simply connected subset R of \mathcal{F} [the complement of a collection of pairwise disjoint convex obstacles, K.R.] such that (i) the boundary ∂R is a sequence of three convex chains, that are tangent at their endpoints, and (ii) R is contained in the triangle formed by the three endpoints of these convex chains*”. Pocchiola and Vegter used pseudo-triangles and pseudo-triangulations as tool for computing the visibility complex of a set of pairwise disjoint convex obstacles. In the early 1990’s pseudo-triangulations were also called geodesic triangulations and found to be a helpful tool as a kinetic data structure for visibility problems of polygonal obstacles. A decade later Streinu associated pseudo-triangulations with rigidity theory to solve the Carpenter’s Rule Problem [36]. In 2008 Rote, Santos, and Streinu published a survey [32] on pseudo-triangulations to outline the results on pseudo-triangulations in until then current literature. Definitions and nomenclature in this master’s thesis are mainly based on this survey.

1.1 Thesis Overview

The main focus of this master’s thesis lies on pointed pseudo-triangulations with maximum face degree four, so called 4-PPTs, and edge flips in 4-PPTs, local transformations that changes one 4-PPT into a different one. Each 4-PPT of a point set can be represented by a vertex in a so called flip graph, where two vertices share

an edge if their corresponding 4-PPTs can be transformed into each other with exactly one edge flip. Chapter 2 presents the terminology and basic definitions on pseudo-triangulations.

There are a lot of different well known applications for triangulations. The field of applications for pseudo-triangulations is smaller, but nevertheless they are a useful data structure that is used for visibility graph algorithms as well as for different problems in the field of robotics (robot arms as bar-and-joint frameworks, collision detection) or as tool for proofs in terms of illumination and guarding problems. An overview on this can be found in Chapter 2.5.

Since a lot of research has been done in the last few years Chapter 3 gives an overview on the state of the art results. We further focus on the question whether the flip graph of 4-PPTs of a set of points is connected or not. Just recently (May 2012) a group of researchers proved the connectedness of the flip graph of combinatorial 4-PPTs, a class of 4-PPTs that is described in Chapter 3.3.

Chapter 4 focuses on recent results on 4-PPTs of different point sets. We elaborate proofs and disproofs of connectedness of the flip graphs of all 4-PPTs of simple polygons, and special point sets like the single chain sets, the double circle and describe them in this chapter. Additionally we introduce a new special point set, a combination of two parallel single circles, and the number of 4-PPTs of selected sets will be studied. Finally, we developed a dual approach to prove the connectedness of the flip graph of a set of points in the plain, that will be explained. The dual idea was also implemented by the author to extend Reisner's flip-software [31] by an automated flip algorithm. We applied this extended software tool and results of experiments and conclusions drawn out of this results will be explained in Chapter 5.3.

2 Background on Pseudo-Triangulations

This chapter gives a basic introduction of the fields of pseudo-triangulations. We will define pseudo-triangles and pseudo-triangulations and take a look at special types of pseudo-triangulations. A local operation called edge flip will be introduced to transform a pseudo-triangulation into a different one and motivates the investigation of the so-called flip graphs of pseudo-triangulations. An interesting aspect of those flip graphs is the investigation of their connectivity. If the flip graph of all pseudo-triangulations of a geometric figure or a point set is connected, each pseudo-triangulation of this figure or set can be transformed into every other by applying the edge flip operation.

2.1 Basic Definitions

Before we introduce pseudo-triangles some definitions are necessary. In the context of this thesis all considered point sets S in the plane are in *general position*, i.e., no three points of S are collinear. A *polygon* with n points is a plane figure where n non-crossing edges connect n points to a closed path. We call a polygon *simple* if there are only non-crossing edges on the path and exactly one inner face exists that is bounded by the closed path. Whereas a simple polygon does not have any interior points, a *pointgon* is a simple polygon with additional points inside the interior face. A simple polygon is *convex* if each inner angle of the bounded face is $< \pi$. The *convex hull* $CH(S)$ of a point set S is the smallest convex polygon that contains S .

We denote a *pseudo- k -gon* as a polygon with exactly k convex points, i.e., the angle outside the border of the polygon is $> \pi$ at these points. These convex points are called *corners* of the pseudo- k -gon. A *pseudo-triangle* is a pseudo-3-gon, a simple polygon with exactly three corners. All other points are characterized as *reflex* points and have an outer angle $< \pi$. To clearly differentiate between these two types of

points, the postulation that a set S of points in the plane is in general position is necessary. Figure 2.1 shows two examples for pseudo-triangles.

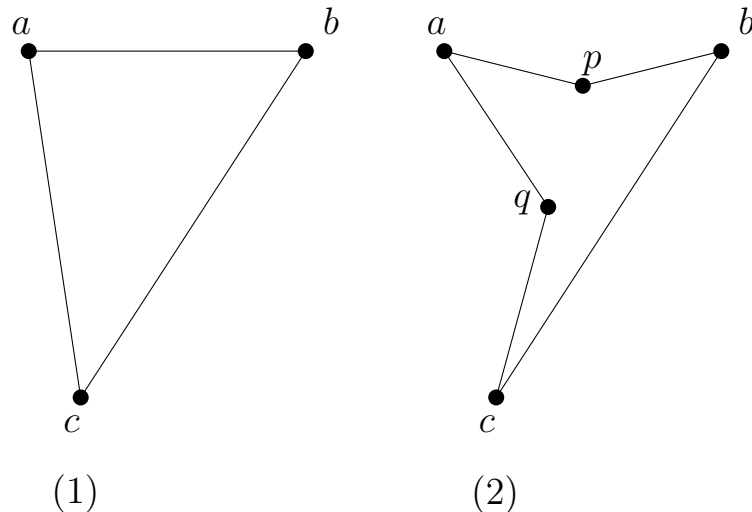


Figure 2.1: (1) A triangle which is a special case of a pseudo-triangle with corners a , b , c and no reflex points. (2) A pseudo-triangle with two reflex points p and q .

At the beginning pseudo-triangulations were also called *geodesic triangulation*, because they can be constructed by inserting non-crossing geodesic paths into a polygon P . A *geodesic path* is the shortest path between two points of P that can consist of diagonals and polygon edges. An edge is called a *diagonal* of a polygon if it is an edge between two vertices of the border of P that crosses the inner area of P . A geodesic path (consisting of ≥ 2 edges) between two consecutive corners (in a cyclic order of all corners) of a polygon is called *side-chain*. We will later mainly deal with pseudo-triangles that have one reflex point, i.e., they have exactly one side chain consisting of two edges. A diagonal of a polygon is defined as *tangent* if one of its endpoints is either a corner of the polygon and the diagonal lies inside the convex angle of this corner or if it is a reflex point of the polygon and the two edges of this reflex point lie on the same side of the supporting line of the diagonal edge. A geodesic-path between two corners always preserves the pointedness (see Section 2.2) of the affected points. Further, a diagonal of a polygon that is part of a geodesic path is always tangent in both of its endpoints (see Figure 2.2) and is also called *bitangent*.

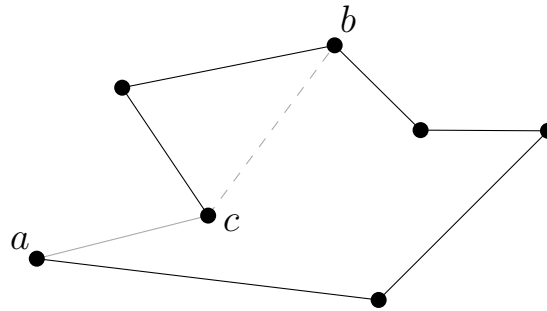


Figure 2.2: The two grey line segments form a geodesic path between the corner a and the corner b . The dashed line segment is a bitangent, since it is tangent to both end points.

We shall now define a pseudo-triangulation on three different geometric structures: on simple polygons, on pointgons, and sets of points. A *pseudo-triangulation* of a simple polygon is a partition of the polygon into pseudo-triangles using only the points of the polygon, whereas a pseudo-triangulation of a pointgon is a tiling of the surrounding simple polygon using all interior points as well. A pseudo-triangulation of an arbitrary point set S in the plane is a pseudo-triangulation of the pointgon that is formed by S and its convex hull $CH(S)$. A *triangulation* is a special case of a pseudo-triangulation, since a *triangle* is a pseudo-triangle with no reflex points. Often bounds for the number of reflex points per pseudo-triangle are given; for example pseudo-triangulations of point sets, where only pseudo-triangles with at most one reflex point are allowed. If there are no special restrictions, a pseudo-triangulation can consist of pseudo-triangles with different numbers of reflex points. We will later see that the number of triangles in a special type of pseudo-triangulations (so-called pointed pseudo-triangulations with face degree ≤ 4) depends on the number of points of the convex hull.

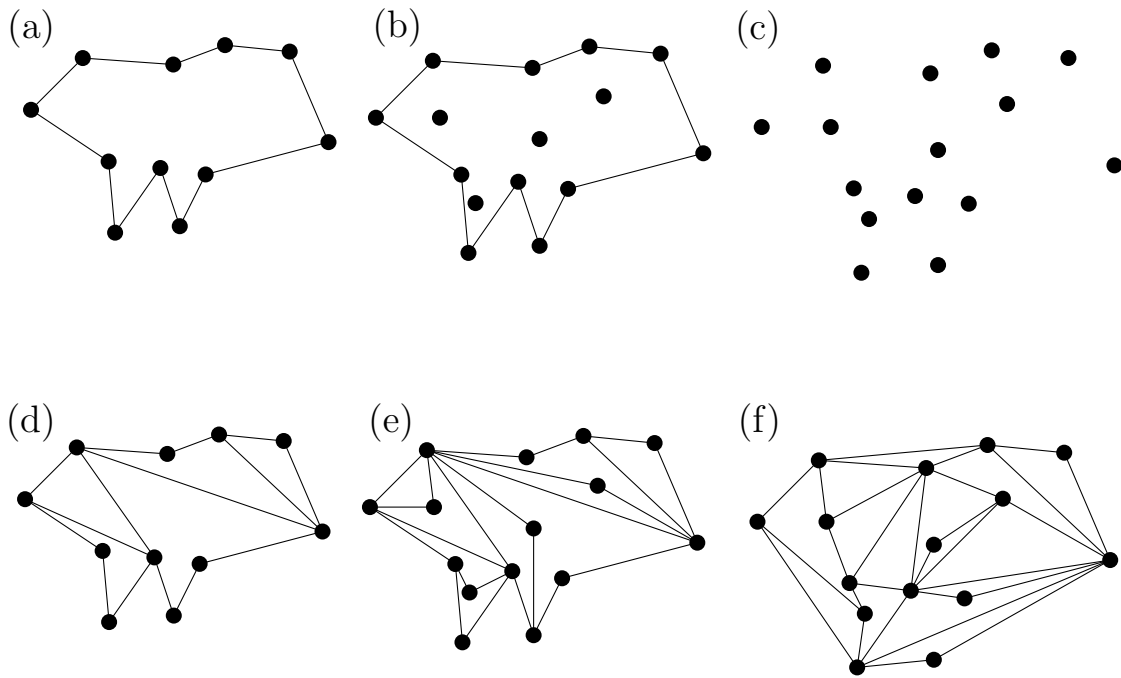


Figure 2.3: A simple polygon (a), a pointgon (b) and a set of points (c). (d)-(f) show pseudo-triangulations of those sets.

2.2 Pointed Pseudo-Triangulation

A special type of pseudo-triangulations are *pointed pseudo-triangulation*. A point of a pseudo-triangulation is called *pointed* if two edges share an endpoint and form an angle $> \pi$ and no other edge lies inside this angle. Consider a point set S of n points in the plane, let $CH(S)$ be the set of points on the convex hull of S . In every pseudo-triangulation all points of $CH(S)$ are *convex*, i.e., they are pointed to the outer face of the convex hull of S . In a pointed pseudo-triangulation all points need to be pointed. Pointed pseudo-triangulations minimize the number of edges in a pseudo-triangulation and are therefore also often named *minimum pseudo-triangulation* [36]. In the next sections we will take a closer look on the number of points, edges and faces of a pseudo-triangulation as well as on special types of pseudo-triangulations that result from the restriction of the degree of points and faces.

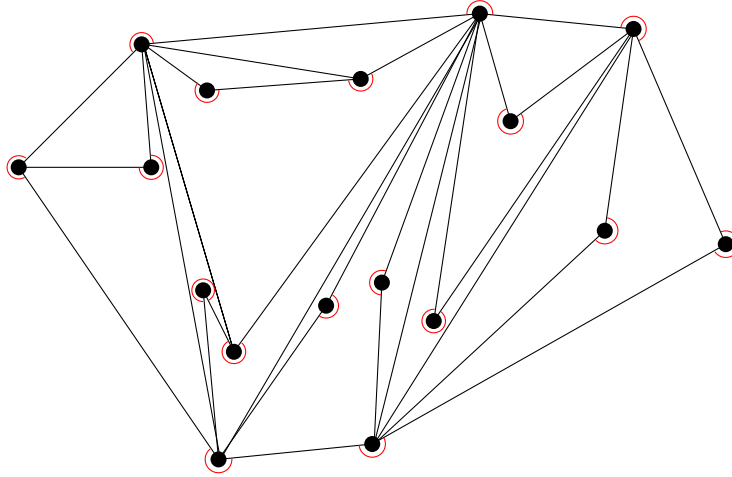


Figure 2.4: A pointed pseudo-triangulation of a set of points. The vertices are pointed into the faces incident to the red marks.

2.2.1 Counting Vertices, Edges and Faces

A pseudo-triangulation of a point set S with n points can be seen as a planar graph, since we do not allow crossing edges. Hence, Euler's formula for planar graphs holds for the number of points n , the number of edges m , and the number of inner faces f of a pseudo-triangulation:

$$n - m + f = 1 \tag{2.1}$$

Using this equation, the number of edges and pseudo-triangles of a pseudo-triangulation of a pointgon P can be determined depending on the number of non-pointed points in the interior of P and the number of reflex points on the surrounding polygon.

Theorem 2.1 (Vertex and face counts in pseudo-triangulations of pointgons [32]). *Let PT be a pseudo-triangulation of a pointgon with n points, n_X of which are non-pointed, and r points of the surrounding polygon are reflex. Then PT consists of $n - 2 + n_X - r$ pseudo-triangles and $2n - 3 + n_X - r$ edges.*

Proof. In a pseudo-triangulation with m edges, these edges form $2m$ angles, $n - n_X$ of them are $> \pi$ (one at each pointed vertex). The number of angles $< \pi$ equals r , the number of reflex points of the surrounding polygon, plus one for each corner of each pseudo-triangle. Let f be the number of inner faces, then we get

$$2m = n - n_X + 3f + r \tag{2.2}$$

The combination of Equations 2.1 and 2.2 leads to the stated number of edges and inner faces, i.e., pseudo-triangles. \square

The number of non-pointed points, n_X , is the maximum in triangulations because a triangulation of a pointgon or a point set cannot have any pointed points in the interior of the convex hull. Therefore, the number of edges in a triangulation is $2n - 3 + n_I$ since $n_X = r + n_I$ for n_I , the number of interior points. For triangulations of point sets, this equals the well-known relation $m = 3n - 3 - h$ for $h = n - n_I$ points on the convex hull and the triangulation consists of $2n - 2 - h$ triangles. By definition $n_X = r = 0$ in pointed pseudo-triangulations of point sets. This leads to $2n - 3$ edges and $n - 2$ pseudo-triangles and minimizes the number of edges. Therefore, pointed pseudo-triangulations are often also called minimum-pseudo-triangulations. The following theorem gives a characterization of pointed pseudo-triangulations.

Theorem 2.2 (Characterization of pointed pseudo-triangulations [32]). *Let S be a set of n points in the plane, and PT a graph embedded on S . Then the following properties are equivalent:*

1. *PT is a pseudo-triangulation with a minimal number of non-crossing edges.*
2. *PT is a pointed pseudo-triangulation of S .*
3. *PT is a pseudo-triangulation of S , consisting of $2n - 3$ edges and $n - 2$ faces.*
4. *PT is non-crossing, pointed and has $2n - 3$ edges.*
5. *PT is pointed, non-crossing and maximal among the pointed non-crossing graphs embedded on S .*

Proof. The equivalence of the first three points (1) \Leftrightarrow (2) \Leftrightarrow (3) follow from Theorem 2.1: the pseudo-triangulation of the point set S is a pseudo-triangulation of the pointgon that consists of $CH(S)$ and its inner points. $CH(S)$ does not have any reflex vertices, hence $r = 0$. The remaining number of edges is then $2n - 3 + n_X$, where n_X is the number of non-pointed vertices. The number of edges becomes minimal for $n_X = 0$. Also, (2) \Rightarrow (4) follows then from Theorem 2.1. From (4), it follows from Theorem 2.1 that PT is pointed and vice versa. PT is maximal among the pointed non-crossing graphs on S since PT is a pseudo-triangulation of a point set. Every additional edge would be an inner edge, i.e., an edge inside a pseudo-triangle. Since pseudo-triangles do not have any interior bitangents, an additional edge would turn a pointed vertex into a non-pointed one. This proves the implication (4) \Rightarrow (5).

The implication (2) \Rightarrow (5) follow by the argument mentioned above. For the implication (5) \Rightarrow (2), we want to show that the graph PT , which is maximal among all non crossing graphs embedded on S and whose vertices are all pointed, is a pointed pseudo-triangulation (Theorem 2.6 in [32]). Since PT is maximal and pointed and a convex hull point always stays pointed when an edges is added, the convex hull edges of S are part of PT . To prove that every interior face of PT is a pseudo-triangle, we consider an interior face F and enumerate its corners from p_1 to p_k , $k \geq 3$. Consider further two paths α_+ and α_- from v_1 to v_3 through the inner of F near to the border and from v_3 to v_3 respectively the other way round. Shortening these paths will result into two geodesic paths. Adding the edges of a geodesic path to PT would not change a pointed vertex into a non-pointed, but since PT is already a maximal graph, the geodesic paths coincide and consist of a border edge of F ; hence, p_1 and p_3 are neighbored corners and F is a pseudo-triangle. \square

2.2.2 Constructing Pointed Pseudo-Triangulations

Now we know how to characterize pointed pseudo-triangulations. Using their properties it is possible to specify an iterative procedure to construct a pointed pseudo-triangulation of a point set. This procedure was presented in a survey on pseudo-triangulations [32] and is based on the *Henneberg-Construction*, an algorithm for constructing minimal rigid graphs [24]. An algorithm for constructing special pointed pseudo-triangulations, so-called 4-PPTs, will be presented in Chapter 3.2.1.

Theorem 2.3. (*Streinu [32]*) *Let S be a set of n points and \mathcal{P} a pseudo-triangulation of S . Then there exists an ordering of the points p_1, p_2, \dots, p_n of S such that \mathcal{P}_i is a pseudo-triangulation of the points p_1, p_2, \dots, p_i for $i = 3, \dots, n$ and \mathcal{P}_{i+1} results by inserting p_{i+1} to \mathcal{P}_i in either one of those two ways:*

1. p_{i+1} becomes a vertex of degree 2 in \mathcal{P}_{i+1} . If p_{i+1} has been inserted into the outer face of \mathcal{P}_i the two new edges are tangent to the boundary of \mathcal{P}_i , otherwise the two edges are on the geodesic between two arbitrary corners of the pseudo-triangle in which p_{i+1} was inserted.
2. p_{i+1} becomes a vertex of degree 3 in \mathcal{P}_{i+1} , by adding p_{i+1} and two edges like above, but then flip one edge of the side-chain opposite to p_{i+1} in the unique triangle that has p_{i+1} as a corner.

Proof. First, we show that in every pointed pseudo-triangulation there exists at least one point of degree two or three. Then we show that removing such a point

edges e lies inside an angle α of the two other edges and $\alpha < \pi$. It is obvious that e is an inner edge; therefore it can be flipped in a new edge e' . Let \mathcal{P}' be the pointed pseudo-triangulation that results from flipping e in \mathcal{P} . In \mathcal{P}' the vertex p'_n has now degree two and can be removed as mentioned above. This results again in a pointed pseudo-triangulation \mathcal{P}_{n-1} with $2(n-1) - 3$ edges. Hence \mathcal{P} can be constructed by inserting a point into \mathcal{P}_{n-1} and flipping the edge e' into e , which corresponds to part two of the theorem. \square

2.3 Flip Graphs of Pseudo-Triangulations

We shall now introduce a local operation that allows us to transform a pseudo-triangulation into another by modifying one edge, i.e., the two adjacent pseudo-triangles. This operation is called *edge flip*. An edge flip allows us to remove one edge of a pseudo-triangulation PT and insert a different one, resulting in a new pseudo-triangulation PT' . In general, one can differentiate between three types of flips. The *deletion flip* removes one edge $e \in PT$ and results in a new pseudo-triangulation with one edge less than PT . In contrast the *insertion flip* inserts a new edge $e \notin PT$ and results in a new pseudo-triangulation with one edge more than PT (Figure 2.6).

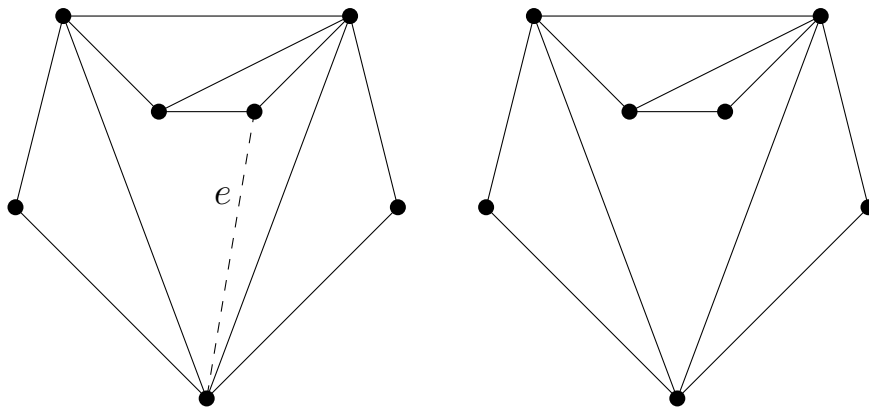


Figure 2.6: Removing or inserting the edge e results again in a valid pseudo-triangulation.

The third, and the most important type for the following sections, is the *diagonal flip*: in [32] it is shown that if removing an edge $e \in P$ does not result in a new pseudo-triangulation, a unique edge $e' \notin P$ exists different from e such that replacing e by

e' produces a new pseudo-triangulation. Such a diagonal flip always affects two adjacent pseudo-triangles that share the edge e . We assume now that removing e results in a face with four corners which is no longer a pseudo-triangle (otherwise it would be an edge-removing flip). Let a, b, c, d be the corners of this pseudo-quadrilateral in counter-clockwise order and let e be the edge that connects the corners a and c , i.e., e forms a diagonal of this pseudo-quadrilateral. After removing e we insert the other diagonal edge e' that connects the other two corners b and d (see Figure 2.7 left). This is only possible if we can insert the new diagonal without

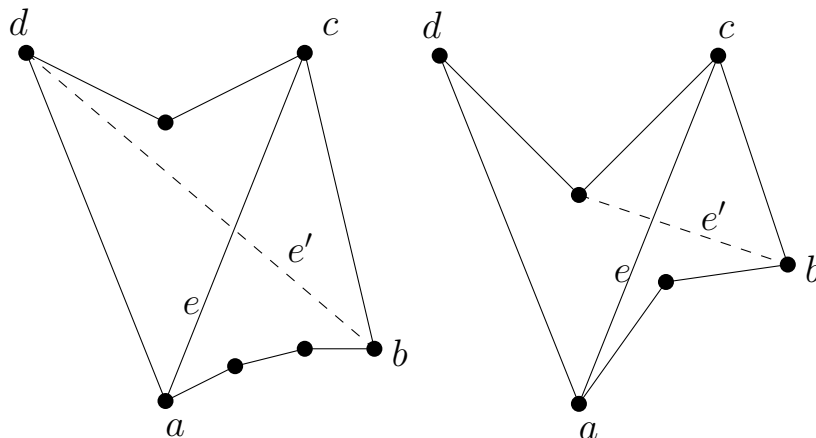


Figure 2.7: Two diagonal flips removing e and inserting e' .

intersecting existing edges. If the new diagonal causes an intersection, we insert e' instead in a way that the geodesic path between the two corners b and d is completed (see Figure 2.7 right).

A diagonal flip neither decreases or increases the number of faces in a pseudo-triangulation, but it can change the degree of the affected faces. In Figure 2.7 (right), the diagonal flip transforms two quadrilaterals into one triangle and a pentagon. It is shown in [32] that an insertion flip always turns one pointed vertex into a non-pointed one, and the inverse operation, the deletion flip, does the reverse. This plays an important role in terms of pointed pseudo-triangulations of point sets. Since all points need to be pointed, only diagonal flips are allowed. In [32] it is further proven that in a pseudo-triangulation of a pointgon P , there exists one flip for each interior edge that is $n - 3 + n_X - r + n_I$ and a flip for each of the $n - n_X - k$ pointed vertices that is not a convex point on the surrounding polygon of P . This leads to $n + 2n_I - 3$ possible flips in each pseudo-triangulation in a pointgon. We will now see that this will be the degree of the so-called flip graph of pseudo-triangulations of pointgons.

Let S be either a simple polygon, a pointgon or a set of points. The *flip graph* of the pseudo-triangulations of S is a graph G where each vertex represents a unique pseudo-triangulation of S . Two vertices of G are connected if the two corresponding pseudo-triangulations can be transformed into each other by one edge flip. There are still many open questions on properties of these flip graphs starting with the most basic ones: is the flip graph of pseudo-triangulations of S connected? Is it still connected if we claim all pseudo-triangulations to be pointed or if we introduce restrictions for the face or vertex degree?

Theorem 2.4 (Properties of the graph of pseudo-triangulations of a pointgon [32]). *Let P be a pointgon with n points in the plane, n_I of which are interior points. The flip graph G of all pseudo-triangulations of P has the following properties:*

1. G is connected.
2. G is an undirected regular graph of degree $n + 2n_I - 3$.
3. The subgraph G' , induced by the pointed pseudo-triangulations of P is connected.
4. G' is regular of degree $k + 2n_I - 3$, where k is the number of convex points of P .

For pseudo-triangulations of a point set S with n points, we have $r = 0$, hence the number of flippable edges, i.e., the degree of the flip graph in a pointed pseudo-triangulation of S is $n + n_I - 3$.

In Chapter 4 we will show that the flip graph of pointed pseudo-triangulations with special degree limitations are connected for certain special point sets but not for others. Chapter 4 gives an approach to prove the connectedness of the flip graph of such a special face-degree-bounded pointed pseudo-triangulation of a point set.

2.4 Degree Limitation

In many cases it is not easy to formulate general statements about pseudo-triangulations of a point set or about their flip graphs. Setting boundaries for either face or vertex degrees reduces the number of pseudo-triangulations, which can be helpful. In a pseudo-triangulation, we can limit either the degree of a point, i.e., the number of edges incident to one point or the degree of a face, i.e., the number of points

that form a pseudo-triangle. Introducing degree limitations raises new questions, for example is a flip graph still connected if we allow only a vertex degree smaller than k , $k \in \mathbb{N}$, in its pseudo-triangulations? In Chapter 3 an overview on results on degree bounded triangulations is given.

As mentioned before it is also possible to limit the face degree, i.e., to restrict the number of reflex points in a pseudo-triangle. In Chapter 4 we will focus on pointed pseudo-triangulations with a maximum face degree of four, also called *4-PPTs*. In a 4-PPT all pseudo-triangles are allowed to have one reflex point at the most, so the bounded faces are either triangles or quadrilaterals. A special property of 4-PPTs of a point set S is that the number d of triangles depends on the number k of points on the convex hull of S , i.e., $d = k - 2$. This can be proven easily by induction, and will be shown in Chapter 3.2 together with the algorithm for constructing 4-PPTs. In that chapter we will present also an algorithm by Kettner et al. [27] that constructs a 4-PPT of a point set that starts with the convex hull and then iteratively inserts the inner points and updates the 4-PPT in parallel.

2.5 Application of Pseudo-Triangulations

One class of application for pseudo-triangulations in computational geometry are so-called visibility-problems. Given a set of objects in the plane, two objects are visible to each other if a straight line segment exists between them and does not intersect any other object. A special problem is the so-called *Art Gallery Problem* or *Museum Problem*. The problem was first stated by Klee as a question to Chvátal [16]: How many guards are necessary to monitor an art gallery room with n walls? In the original problem, a guard can survey 360° around his fixed position. In 1975 Chvátal [16] proved that $\lfloor \frac{n}{3} \rfloor$ guards are always sufficient to guard a polygon of n vertices and three years later Fisk [19] gave a very short proof for the upper bound by using triangulations. The art gallery room is a simple polygon with n vertices that can be triangulated. There further exists a three coloring of this triangulation. Placing the guards at the vertices of the polygon that are colored in the least common color leads to a number of necessary guards of $\leq \lfloor \frac{n}{3} \rfloor$. When using so-called π -guards, guards that have a field of view of 180° , Tóth [37] showed in 2000 that $\lfloor \frac{n}{3} \rfloor$ guards are sufficient if the location of the guards is not restricted to vertices. Considering vertex- π -guards, i.e., π -guards who are located at a vertex of the polygon, upper bounds for the number of necessary guards were $\lfloor \frac{3n-5}{4} \rfloor$ and then $\lfloor \frac{5n}{6} \rfloor$, proved

by Tóth [37] using a special composition of polygons and by Brumberg et al. [15] respectively in 2005. These bounds were improved by Speckmann and Tóth [35] using pseudo-triangulations. They showed that a pseudo-triangle with m vertices can be surveyed by $\lfloor \frac{2m-3}{3} \rfloor$ vertex- π -guards. Based on this result, Speckmann and Tóth proved a new upper bound for the number of edge-aligned vertex- π -guards, vertex- π -guards whose one border of field of view coincides with a polygon edge. The introduction of three different allocations for edge-aligned vertex- π -guards in a pseudo-triangulation of the polygon that sum up to a total number of $2n - k$ guards, leads to a maximum of $\lfloor \frac{2n-k}{3} \rfloor$ edge-aligned vertex- π -guards that are necessary to guard a simple polygon with n vertices, k of them convex. A second result using pseudo-triangulations for solving the art gallery problem is $\lfloor \frac{n}{2} \rfloor$ as tight upper bound for the number of general vertex- π -guards (no edge-alignment required) to guard a simple polygon with n points. Again, the proof is based on the number of vertex- π -guards that are necessary to monitor one pseudo-triangle.

Another application of pseudo-triangulations is a so-called *kinetic data structure* for collision detection [32] of moving objects. Consider a set of simple polygons in the plane and a pseudo-triangulation of the space between the objects. The movement of the objects changes the location of the vertices of the pseudo-triangulation and the pseudo-triangulation changes. In a certain range, the objects can move and the pseudo-triangulation gets distorted, but it still stays a valid pseudo-triangulation. In [32] a set of easy checkable properties, which ensure that a pseudo-triangulation stays valid while its points are moving in the plain, is mentioned. A pseudo-triangle whose vertices are moving in the plane stay a valid pseudo-triangle as long as

- no two adjacent vertices coincide;
- the three corner angles remain positive;
- all other angles remain larger than π .

Consider a pseudo-triangulation of a set of convex polygons whose vertices move. It will be a valid pseudo-triangulation as long as

- all pseudo-triangles remain valid;
- all obstacles remain convex polygons;
- and all exterior angles at the convex hull vertices remain larger than π .

If one of these points is violated, the pseudo-triangulation needs to be updated by a flip. Compared to triangulations, pseudo-triangulations have the advantage that they can consist out of fewer faces, i.e., the update-process is less expensive. Agarwal et al. [1] described an algorithm for maintaining pseudo-triangulations of the space between moving or deforming polygons and analyzed the performance of pseudo-triangulations as kinetic data structure.

A related problem is a specification of the *carpenter's ruler problem* [32, 11]. Consider a carpenter's ruler, i.e., a polygonal linkage of n segments in the plane, that is bent in a complicated way. One question that arises is, whether it is possible to straighten the ruler by moving the segments while avoiding self-intersections. Connelly et al. [18] proved that it is possible to straighten polygonal arcs and to convexify polygonal cycles, by continuously moving their vertices but preserving the length of their edges and avoiding self-intersection of their edges. Streinu [36] used pseudo-triangulations as a tool for a convexification algorithm for simple polygons as follows.

Algorithm 1 The Convexification Algorithm by Streinu [36].

1. **Initialization:** Pseudo-triangulate the polygon. Remove a convex hull edge to obtain a pseudo-triangulation expansive mechanism.
 2. **Repeat until the polygon becomes convex:**
 - **(Next Event)** Pin down an arbitrary edge and move the mechanism until an alignment events occurs: two extreme edges at a vertex align.
 - **(Freeze or Flip)** If the aligned edges were polygon edges, freeze them into a single edge by eliminating the common vertex, and recompute a compatible pseudo-triangulation mechanism. If one of the aligned edges is an added edge, drop it and replace it by the edge extending over the two aligned edges.
-

Consider a simple (not convex) polygon with n points on the hull and a pointed pseudo-triangulation of the set of corners of the polygon that is created by adding $n - 4$ non-crossing edges to the polygon, such that each vertex is pointed and one convex hull edge is missing. The additional edges behave like the polygon edges, i.e., they cannot bend or stretch. The resulting mechanism can now be used to convexify the polygon by pinning one edge and rotating two other edges around the endpoints of the pinned edge. The additional edges ensure an expanding non-crossing motion, which is possible until two edges align. If this happens, the pseudo-triangulation

needs to be updated either by an edge flip or by freezing the joint of the two aligned edges and treat them as one edge.

3 Overview on related research results

This chapter gives a brief overview on the state-of-the-art knowledge about connectivity of flip graphs of triangulations and pseudo-triangulations in general and upper bounds for counting pseudo-triangulations. A closer look is taken on minimum pseudo-triangulations and an introduction to degree limited pseudo-triangulations will then lead to the research question of this theses.

3.1 Connectivity and Counting

As already mentioned in Chapter 2, every point set S has a corresponding flip graph, a graph where each vertex represents a unique pseudo-triangulation of S . Two vertices are connected with an edge if the two corresponding pseudo-triangulations can be transformed into the other with one edge flip.

In 2001 Brönniman et al. [14] showed that the flip graph of pointed pseudo-triangulations (PPT) of a set S of n points in the plane is connected and stated $\mathcal{O}(n^2)$ as upper bound for the diameter of the graph. In a flip graph, this means that it is the maximum of all shortest flip sequences between two distinct PPTs. In [14] Brönniman et al. introduce a *canonical sorted pseudo-triangulation* and show that with at most $\mathcal{O}(n^2)$ flips, every PPT of S can be transformed into this canonical form. By reversability of flip sequences, the flip graph of all PPTs of an arbitrary point set is connected. Furthermore, they give an algorithm for determining the number of different PPTs of a point set using a total order on the set of edges and the greedy flip algorithm by Pocchiola and Vegter [30] in $\mathcal{O}(n^2)$ time per pseudo-triangle. Experimental applications of this algorithm on the point sets of Aichholzer et al. [4] showed that for $n \leq 10$, the number of triangulations of a point set S is less than the number of PPTs of S . Both quantities are equal if the points in S are

in convex position. It has also been shown that the number of PPTs is minimal for point sets in convex position. [4, 5].

In 2002 Bereg [13, 12] published an algorithm, based on Avis' and Fukuda's reverse search technique, which enumerates PPTs in $\mathcal{O}(\log n)$ time per pseudo-triangle and needs linear space. He further shows that the diameter of a flip graph of all PPTs of a point set S with n points is at most $(n-1)(n-4)$.

In 2004 Singh and Mehta [34] were able to generalize Beregs algorithm for enumerating all pseudo-triangulations. They showed that the flip graph of pseudo-triangulations of a point set S including n_X non-pointed points is connected for fixed n_X , i.e., in that flip graph no edge exists between two pseudo-triangulations with different number of non-pointed points.

The upper bound for the diameter of the flip graph of PPTs of a set S of n points was improved by Bereg [12] to $\mathcal{O}(n \log n)$, which is even smaller than the diameter of the flip graph of triangulations of S .

In [9] Aichholzer et al. studied the number of PPTs on special point sets, such as the double circle, the double chain or the single chain¹. In [2] a table of extremal sets for triangulations is given and it shows that the double circle actually minimizes the number of triangulations for $5 \leq n \leq 11$ using the results of [8]. For $12 \leq n \leq 20$ the double circle is still the best known example for a set of n points with a number of triangulations closest to the calculated lower bounds. The double chain was believed to maximize the number of triangulations until the double zig-zag chain was found to deliver an asymptotically bigger number of triangulations. Since pseudo-triangulations are a generalization of triangulations; these sets can also deliver interesting results for the number of pseudo-triangulations and pointed pseudo-triangulations.

The double circle with n points has asymptotically $\Theta(\sqrt{12}^n n^{-\frac{3}{2}})$ triangulations [33]. In [9] the asymptotical numbers of pseudo-triangulations and pointed pseudo-triangulations of the double circle are presented, $\Theta^*(\sqrt{40}^n)$ and $\Theta^*(\sqrt{28}^n)$ respectively². In Chapter 4 we will present a closed formula for the number of 4-PPTs of the single chain. In comparison, the number of pseudo-triangulations of the single chain with n points is approximately $3^{n-2}C_{\frac{n-3}{2}}$ and the number of pointed pseudo-triangulations is $2^{n-2}C_{n-3}$, with an error of 12.5% and 4% respectively, for $n \rightarrow \infty$ and C_n being the n-th Catalan number [9]. Consider now the double chain with

¹Detailed definitions of the single chain, the reverse single chain and the double circle are given in Chapter 4.3 and 4.4

²The asterisk indicates the neglect of polynomial factors.

$n = l + m + 4$ points, where $l + m$ inner points form two disjoint chains of length l and m . The average number of pseudo-triangulations and pointed pseudo-triangulations of that point set is given by $\Theta(20^n n^{-\frac{7}{2}})$ and $\Theta(12^n n^{-\frac{7}{2}})$ respectively. Those numbers might be interesting to be compared with the number of 4-PPTs of the muffin set (see Chapter 4).

3.2 Degree Limitation

In terms of triangulation Aichholzer et al. [7] and Hackl [21] investigated flip graphs of degree bounded triangulations. Restricting the vertex degree of a triangulation by k means that all allowed flip operations result in a triangulation where all points have a degree of at most k . It has been shown that for a maximum vertex degree of $k \leq 6$, the flip graph of triangulations of a set S of n points in convex position is not connected. For $k \geq 6$ it was further shown in [7] that the flip graph is connected and has a diameter of $\mathcal{O}(n^2)$. It was further shown that the flip graph of triangulations of arbitrary point sets is not necessarily connected for any k . If we allow a more relaxed vertex degree bound during intermediate steps of a sequence of flips between two degree-bounded triangulations, (i.e., an intermediate flip results always in a triangulation where all vertices have a degree $\leq k + 4$) then a diameter of $\mathcal{O}(n \log n)$ can be reached [7].

For pseudo-triangulations it is known that there exists a pointed pseudo-triangulation for every set of n points in the plane, where all points have a vertex degree of at most 5 [27]. This result was proven by describing a recursive algorithm to generate a pointed pseudo-triangulation of a given point set. It is possible to report such a pseudo-triangulation in $\mathcal{O}(n \log n)$ time. An example for a set that enforces a vertex degree of 5 was given by [27] as any completion of Figure 3.1 to a pseudo-triangulation. What is not yet known is if there exists any vertex degree limitation k such that the flip graph of pointed pseudo-triangulations with maximum vertex degree k is connected. Hackl [21] introduced a special point set and gave an example for a pseudo-triangulation with a maximal vertex degree of 9, that is a singleton in the flip graph of pseudo-triangulations with maximal face degree 9 of this set.

3.2.1 Constructing 4-PPTs

In terms of pseudo-triangulations we cannot only bound the vertex degree but also the face degree. In Chapter 2 we introduced 4-PPTs, i.e., pointed pseudo-

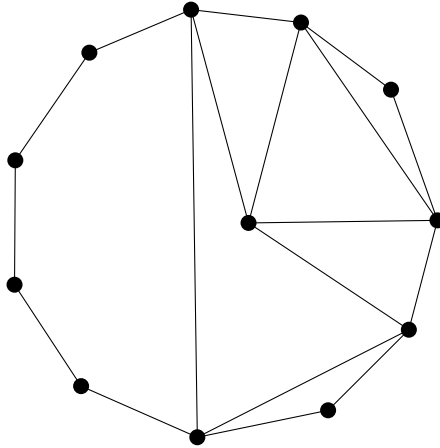


Figure 3.1: Any pseudo-triangulation completing this figure enforces a maximum vertex degree ≥ 5

triangulations with maximum face degree 4. In [27] Kettner et al. showed that for every set S of n points in plane, there exists a 4-PPT which can be constructed in $\mathcal{O}(n)$ time. The proof is given by an iterative algorithm that starts with the convex hull of the point set S . This construction algorithm was implemented by Reisner [31] in an edge flip software tool, which was later extended to investigate the dual approach on proving the connectivity of the flip graph of 4-PPTs (see Chapter 5). As mentioned before, the algorithm starts with constructing the convex hull of the point set S . After triangulating the convex hull, we iteratively insert the inner points. Such a new interior point can be inserted either into an already existing triangle or into a 4-gon. In the first case, the new point will be connected to two arbitrary corners of the triangle. This results in a new (smaller) triangle and an additional 4-gon (see Figure 3.2). If we insert a new inner point into a 4-gon, we have to distinguish between three different situations (Figure 3.3).

In the first case (Figure 3.4 left), the new point lies in the intersection of four half-planes: the extension of the two edges of the side-chain and the supporting lines of the two edges of the 4-gon. In this first situation, the point will be connected with the two corners of the 4-gon which are adjacent to the reflex point and we form two new 4-gons. In the other two cases the new point lies in the intersection of three half-planes: again the extensions of the two edges of the side-chain and the supporting line of only one of the edges (Figure 3.4, right). Both cases are equivalent, because of the symmetry. Two new edges are drawn from the new point to the reflex point

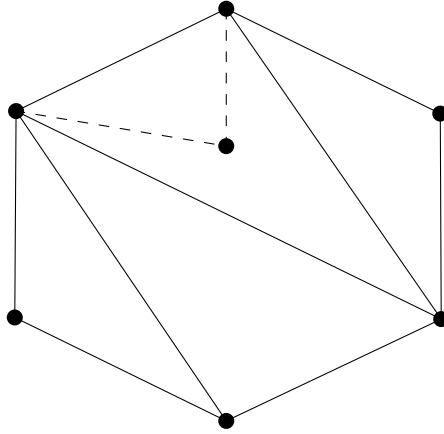


Figure 3.2: Inserting a point into a triangle, new edges are dashed.

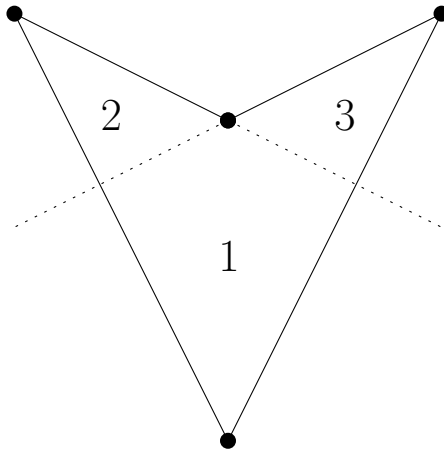


Figure 3.3: Three areas for inserting a point into a 4-gon.

of the 4-gon and the corner opposite of the reflex point, respectively. This results again in two new 4-gons.

As mentioned in Section 2.4, the number of triangles f_t in a 4-PPT of a point set S , depends on the number of points of $CH(S)$. If we take a look at the construction algorithm above, it is easy to count the number of triangles. Let $k = |CH(S)|$ be the number of points on the convex hull of S . The triangulation of the convex hull leads to $k - 2$ triangles. During the whole constructing process, the number of triangles remains the same. A new triangle is only created by inserting a point into an existing triangle and splitting it into a triangle and a 4-gon; hence, $f_t = k - 2$. Accordingly, we can determine the number of 4-gons f_q . With each new inserted point, we create a new 4-gon; hence, $f_q = n_I = n - k$.

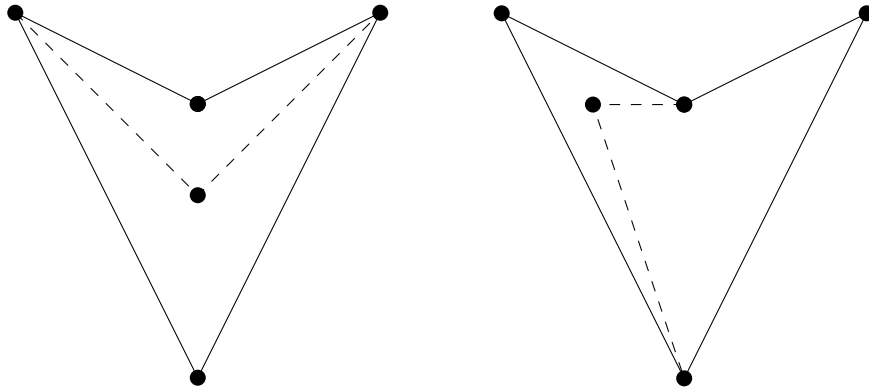


Figure 3.4: Two ways of inserting a point into a four sided pseudo-triangle. New edges are dashed.

In Chapter 5 we will refer to this construction as *Super-Easy-Construction* and will use it to prove a first conjecture about the existence of so-called alternating paths in the dual graph of a 4-PPT.

3.3 Abstract Pseudo-Triangulations

Until now, we studied pseudo-triangulations as a geometric graph with noncrossing straight-line edges that are embedded in the plane. We will further refer to this as *geometric* pseudo-triangulation. A lot of interesting results have been obtained by studying the combinatorial analogs of pseudo-triangulations, so-called *abstract pseudo-triangulation* or *combinatorial pseudo-triangulation*. To specify a combinatorial pseudo-triangulation, the combinatorial pseudo-triangulation labeling (*CPT-labeling*) was introduced [28]. Consider a plane graph G , where each angle that is induced by the edges of G is labeled either *small* or *big*. We call such a labeling a *CPT-labeling* if the following requirements are fulfilled:

- Every bounded face of G has exactly three angles labeled with *small*.
- All angles of the unbounded face of G are labeled *big*.
- No vertex of G is incident to more than one angle that is labeled *big*.

A combinatorial (or abstract) pseudo-triangulation is now defined as the (not necessarily straight-line) embedding of a graph G in the plane together with a CPT-labeling. For *combinatorial pointed pseudo-triangulations*, we further require that every vertex in G has exactly one angle labeled *big*. For graphic representation of

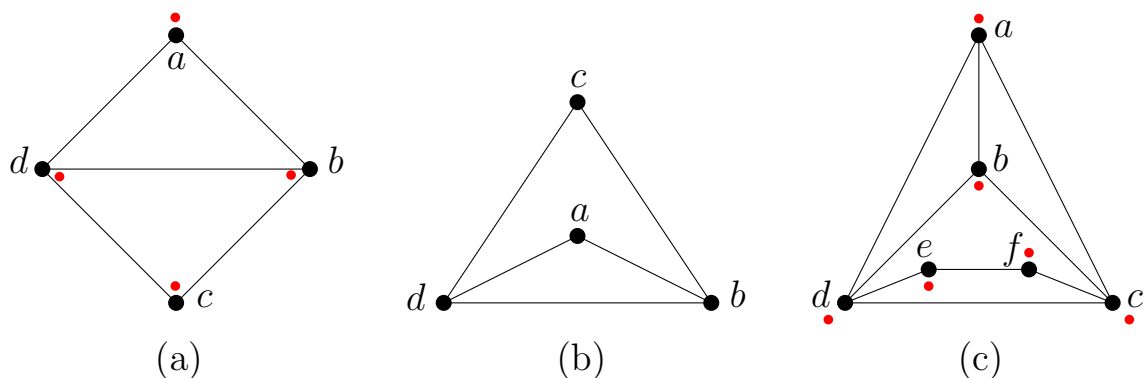


Figure 3.5: A CPT (a), an embedding of (a) as geometric pseudo-triangulation (b), a non-stretchable CPT

combinatorial pseudo-triangulations it is common to mark the *big* angle with an extra dot. Note that it is not always possible to find a straight-line embedding of a combinatorial pseudo-triangulation or an embedding that draws *big* angles $> \pi$ and *small* angles $< \pi$. Such CPTs are called *non-stretchable*. Figure 3.5 (c) shows such a non-stretchable CPT. In a corresponding geometric pseudo-triangulation the points a , c and d need to be pointed into the same face. Since a, c and d form a triangle they can only be pointed into the exterior face. If we draw the triangle a, c, d we can either place the point b inside this triangle, which would turn b into an unpointed vertex, or we can place b outside the triangle, which would then turn one of the vertices a , c or d into an unpointed one. Hence it is not possible to find a geometric pseudo-triangulation that is equivalent to the CPT in Figure 3.5 (c). Nevertheless, every geometric pseudo-triangulation is always a combinatorial pseudo-triangulation.

3.3.1 Flips in Abstract Pointed Pseudo-Triangulations

As in terms of geometric pseudo-triangulations the edge-flip operation is defined for combinatorial pseudo-triangulations, since they are a generalization of geometric pseudo-triangulations. The removing, insertion and diagonal flips are defined the same way as for pseudo-triangulations (see Chapter 2.3). Figure 3.6 shows an abstract pointed pseudo-triangulation of a 5-gon where a triangle and a 4-gon share one edge e . The possibilities for flipping e in the degree-bounded setting (face degree ≤ 4) are indicated by dashed lines.

Taking a closer look at this diagonal flip, we can see that this type of flip can

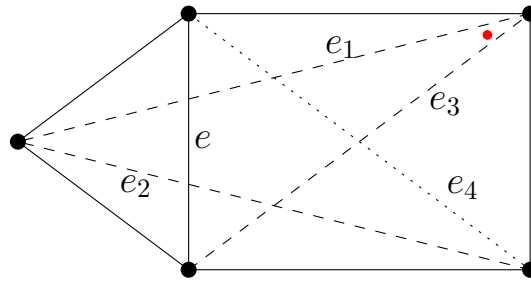


Figure 3.6: A diagonal flip of edge e can result in either e_1, e_2 or e_3 . Flipping e to e_4 would no longer result in an CPT.

result in different graphs and the pseudo-triangulations before and after the flipping may not exist in the same embedding (Figure 3.7c).

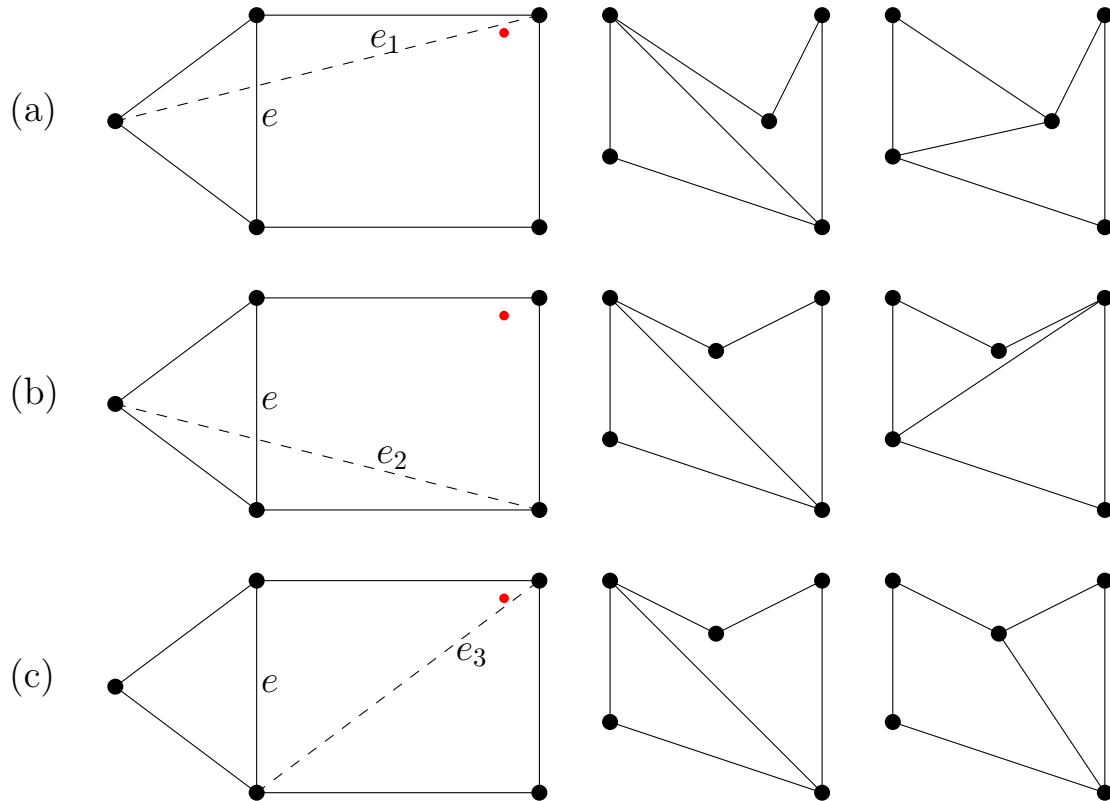


Figure 3.7: (a) and (b) show flips that exist in one embedding, (c) represents a flip that results in a valid CPT, that cannot be embedded the same way as it could be before the flip.

In [32], [28] and [20] the interested reader will find more information on ab-

stract pseudo-triangulations with regard to rigidity aspects and the so-called *Laman Graphs*.

3.3.2 Coloring of 4-PPTs

In Chapter 5.1.1 the dual graph of a pseudo-triangulation will be introduced. A combined embedding of a pseudo-triangulation and its dual graph allows to visualize the three colorability of a 4-PPT. Graph coloring is a big branch of graph theory. A coloring of a graph assigns a color to each vertex or edge. A *proper vertex coloring* of a graph is the assignment of colors to the vertices in a way that no two adjacent vertices have the same color. A *proper k -coloring* uses at most k colors to color the graph. The decision whether a given graph can be colored with k colors in a proper way is NP-complete (for $k > 2$). Nevertheless, the *Four Color Theorem* states that for every planar graph, there exists a proper k -coloring with $k \leq 4$. Aichholzer et al. [3] showed that 4-PPTs are 3-colorable. The proof of the theorem uses the concept of abstract pseudo-triangulations.

Theorem 3.1. [3] *For every pointed pseudo-triangulation with maximum face degree four there exists a proper coloring with three colors, that can be found in linear time.*

Proof. Since every geometric 4-PPT is also a combinatorial 4-PPT, we introduce a merge operation to shrink the given geometric 4-PPT to a combinatorial triangulation that can be colored with three colors in linear time. The merge operation merges a reflex point of a 4-gon with its opposite corner by identifying them (see Figure 3.8).

The remaining graph is still a valid CPT. Repeating this merge operation for each of the remaining four-sided pseudo-triangles leads finally to a combinatorial triangulation. In order to avoid degenerated cases, it is necessary to first merge inner vertices of vertex degree two before merging other vertices. Once the triangulation is build, the remaining vertices can be colored with 3-colors in linear time. Finally each merge step is retracted again and every new vertex gets the color of the merged vertex. In this manner, the coloring remains a proper 3-coloring, since the two vertices that were merged before do not share an edge in the 4-PPT. \square

3.3.3 Recent research results on CPPTs

In the previous sections we gave a short introduction to abstract or combinatorial pseudo-triangulations. During the Pseudo-Triangulation week in Alcalá (Spain) in

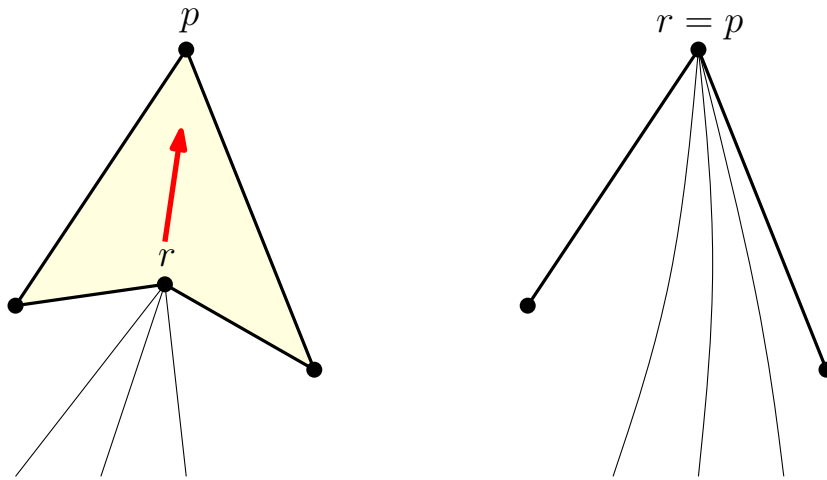


Figure 3.8: Merging step: the reflex point r of a pseudo-triangle is merged with its opposite corner.

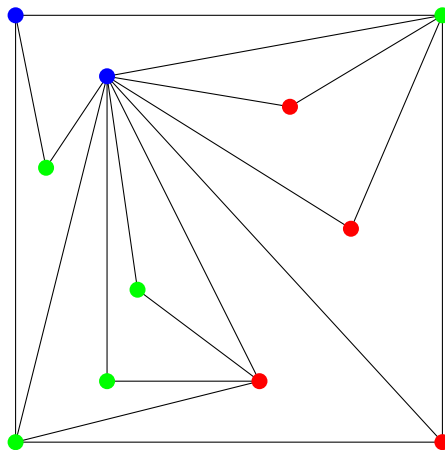


Figure 3.9: A valid 3-coloring of a 4-PPT due to the algorithm presented in Theorem 3.1.

May 2012 [6] a proof that the flip graph of abstract pointed pseudo-triangulations with a facedegree of at most 4 (4-CPPT) of point sets with three points on their convex hull is connected, was accomplished. The flip graph is even connected if we allow only edges incident to a triangle to be flipped. Unfortunately, this result does not prove the connectedness of the flip graph of geometric pointed pseudo-triangulations with a facedegree ≤ 4 (4-PPT), since a sequence of 4-CPPTs that differ by one flip may not exist in the same embedding.

3.4 Research Question

There are still a lot of open questions in the field of pseudo-triangulations, especially when we introduce conditions and restrictions such as vertex or face degree bounds. The main question that is outlined in the next chapters is, whether the flip graph of all 4-PPTs of a point set is connected or not. Even if we know that the flip graph is connected for abstract 4-PPTs, it has not been possible to prove it for geometric 4-PPTs until now. The answer depends obviously on the point sets on which we construct our 4-PPTs. First, we show that the flip graph of 4-PPTs of simple polygons is not connected. Looking at 4-PPTs of point sets, we will first prove connectedness of the flip graphs for special point sets. Those proofs use symmetries of the point set that allow an inductive construction of the flip graph. Then a dual approach will be introduced to investigate the connectedness of flip graphs of 4-PPTs of arbitrary point sets with exactly three points on the convex hull. This dual idea was further implemented to extend Reisner's flip software [31]. An approach for an automated flip algorithm brought some interesting results, which will be discussed in Chapter 5.2.

4 Special Point Sets And Their Flip Graph

This chapter presents results of investigations on the connectedness of flip graphs of pseudo-triangulations on special point sets. We first take a look at 4-PPTs of simple polygons and ≥ 5 -PPTs of point sets and show that for both examples exist whose flip graphs are not connected. Then we prove that the flip graphs of all 4-PPTs of the single chain set and the reverse single chain set with n points are connected for all $n \in \mathbb{N}$. For the single chain we also present a closed formula for the number of 4-PPTs that exist on that set. Another special set whose flip graph of all 4-PPTs is connected is the double circle, a set that also appeared to be special in terms of minimizing the number of triangulations. Finally, the connectedness of 4-PPTs of a set formed by two parallel circular arcs, called muffin set, will be shown.

4.1 Simple Polygons

A 4-PPT of a simple convex polygon of n points in the plane is equivalent to a triangulation of the polygon, since there are no points inside the convex hull. It is well known that the flip graph of all triangulations of a simple convex polygon is connected [26]. When the convexity is disregarded, the connectedness of the flip graph is not maintained and leads to the following theorem:

Theorem 4.1. *The flip graph of all 4-PPTs of a simple polygon of n points in the plane can be disconnected.*

Proof. Figure 4.1 shows two different 4-PPTs of the same simple polygon with 10 points. Obviously no inner edge of these 4-PPTs can be flipped; hence, they represent two singletons in the flip graph of this polygon. \square

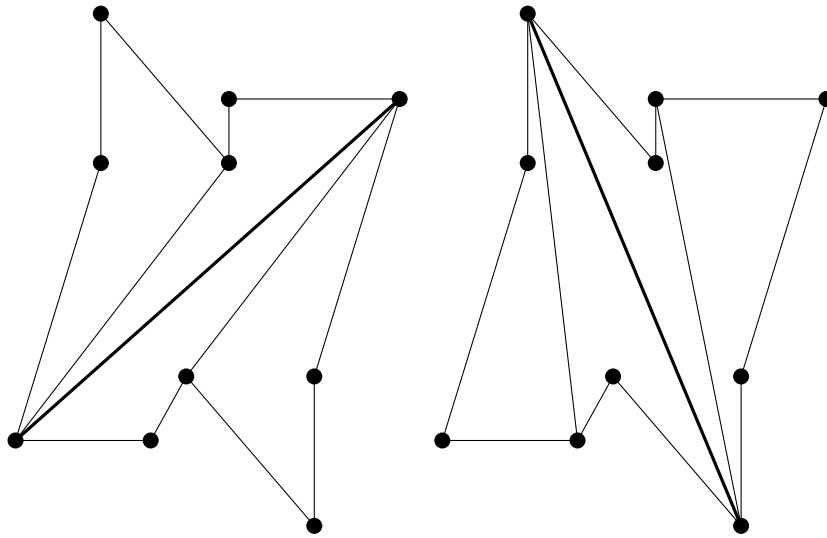


Figure 4.1: Two singletons in the flip graph of 4-PPTs of a simple polygon with 10 points.

4.2 Flip graph of ≥ 5 -PPTs

Given a set of n points in the plane, we define a ≥ 5 -PPT as a pointed pseudo-triangulation with at least one five-sided pseudo-triangle. We can show now that the flip graph of all ≥ 5 -PPTs of a set of points can be disconnected [10].

Theorem 4.2. *The flip graph of all ≥ 5 -PPTs of a set of points can be disconnected.*

Proof. We prove this theorem by constructing a counterexample with 8 points. Therefor we consider a hexagon with two points inside the convex hull (see Figure 4.2).

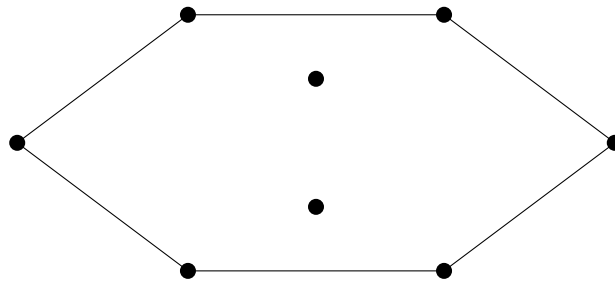


Figure 4.2: Constructing a counter example with 8 points

A ≥ 5 -PPT of this set has exactly one pseudo-triangle with 5 points and 5 triangles,

because 6 points of the set are on the convex hull. There are two ways to draw such a pentagon with the two adjacent reflex points, and six ways to draw a pentagon where the two reflex points are not adjacent. The eight ways to draw those pentagons in our special set are showed in Figure 4.3. Once the pentagon is fixed, only convex

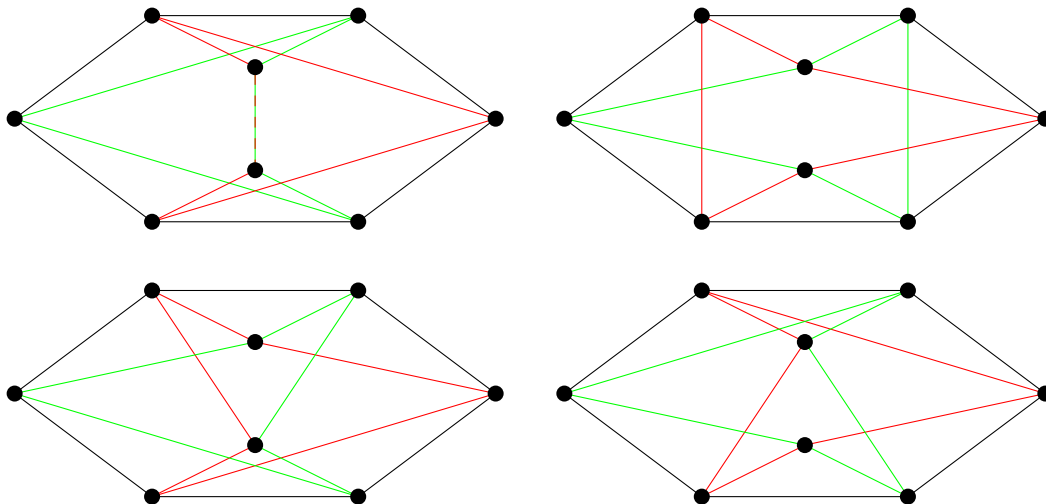


Figure 4.3: Eight ways to draw a pseudo-5-gon on this special set. Note that each pseudo-5-gon and its symmetric equivalent are plotted in the same figure.

polygons remain to be pseudo-triangulated. Therefore, all other faces in the ≥ 5 -PPT of this set must be triangles. Since we only have one pentagon in our PPT, we need to ensure that no flip of an edge incident to this pentagon and a triangle, transforms these faces into two 4-gons. Observing Figure 4.3 and considering all possible triangles to complete the figures to a ≥ 5 -PPT it can be seen that only flips of edges incident to two triangles are possible. Therefore, no flip sequence that changes the position of the pentagon exists. The flip graph of all ≥ 5 -PPT of a set of n points, which includes one of the examples of Figure 4.3 as a subgraph and whose other faces are triangles is not connected. \square

4.3 The Single Chain

4.3.1 Connectivity of the Flip Graph

A special set of points is the so-called *single chain*. Consider a set S of $n > 3$ points in the plane, such that $|CH(S)| = 3$, $n - 1$ points form a convex polygon and one point t , outside the polygon, sees all edges of the polygon but one. In terms of

visibility, a point p_1 sees another point p_2 , i.e., p_2 is visible for p_1 , if it is possible to draw an edge p_1p_2 without crossing any other edge, especially the edge of the polygon. We further define that a point p_1 sees an edge p_2p_3 if the triangle $p_1p_2p_3$ is empty, i.e., no other point lies inside and no edge is separating one corner of the triangle from the other two. The *reverse single chain* is another special set S' of n

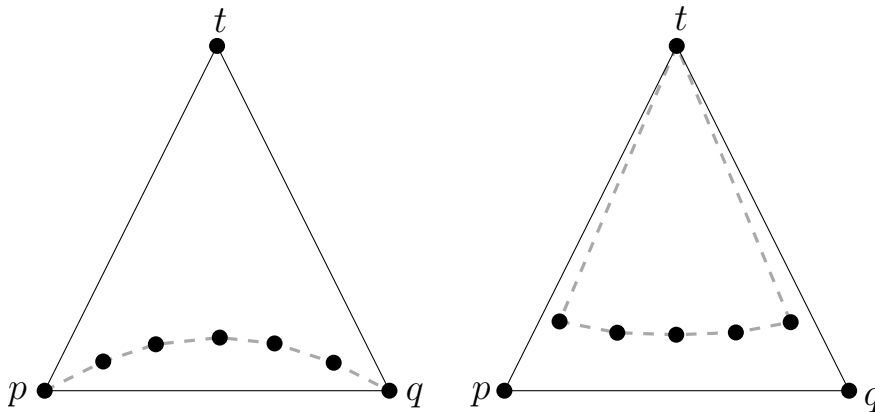


Figure 4.4: Example for a single chain set (left) and a reverse single chain set(right) for $n = 8$.

points in the plane, such that $|CH(S')| = 3$ and $n - 3$ interior points together with one convex hull point t form a convex polygon and all points of this polygon are visible by the two other exterior points p and q . An example of each set is given in Figure 4.4. Hackl and Pilz [23] proved, that the flip graphs of the single chain set and the reverse singles chain set are connected (Theorem 4.3 and Theorem 4.4).

Theorem 4.3. *Given a single chain set S with $n \geq 3$ points. Then the flip graph G of all 4-PPTs of S is connected, even if we allow only to flip edges incident to an triangle.*

Proof. Hackl and Pilz [23] proved Theorem 4.3 with the inductive construction of the flip graph. The case $n = 3$ is trivial, so $n = 4$ will be the basis for further steps (Figure 4.5). We will now show that we can split the flip graph G into three disjoint and connected subgraphs $r(G)$, $l(G)$ and $m(G)$, and show that these subgraphs are also connected with each other. Let $\{t, p, q\} \in S$ be the points on the convex hull of S and $S \setminus \{t\}$ is the convex set (as in Figure 4.5). The *left side* of G , $l(G)$ is the set of all 4-PPTs of S in which q is only adjacent to t and p . In the same way

¹Figures 4.5, 4.6 and 4.9 in this section were provided by Hackl and Pilz [23].

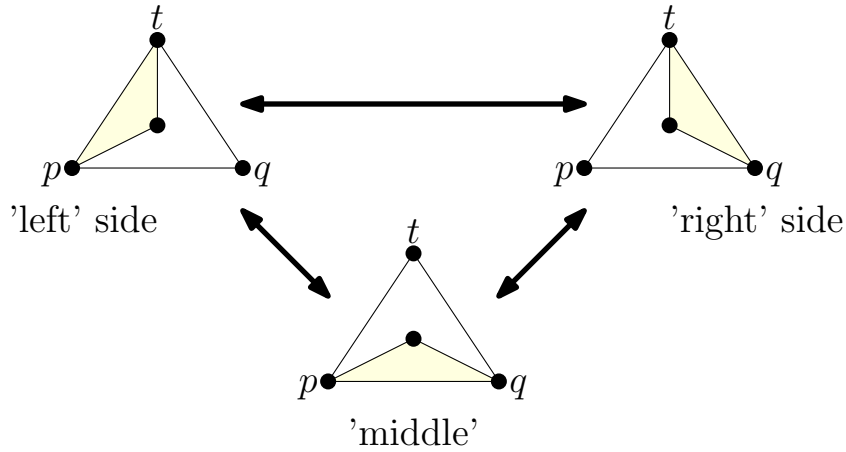


Figure 4.5: Flip graph for the single chain with $n = 4$.¹

we define the *right side* of G , $r(G)$ to be the set of all 4-PPTs where p is only adjacent to t and q and not to any interior point. The *middle* of G , $m(G)$ are all 4-PPTs in which q as well as p are adjacent to at least one interior point. Assume

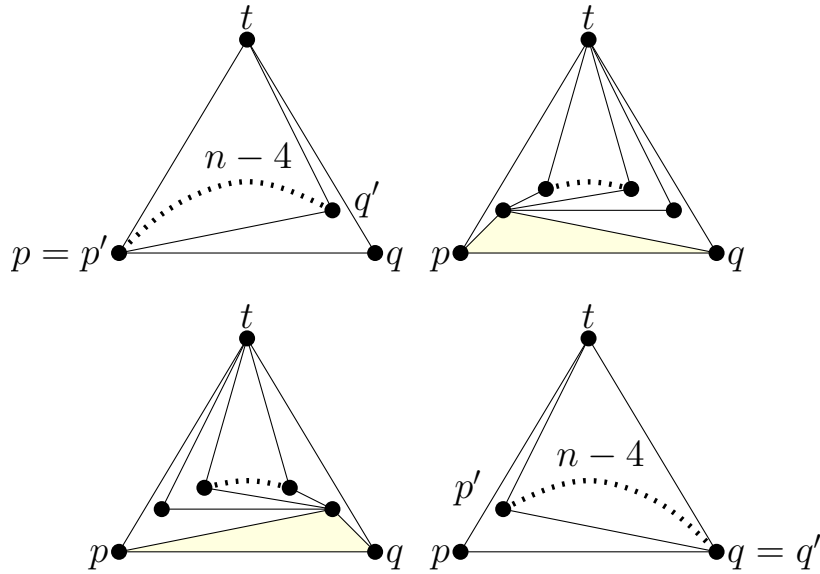


Figure 4.6: Each 4-PPT in $m(G)$ is connected to one in $r(G)$ or $l(G)$

now that the flip graph G' of a single chain set S' with $n - 1$ points is connected and $CH(S') = \{t', p', q'\}$. By adding a new point q to all 4-PPTs of G' such that q' becomes an interior point and q is only connected to t' and p' we create a new left side of G , the flip graph of the new set $S = S' \cup \{q\}$ with $|CH(S)| = 3$. Since G'

was connected, $l(G)$ is now also connected. Analogous we can create a new right side of G by adding a new point p to all 4-PPTs in G' and with the same argument as before, $r(G)$ is connected. Since $|CH(S)| = 3$, Theorem 2.1 verifies that we have exactly one triangle among the pseudo-triangles in each 4-PPT of S . The special point set enforces that in all 4-PPTs in $m(G)$ the baseline pq is part of this triangle. Additionally there exists exactly one 4-PPT for each of the $n - 3$ triangles including the edge pq . Flipping a triangle edge incident to either p or q results in a 4-PPT that is part of $r(G)$ or $l(G)$, respectively (Figure 4.6). Therefore, G is connected. \square

Figure 4.7 shows the flip graph of the single chain set for $|S| = 6$ points. Interestingly only two of the three different flip types that are described in section 5.1.2 occur here. Next, we will show, that the flip graph of the very similar point set, the

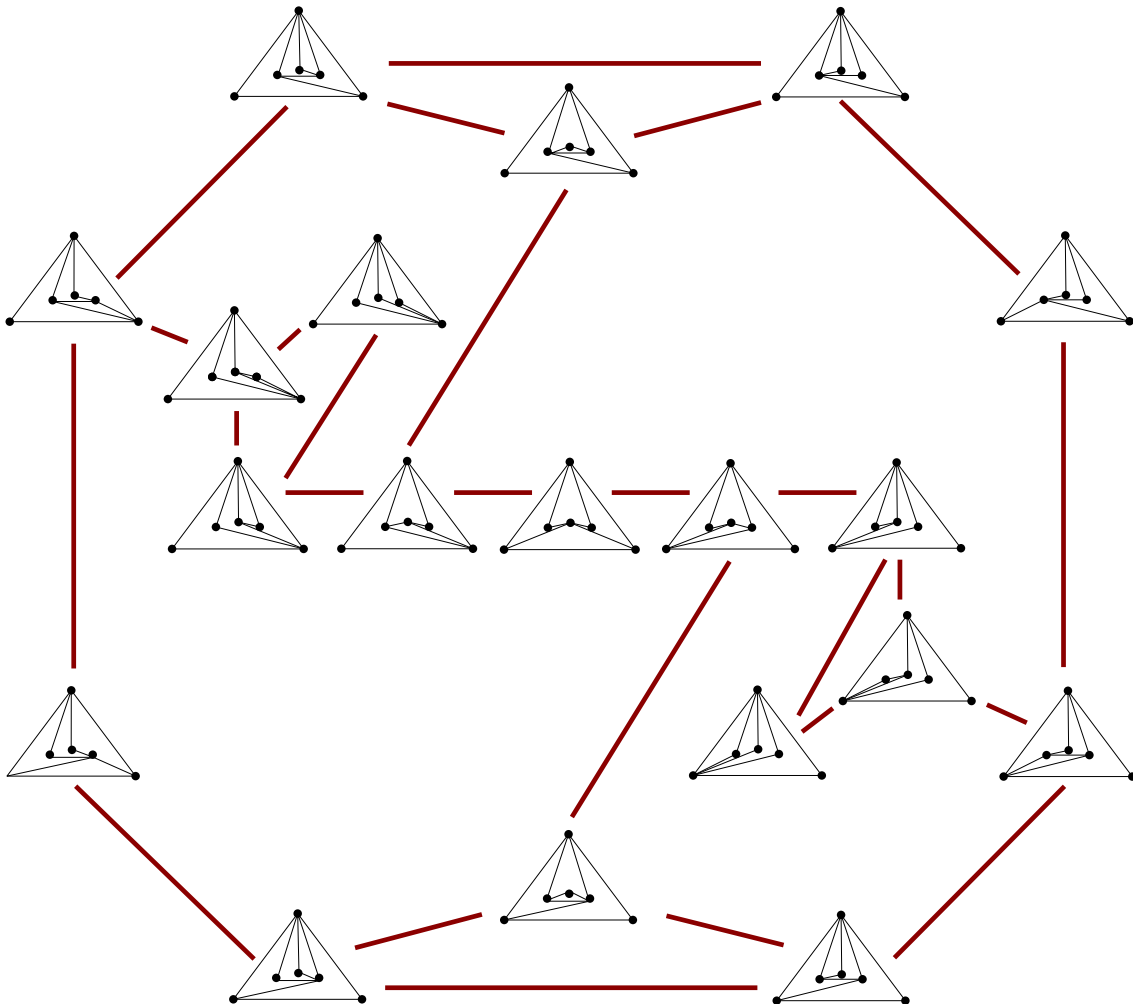


Figure 4.7: Flip graph of the single chain set for $n = 6$.

reverse single chain, is also connected.

Theorem 4.4. *Let S be a reverse single chain set with $n \geq 3$ points. Then the flip graph G of all 4-PPTs of S is connected, even if we allow only to flip edges incident to an triangle.*

Proof. This proof by Hackl and Pilz [23] follows the general idea of the proof of Theorem 4.3 but needs to be explained in more detail. Let G be the flip graph where each vertex corresponds to one 4-PPTs of S . We again define the left, right and middle of G , $l(G)$, $r(G)$ and $m(G)$ as above. Let G' be the flip graph of the reverse single chain set S' with $n - 1$ points and we assume G' is a connected graph. We will create now $r(G)$ by adding another vertex to the chain and show that $r(G)$ is a connected graph. Figure 4.8a represents the set S' with $n - 1$ points, i.e., $n - 4$ of them are part of the interior chain.

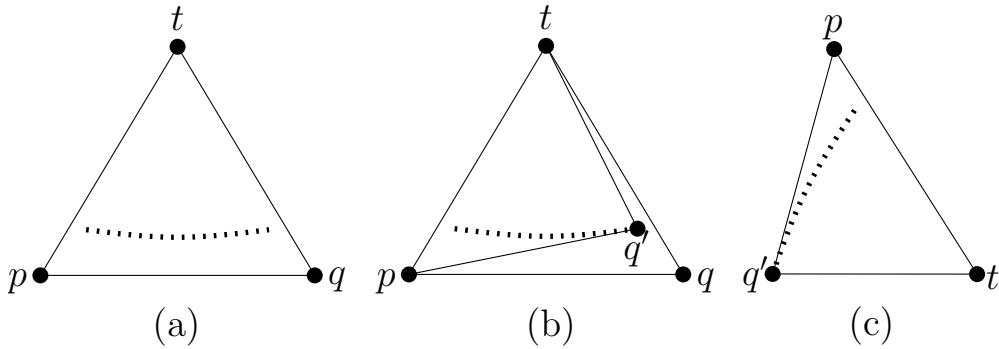


Figure 4.8: (a) Representation of a reverse single chain set S' with $n - 1$ points. (b) Extending the chain by q' . (c) This pointgon is a single chain set, its flip graph of 4-PPTs is connected.

We extend the interior chain by adding a vertex q' to the right end of the chain of S' in way that the resulting set S is again a valid reverse single chain set. Drawing the edges $q't$ and $q'p$ has the consequence that every 4-PPT of the pointgon $P = S \setminus \{q\}$ that is bounded by the triangle $q'tp$ is part of $r(G)$ (Figure 4.8b). Hence, if the flip graph of 4-PPTs of P is connected, $r(G)$ is connected. Taking a closer look at P , we see that this set fulfills all the requirements for being a single chain set with $n - 1$ points and the baseline $q't$ (Figure 4.8c). From Theorem 4.3 it follows that the flip graph of 4-PPTs of P is connected and hence, $r(G)$ is connected. Equivalently it can be shown that $l(G)$ is connected by adding the point p' to the left side of the interior chain. To prove that the whole graph G is connected, we will show that all 4-PPTs

in $m(G)$ are connected in chains, that finally result in a 4-PPT that is either part of $r(G)$ or $l(G)$. Let now a and b be the leftmost and rightmost point of the inner chain, respectively (see Figure 4.9). Consider the 4-PPT $\mathcal{P} \in m(G)$ with the triangle

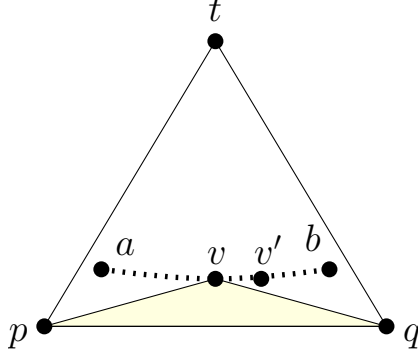


Figure 4.9: Flipping the edge pv or vq of the triangle pvq results again in an 4-PPT in $m(G)$ unless $v = b$ or $v = a$.

paq . Flipping the edge pa results in a 4-PPT $\mathcal{P}' \in l(G)$. Due to symmetry reasons flipping the edge bq in the 4-PPT $\mathcal{P}'' \in m(G)$ with the triangle pbq results in a 4-PPT $\mathcal{P}''' \in r(G)$. Therefore consider a 4-PPT in $m(G) \setminus \{\mathcal{P}, \mathcal{P}''\}$ with the triangle qvp and $v \in S \setminus \{q, p, t, a, b\}$. W.l.o.g. flipping pv and qv is symmetric, so assume now we flip the edge qv . This flip produces a new triangle edge pv' , with v' being a neighbor of v in the chain, closer to b than v was before. If $v' = b$, the resultant 4-PPT is part of $r(G)$. So consecutive flipping of the edge qv , v representing the current corner (top) of the triangle opposite the baseline, moves the top of the triangle along the chain of interior points, finally resulting in a 4-PPT in $r(G)$. On the other hand, flipping the edge pv will move the top of the triangle into the other direction, finally resulting in a 4-PPT in $l(G)$. Hence, starting with any 4-PPT in the subgraph $m(G)$, there exists always two flip sequences, one resulting in a 4-PPT in the subgraphs $r(G)$ and the other resulting in a 4-PPT in $l(G)$. We can conclude that G is connected. Note that the subgraph $m(G)$ is not a connected graph in this case, i.e., $m(G)$ exists of several disjoint chains (see Figure 4.10). Consequently there exist more than one 4-PPT per fixed triangle that has pq as baseline. \square

4.3.2 Counting 4-PPTs of The Single Chain

Consider the single chain set S of $n \geq 3$ points in the plane with $|CH(S)| = 3$ as defined in the previous section 4.3. Following the idea of the proof of Theorem 4.3,

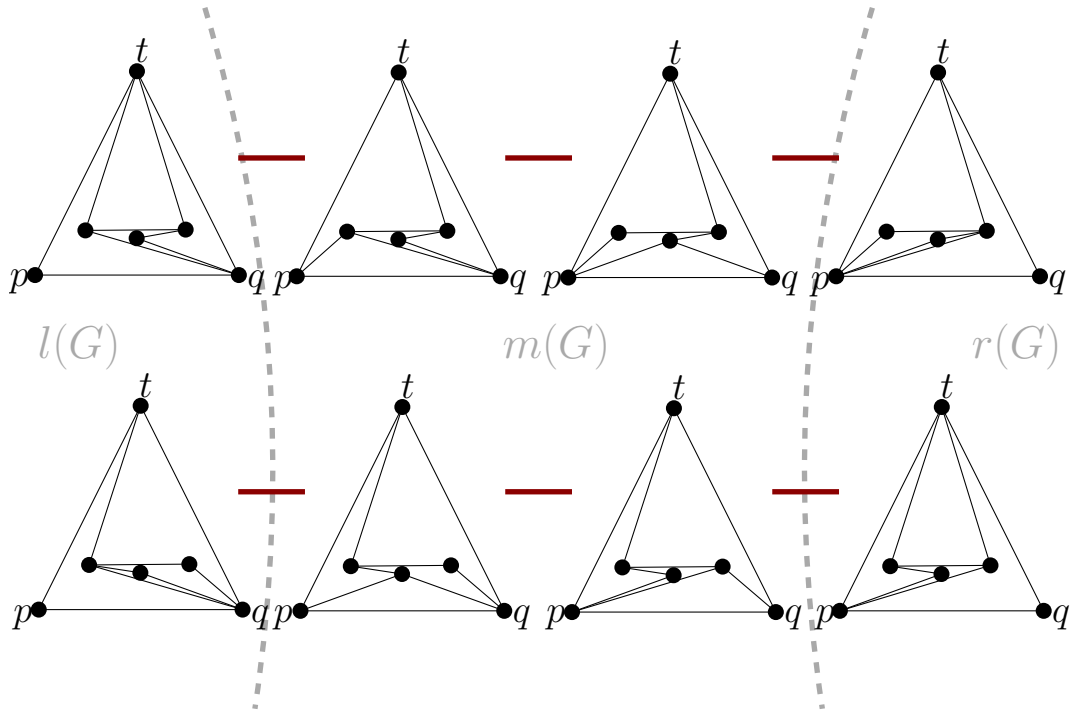


Figure 4.10: Two subgraphs of $m(G)$ that are not connected in $m(G)$.

we can count the number of different 4-PPTs of such a set. Let $N(n)$ be the number of all 4-PPTs of S , G the flip graph of the 4-PPTs of S , i.e., $N(n)$ is the number of vertices of G . As seen before, the left side of G , $l(G)$, is connected and since the number of vertices in $l(G)$ is the number of all 4-PPTs of the single chain set S' with $|S'| = n - 1$, we have $N(n - 1)$ vertices in $l(G)$. Analogously, we have $N(n - 1)$ vertices in $r(G)$, the right side of G . In the middle of G , $m(G)$, we have all 4-PPTs with the triangle incident to the baseline of S . This means for each of the $(n - 3)$ choices of the third point of the triangle, we have one 4-PPT. Since

$$\{l(G) \cap r(G)\} \cup \{l(G) \cap m(G)\} \cup \{r(G) \cap m(G)\} = \{\}$$

$$\text{and } l(G) \cup r(G) \cup m(G) = G$$

we have

$$\begin{aligned}
N(n) &= 2N(n-1) + n - 3, & n \geq 3 & \quad (4.1) \\
N(1) &= N(2) = 0 \\
N(3) &= 1
\end{aligned}$$

This recursion can be solved by consecutive substitution.

$$\begin{aligned}
N(n) &= 2N(n-1) + n - 3 \\
&= 2(2N(n-2) + n - 1 - 3) + n - 3 \\
&= 2^2N(n-2) + (2n + n) - 2 - (2 \cdot 3 + 3) \\
&= \dots \\
&= 2^k N(n-k) + n \sum_{i=0}^{k-1} 2^i - \sum_{i=1}^{k-1} 2^i i - 3 \sum_{i=0}^{k-1} 2^i
\end{aligned}$$

Using $N(n-k) = 1$ for $k = n-3$ leads to

$$\begin{aligned}
N(n) &= 2^{n-3} \cdot 1 + n \sum_{i=0}^{n-4} 2^i - \sum_{i=1}^{n-4} 2^i i - 3 \sum_{i=0}^{n-4} 2^i \\
&= 2^{n-3} \cdot 1 + (n-3) \sum_{i=0}^{n-4} 2^i - \sum_{i=1}^{n-4} 2^i i
\end{aligned} \quad (4.2)$$

The sums that appear in Equation 4.2 can be replaced by their explicit expressions.

$$\sum_{j=0}^m 2^j = 2^{m+1} - 1 \quad (4.3)$$

$$\sum_{j=1}^m 2^j j = 2^{m+1}(m-1) + 2 \quad (4.4)$$

Equation 4.2 combined with the adapted properties 4.3 and 4.4 leads to the following result.

$$N(n) = 2^{n-3} + (n-3)(2^{n-3} - 1) - (2^{n-3}(n-5) + 2) \quad (4.5)$$

Simplifying Equation 4.5 leads to the following closed formula for the recursion 4.1:

$$N(n) = 3 \cdot 2^{n-3} - n + 1, \quad n \geq 3 \quad (4.6)$$

The first values of this integer series are displayed in Table 4.1. The sequence is listed in “The On-Line Encyclopedia of Integer Sequences” with the composite number A079583 [17]. This sequence, i.e., the corresponding formula, can also be obtained by studying the infinite sequence of strings. $x(1) = a$, $x(2) = aba$, $x(3) = ababbaba$, ... where $x(n+1) = x(n) \oplus "b"^{n-1} \oplus x(n)$, for $n \geq 1$, and none of the borders $x(1)$, $x(2)$, ..., $x(n-1)$ of a string $x(n)$ covers $x(n)$ for $n \geq 2$. This means that the string $x(n+1)$ consists of the concatenation of two times the string $x(n)$ and $n-1$ times the string "b" inbetween. Then the length of $x(n+1)$ is given by

$$N(n+3) = 3 \cdot 2^n - n - 2 \quad [17].$$

n	1	2	3	4	5	6	7	8	9	10	...	50
$N(n)$	0	0	1	3	8	19	42	89	184	375	...	$\sim 4.22 \times 10^{14}$

Table 4.1: The number $N(n)$ of vertices in the flip graph of all 4-PPTs of the single chain set with n points.

4.3.3 Counting 4-PPTs of The Reverse Single Chain

Let S now be the reverse single chain set with n points, $N'(n)$ be the number of 4-PPTs of S and G the flip graph of 4-PPTs of S . Furthermore, let $N'_r(n)$ and $N'_l(n)$ be the number of 4-PPTs in $r(G)$ and $l(G)$, respectively. In the proof of Theorem 4.4 we have seen that the number of 4-PPTs in $r(G)$ equals the number

of 4-PPTs of a single chain set $P = S \setminus \{q\}$ that consists of $n - 1$ points. With Equation 4.6 we get

$$N'_r(n) = N'_l(n) = N(n - 1) = 3 \cdot 2^{n-4} - n + 2, n \geq 4$$

For revealing the number of 4-PPTs in $m(G)$ we follow the idea of the disjoint chains in $m(G)$. In the proof of Theorem 4.4 we stated that for each 4-PPT in $m(G)$ two flip sequences can be found that form a chain in $m(G)$ that has its ends in $r(G)$ and $l(G)$, respectively. Such a chain in $m(G)$ consists of $n - 4$ vertices since in a 4-PPT in $m(G)$ the triangle with the baseline pq has one of the interior points of S as its third corner. There exist $n - 3$ interior vertices in S but only $n - 4$ of them are candidates for the third point. Due to the special configuration of the reverse single chain set one is 'blocked' by an edge that ends in the corner t of S and will always be omitted in those flip sequences (see Figure 4.11a-b). Consider Figure 4.11c, if the edge vt exists in a 4-PPT of a single chain set in which the triangle pvq exists too, completing the two triangles ptv and vtq to a 4-PPT would lead to two more triangles in the whole 4-PPT, which contradicts with the fact that we only have one triangle in a 4-PPT of a reverse single chain set.

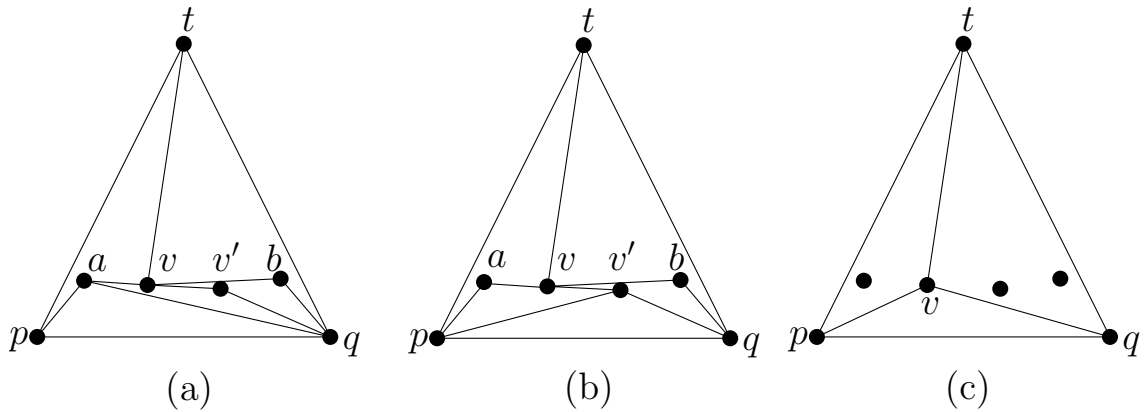


Figure 4.11: (a)-(b) Flipping edge qa results in a new edge pv' . Point v is omitted.
(c) This case cannot occur in a 4-PPT of a reverse single chain set.

To count the number of chains we can easily count their ends in $r(G)$ or $l(G)$, respectively. W.l.o.g. we count the number of possible ends of such chains in $r(G)$. That are all 4-PPTs in $r(G)$ in which the triangle is incident to the edge tb . Consider now the single chain set $P = S \setminus \{q\}$. We have $(n - 4)$ 4-PPTs of P with the triangle

incident to the baseline tb . Hence, this equals the number of 4-PPTs of S in $r(G)$ that can be transformed by one flip into a 4-PPT in $m(G)$. Consequently we get

$$N'_m(n) = (n - 4) \cdot (n - 3), n > 4$$

Summing all up yields to

$$N'(n) = 2 \cdot (3 \cdot 2^{n-4} - n + 2) + (n - 4) \cdot (n - 3), n > 4$$

n	1	2	3	4	5	6	7	8	9	10	...	50
$N'(n)$	0	0	1	3	8	22	50	104	208	410	...	$\sim 4.22 \times 10^{14}$

Table 4.2: The number $N'(n)$ of vertices in the flip graph of all 4-PPTs of the reverse single chain set with n points.

4.4 The Double Circle

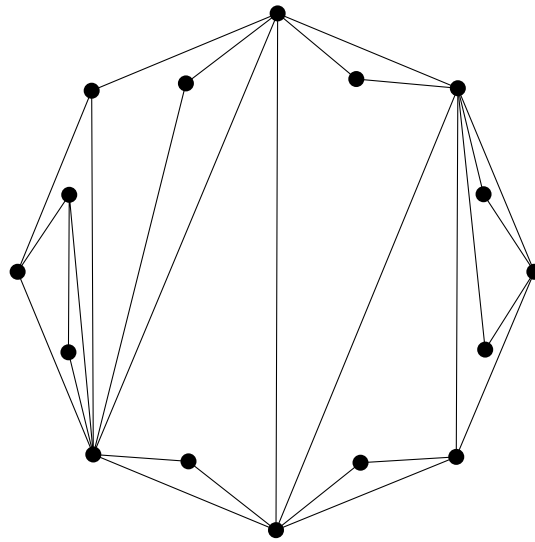


Figure 4.12: Example of a 4-PPT of the double circle with $n = 16$ points.

In terms of triangulations, the double circle is a very interesting set, since for $5 \leq n \leq 11$, it is known to be the set of n points in the plane that minimizes the

number of triangulations [2] and for $12 \leq n \leq 20$ it is still the best known example for a set of n points with the smallest number of triangulations. This special set is defined the following way. Let $n = 2m$, $m > 2$ be the cardinality of S , a set of points in the plane. S is called *double circle* if the convex hull consists of m points and each of the m inner points is set sufficiently close to exactly one edge of the convex hull (see Figure 4.12). A point p is said to be *sufficiently close* to an edge e , if no edge between any two points of $S \setminus \{p\}$ can separate p and e [9].

Theorem 4.5. *Let S be the double circle set with $n = 2m$ points and $m > 2$. Then the flip graph G of all 4-PPTs of S is connected, even if we allow only to flip edges adjacent to a triangle. The following proof was provided by Aichholzer and Hackl [22].*

Proof. First we will define a special type of 4-PPTs of S , the *lense shutter* (Figure 4.13). There exists one edge each between a convex hull point and an interior point. We call these edges *shutter edges* and they are marked in bold in Figure 4.13. Let G be the flip graph of all 4-PPTs of S . We first show that there exists a path in

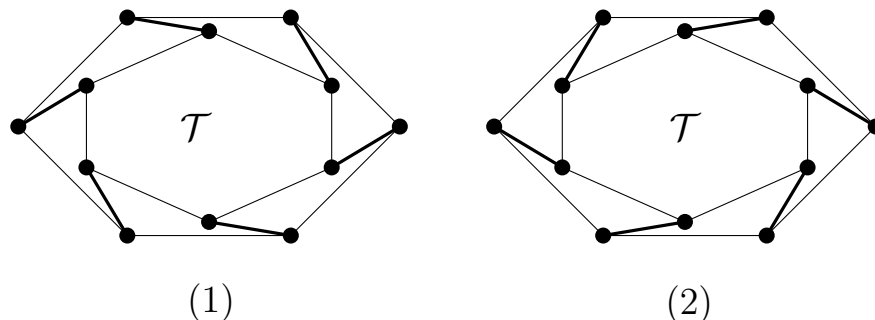


Figure 4.13: The clockwise (1) and counterclockwise (2) lens shutter.²

G that connects the clockwise lens shutter with the counterclockwise lens shutter, i.e., there exists a sequence of flips of triangle edges that changes the orientation of the lens shutter. Then, we will prove that we can allocate one shutter edge to each point of the interior circle and that we can easily change the orientation of a single shutter edge. Finally, we show that we can remove disturbing edges that start with a convex hull point but are not shutter edges and that would destroy a lens shutter 4-PPT.

²The Figures 4.13-4.16 were provided by Aichholzer and Hackl [22].

Claim 1. There exists a sequence of flips to change the orientation of a lense shutter 4-PPT.

Let p be an interior point of S , then e_p is the sufficient close convex hull edge that correspond to p . An edge between p and one end point of e_p is called shutter edge of p . In the two lens shutter 4-PPTs, each point of the convex hull has exactly one shutter edge. If we consider the clockwise lens shutter, we have m pseudo-triangles incident to the convex hull and a triangulation \mathcal{T} of the convex polygon \mathcal{P} of the interior points (Figure 4.13 (1)). Since we allow only to flip edges adjacent to a triangle, all flipable edges are either part of \mathcal{T} or the edges of \mathcal{P} . Flipping an edge of \mathcal{P} results in an triangle that is adjacent to a shutter edge and a flip of this shutter edge results in a new reverse oriented shutter edge. This leads to a sequence of $m+1$ flips, which changes the orientation of the shutter edges (see Figure 4.14). \square

Claim 2. The flip graph of triangulations of \mathcal{P} is connected. Hence, the 4-PPTs that include \mathcal{P} form a connected subgraph of G .

The flip graph of all triangulations of a convex polygon is connected. Hence, the flip graph of triangulations of \mathcal{P} is connected. \square

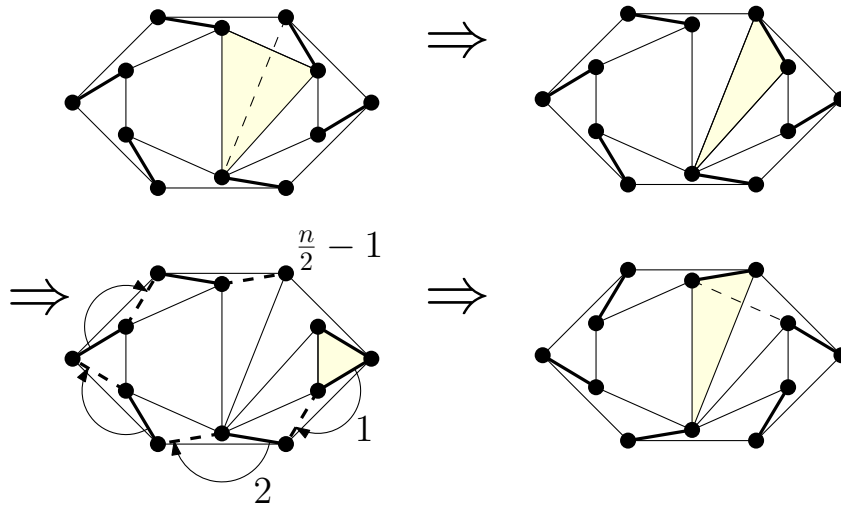


Figure 4.14: Flip sequence to change the orientation of the shutter lense.

Now we want to show that every 4-PPT can be flipped into a lens shutter.

Claim 3. It is possible to achieve that each interior point has exactly one shutter edge.

Therefore, we consider a 4-PPT where at least one interior point p is incident to both its shutter edges s_p and s'_p . Then these two edges form a triangle together with

the convex hull edge e_p . Hence, either s_p or s'_p can be flipped such that only one shutter edge remains. \square

Now we look at the case where each interior point has exactly one shutter edge, but not all shutter edges are yet oriented in the same direction.

Claim 4. There always exists a sequence of flips to change the orientation of a single shutter edge.

Consider Figure 4.15(a), the orientation of the shutter edge of the interior point p shall be changed, i.e., edge pb should be flipped to pa , such that we achieve a 4-PPT with all shutter edges orientated counter clockwise. If, like in Figure 4.15 (a), pb is incident to a triangle, a flip of pb results in the new edge pa (note that $v' = v''$ is possible). If pb is not incident to a triangle, we only have one other option, Figure 4.15 (b), because we excluded the case in Figure 4.15 (c) by only considering 4-PPTs with one shutter edge per interior point. Consider now the situation in Figure 4.15b; the edge e' can either be incident to a triangle (Figure 4.15 (d)) or to a pseudo-triangle. The latter can only occur in situation 4.15 (e). If e' is incident to a triangle, we need to differentiate between two situations, $v' \neq c$ and $v' = c$. In the first case, we can flip e' to receive a triangle having pb as edge. In the second case, we can flip qc , which results in a 4-PPT where pb is incident to a triangle. In addition the also wrongly orientated shutter edge of point c has been corrected. If the edge e' is incident to a pseudo-triangle, then $e'' = qa$ can be incident to a triangle, Figure 4.15 (e). In this case e'' can be flipped and consequently e' becomes incident to a triangle, as we had in Figure 4.15 (d). The situation when e'' is not incident to a triangle is shown in Figure 4.15 (f). In this unique local situation, one can clearly see that the edge e''' needs to be a flipable edge. For $v' \neq d$, flipping e' results again in the situation sketched in Figure 4.15(e). If $v' = d$ five flips are necessary to change the orientation of the shutter edge of p . Those flips are sketched in Figure 4.15 (g)-(k). The sequence starts with the flip of the correctly oriented edge rd , since this is necessary to get the triangle incident to e'' . The last flip fixes then the edge rd again. \square

So far we have shown that the orientation of single shutter edges can be changed and we can find a flip sequence to assimilate their orientation.

Claim 5. There always exists a sequence of flips that removes edges which start in a convex hull point but are not shutter edges, to achieve a lense shutter 4-PPT.

In the right illustration in Figure 4.16, the green colored edges are the edges to be gained, the red ones are forbidden to flip in. Assume at least one green edge

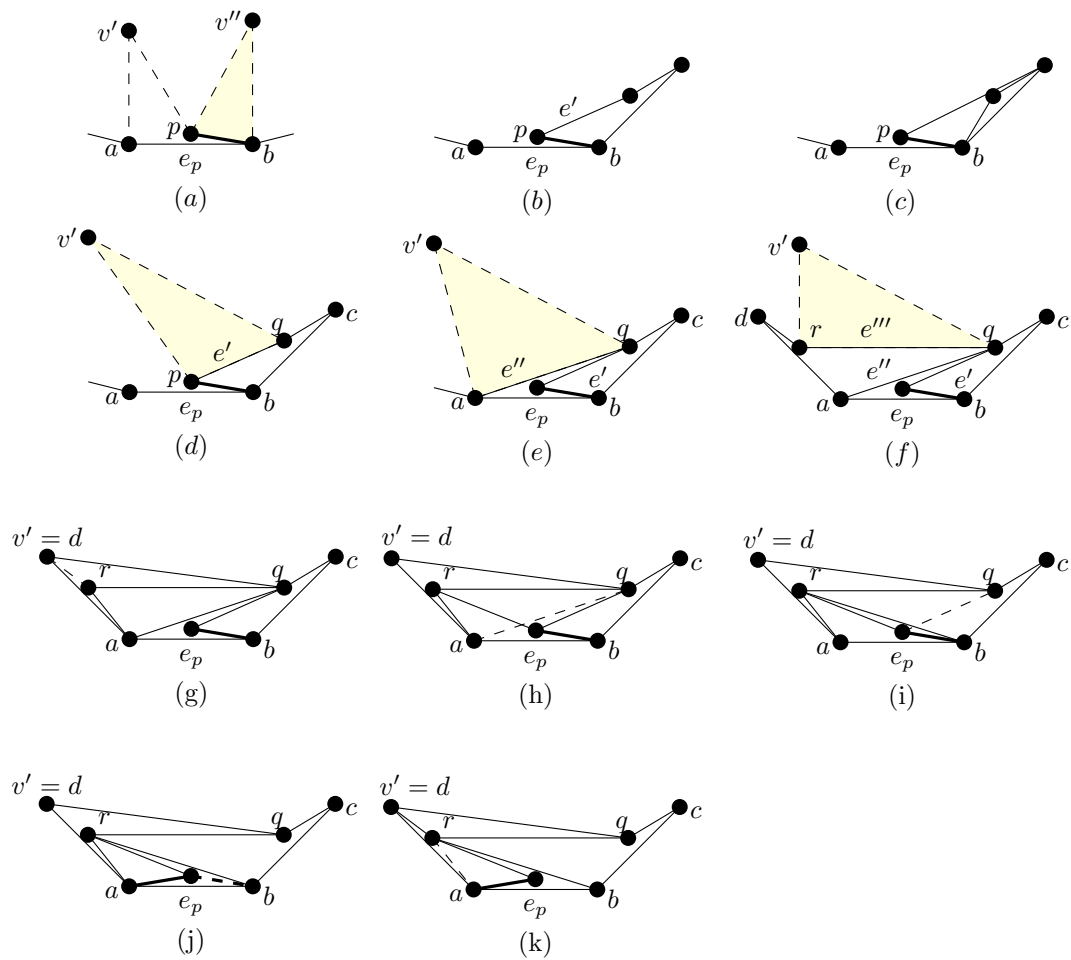


Figure 4.15: Flip sequence to change the orientation of the shutter lens.

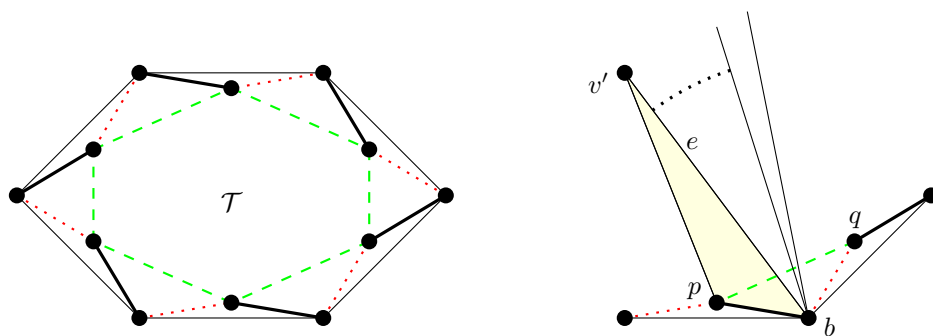


Figure 4.16: Creating the inner polygon edges to finally achieve a lense shutter 4-PPT.

pq (in Figure 4.16 right) needs to be flipped into the 4-PPT. Since it does not yet exist, there exists a fan of (at least one) disturbing edges. Let $e = bv$ be an edge that we want to remove without creating a red edge. Since the red and the green edge incident to p are not yet part of the 4-PPT, e is an edge of the triangle $v'pb$ and can be flipped. We can proceed in the same way with all other edges of this fan, until the last flip results in the green edge. With this final claim, we have shown that every 4-PPT of the double circle can be transformed into a lense shutter 4-PPT. \square

Together, Claim 1 - Claim 5 combined proved that the flip graph of all 4-PPTs of the double circle is connected. \square

4.5 The Muffin Set

Let S be a single chain set with $k + 3$ points, further let q and r be the end points of its baseline and t the third corner (top) on the convex hull. We introduce now a new special set $M_{k,m}$, called the *muffin set*, with $n = k + m + 4 \geq 4$ points in the plane. We define the muffin set by extending the convex hull of S by $m + 1$ points, such that all new points see all edges of the convex polygon in S formed by q , r and all the interior points of S . Let p and s be the leftmost and the rightmost point, respectively, of the set of new points including t . We dub the points p , q , r and s corners of the muffin. Further, we call the set of k interior points the *lower chain* and the set

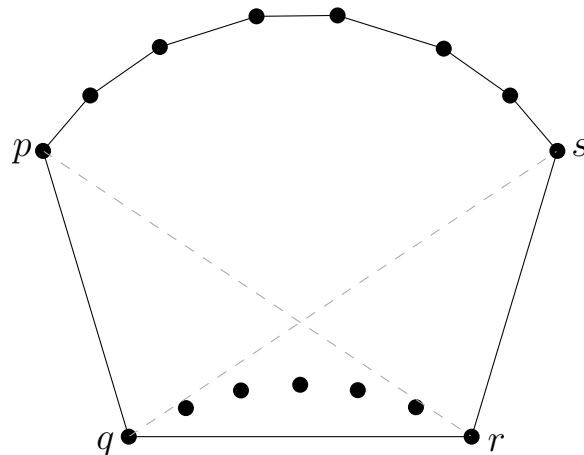


Figure 4.17: The special set $M_{5,6}$.

$CH(M_{k,m}) \setminus \{p, q, r, s\}$ of m points the *upper chain*. By definition the lower chain lies below the supporting lines of pr and sq , respectively (see Figure 4.17).

Theorem 4.6. *The flip graph of the set $M_{k,m}$ is connected $\forall k, m \in \mathbb{N}$, even with the restriction that only edges incident to a triangle are allowed to be flipped.*

Proof. The flip graph of $M_{0,0}$ and $M_{1,0}$ is clearly connected, since $M_{0,0}$ forms a simple 4-gon and $M_{1,0}$ forms a 4-gon with one point inside the convex hull (see Figure 4.18 and Figure 4.19). Likewise the flip graph of $M_{0,m}$ is connected, since $M_{0,m}$ is a simple

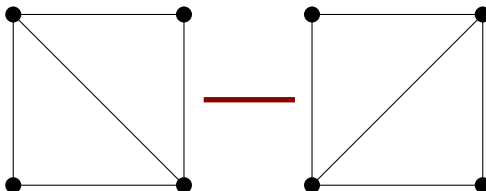


Figure 4.18: The flip graph of $M_{0,0}$ is connected.

convex polygon with $(m+4)$ points on the convex hull. In order to show that the flip graph of $M_{k,m}$ is connected, we first show that this holds for the flip graph of $M_{1,m}$ and use this result as basis for proving it for $M_{k,m}$. Let $G_{1,m}$ now be the flip graph of all 4-PPTs of $M_{1,m}$. As $|CH(M_{1,m})| = m+4$ the 4-PPT consists out of $(m+2)$ triangles and one 4-gon \mathfrak{q} . Similar to the proof of the connectivity of the flip graph of the single chain sets, we can separate the flip graph $G_{1,m}$ into three connected and disjoint subgraphs $r(G_{1,m})$, $l(G_{1,m})$, $m(G_{1,m})$, depending on the position of the single 4-gon \mathfrak{q} . Let $r(G_{1,m})$ be the subgraph of $G_{1,m}$ with all 4-PPTs in which \mathfrak{q} has the single inner point t as its reflex point and qr, tq are fixed edges of \mathfrak{q} , call it the *right side* of $G_{1,m}$. The left side, $l(G_{1,m})$, is defined analogously. Let $m(G_{1,m})$ be all 4-PPTs with one triangle that has the points q , r and t as its fixed corners. Figure 4.20 shows the three classes of 4-PPTs of $M_{1,5}$. Again we have

$$\{l(G_{1,m}) \cap r(G_{1,m})\} \cup \{l(G_{1,m}) \cap m(G_{1,m})\} \cup \{r(G_{1,m}) \cap m(G_{1,m})\} = \{\}$$

$$\text{and } l(G_{1,m}) \cup r(G_{1,m}) \cup m(G_{1,m}) = G_{1,m}.$$

Claim 1. The subgraphs $l(G_{1,m})$, $r(G_{1,m})$ and $m(G_{1,m})$ themselves are connected graphs.

Let u be the corner of \mathfrak{q} that is part of the upper chain. It takes one flip (with an adjacent triangle) to move the upper corner of \mathfrak{q} to one neighbored point on the upper chain. Once the 4-gon is fixed, the remaining points form one or two convex polygons which need to be triangulated. The subgraph of $G_{1,m}$ where \mathfrak{q} is fixed

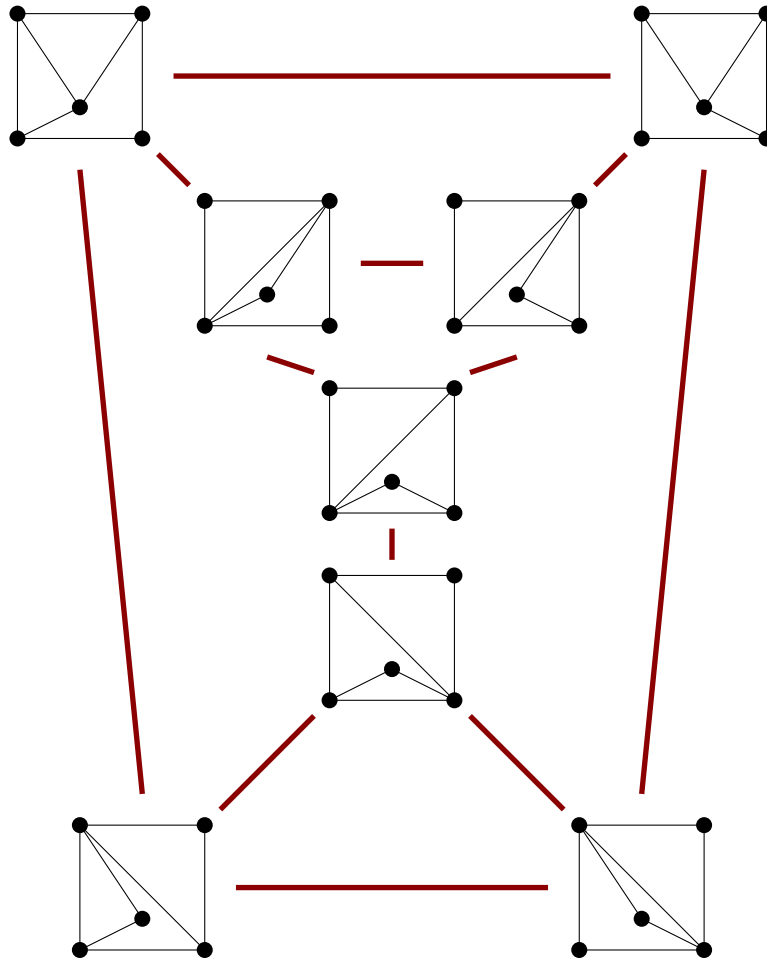


Figure 4.19: The flip graph of $M_{1,0}$ is connected.

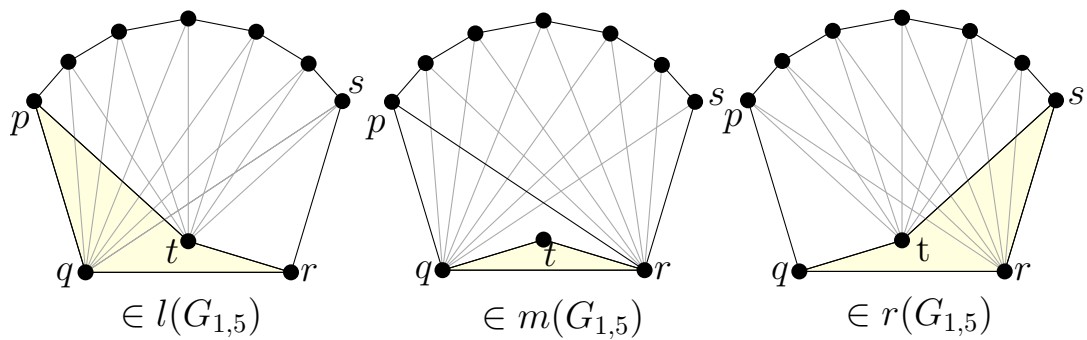


Figure 4.20: Representatives for vertices of $r(G_{1,5})$, $l(G_{1,5})$ and $m(G_{1,5})$. The gray lines correspond to other possibilities for q .

is then connected, because the flip graph of a triangulation of a convex polygon is connected. \square

Claim 2. The flip graph $G_{1,m}$ is connected.

To connect $l(G_{1,m})$ with $m(G_{1,m})$ and $r(G_{1,m})$, consider the 4-PPT with \mathfrak{q} having the corners (p, q, r) , the reflex point t and a triangle spanned by (p, t, r) . Flipping the edge pt results in a 4-PPT that is part of $m(G)$, whereas flipping the edge tr results in a 4-PPT that is part of $r(G)$ (see Figure 4.21). Hence, $G_{1,m}$ is connected. \square Now we show by induction that the flip graph of the set $M_{k,m}$ is connected. But

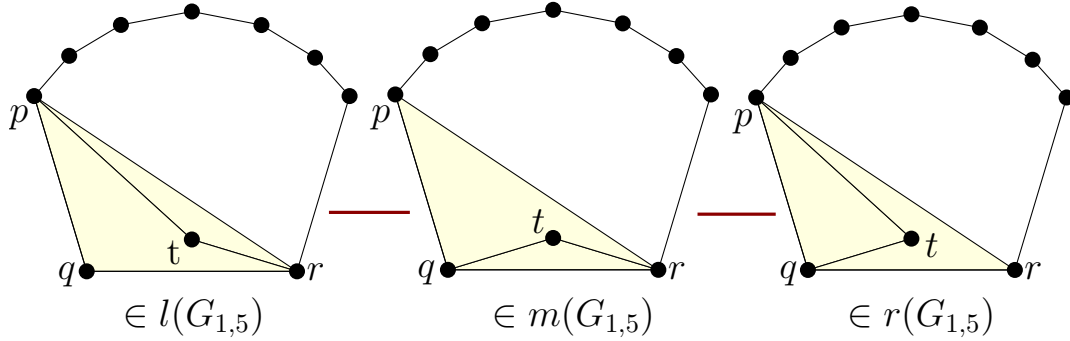


Figure 4.21: Part of the flip graph $G_{1,5}$ that show a connection between the connected subgraphs $r(G_{1,5})$, $l(G_{1,5})$ and $m(G_{1,5})$.

first we state some properties of the set $M_{k,m}$.

Claim 3 (Properties of $M_{k,m}$). Let $M_{k,m}$ be the muffin set with $k+m+4$ points with 4 corners, k points on the lower chain and m points on the upper chain. A 4-PPT \mathcal{P} of $M_{k,m}$ has the following properties:

1. \mathcal{P} has $(k+m+2)$ faces.
2. \mathcal{P} consists of $(m+2)$ triangles and k 4-gons.
3. Exactly one triangle exists that is not incident to any edge of the upper chain.

We designate this the *lower triangle*.

Property 1 follows directly from Theorem 2.2. Since $|CH(M_{k,m})| = (m+4)$ and the number of triangles in a 4-PPT always equals the number of points on the convex hull minus two, we get $(m+2)$ triangles. Since we have $(k+m+2)$ faces in all, the remaining k faces are 4-gons and this proves property 2. Property 3 is based on the characteristics of the special set $M_{k,m}$ that all edges on the upper chain (including

corners (p, s)) are incident to a triangle; therefore, we have $(m + 1)$ *upper triangles* and one which is not incident to any edge of the upper chain. \square

As we have seen above $\forall m$ the flip graph of $M_{1,m}$ is connected. Assume now that the flip graph of $M_{k-1,m}$ is connected $\forall m$. We divide the graph of $M_{k-1,m}$ similar to the previous example into disjoint subgraphs $r(G_{k-1,m})$, $l(G_{k-1,m})$, $m(G_{k-1,m})$, $m_l(G_{k-1,m})$ and $m_r(G_{k-1,m})$. Let $r(G_{k-1,m})$ be all 4-PPTs of the point set with no inner edge incident to the corner q and $l(G_{k-1,m})$ all 4-PPTs of the set with no inner edge incident to the corner r . Then we have three subgraphs with inner edges incident to q and r , $m(G_{k-1,m})$, $m_l(G_{k-1,m})$ and $m_r(G_{k-1,m})$. $m(G_{k-1,m})$ includes all 4-PPTs with the lower triangle tqr where t is a point of the *lower chain*. $m_l(G_{k-1,m})$ includes all 4-PPTs with one 4-gon \mathfrak{p} that has the baseline qr of the muffin as edge between its two corners q and r , the third corner on the *upper chain* and its reflex point being the leftmost point of the lower chain. We define $m_r(G_{k-1,m})$ analogously (see Figure 4.22). Now we want to construct the flip graph $G_{k,m}$ and show that it

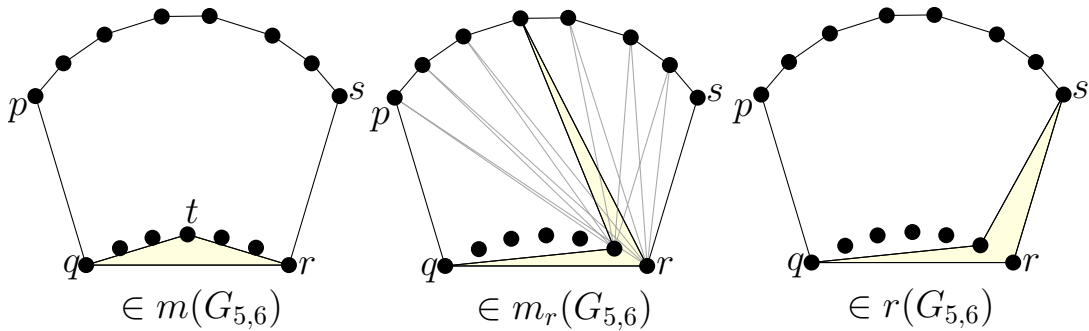


Figure 4.22: Scheme of representative 4-PPTs of $m(G_{5,6})$, $m_r(G_{5,6})$ and $r(G_{5,6})$. Gray lines correspond to other possibilities for \mathfrak{p}

is a connected graph. Therefore, we construct $r(G_{k,m})$ out of $G_{k-1,m}$ by adding to each 4-PPT of $M_{k-1,m}$ a new corner r' such that the original corner r becomes part of the lower chain. In the same way, $l(G_{k,m})$ can be constructed by adding a new corner q' to all 4-PPTs of $M_{k-1,m}$.

Claim 4. $r(G_{k,m})$ and $l(G_{k,m})$ are each connected graphs.

The flip graph of $M_{k-1,m}$ is connected, adding one point to each 4-PPT representing a vertex in $G_{k-1,m}$ obtains the connectedness. Analogously $l(G_{k,m})$ is connected. \square To show that $m_r(G_{k,m})$ is a connected graph, we first show that we can move the corner of \mathfrak{p} which lies on the upper chain to any other point of this chain. We

will then see that for \mathfrak{q} fixed, the subgraph of $m_r(G_{k,m})$ consisting of all 4-PPTs $m_r(G_{k,m})$ including \mathfrak{q} is connected as well.

Claim 5. The upper corner of the special 4-gon \mathfrak{q} can be moved easily along the upper chain.

Consider the 4-gon \mathfrak{q} with its reflex point t and the corner u on the upper chain. To simplify matters call this corner the *upper corner* of \mathfrak{q} . Let x be the left neighbor of u on the upper chain and y the right neighbor. To move the upper corner along the upper chain, one needs either an upper triangle with the points (u, t, x) to move the upper corner of \mathfrak{q} with one flip to x , or the upper triangle (u, r, y) to move it with one flip to y (see Figure 4.23 (a)). \square

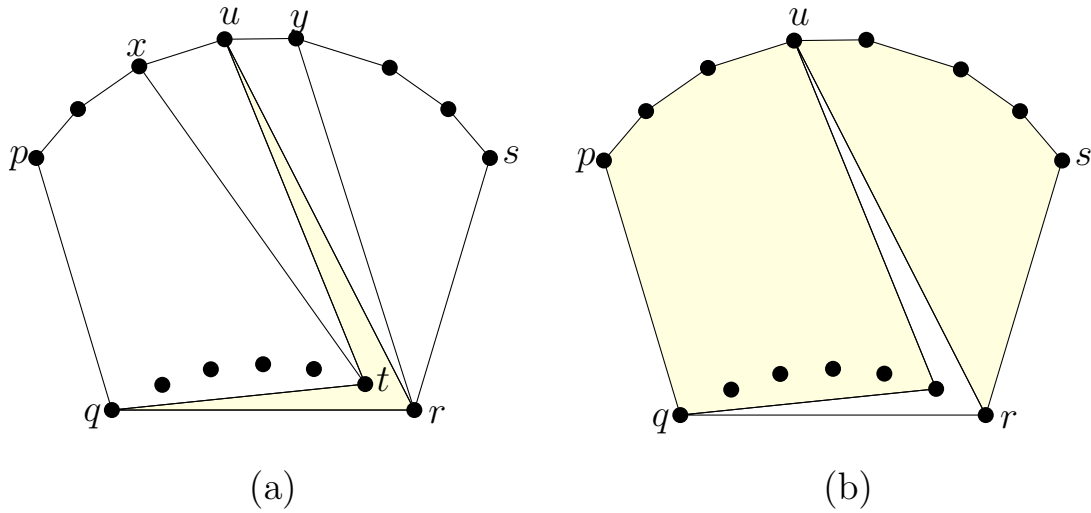


Figure 4.23: (a) Illustrating Claim 5. (b) \mathfrak{q} separating $M_{5,6}$ into a simple convex polygon with 6 points and the set $M_{4,2}$

Claim 6. Each subgraph of $m_r(G_{k,m})$ with fixed 4-gon \mathfrak{q} is connected.

Given a 4-PPT in $m_r(G_{k,m})$ with the fixed 4-gon \mathfrak{q} consisting of the edge qr and a corner u leaving j points of the upper chain to the right of u and i points to the left of u , \mathfrak{q} separates the set $M_{k,m}$ into a simple convex polygon with $(j + 3)$ points and a muffin set $M_{k-1,i}$ whose 4-PPTs lie in $r(G_{(k-1,i)})$ (see Figure 4.23 (b)). In the subgraph of $G_{k,m}$, all edges are fixed but the inner edges of the mentioned polygon are connected, since the flip graph of a simple convex polygon is connected. By assumption, the flip graph of $M_{k-1,i}$ is also connected. \square

Note 5 and Note 6 prove that $m_r(G_{k,m})$ is a connected graph. Due to the symmetry of $M_{k,m}$ the same arguments hold for $m_l(G_{k,m})$. Now we know that four of

the five previous defined subgraphs of $G_{k,m}$ are connected graphs. We can further show that they are also connected with each other.

Claim 7. The subgraph $l(G_{k,m})$ is connected with both subgraphs $m_r(G_{k,m})$ and $m(G_{k,m})$, and the subgraph $r(G_{k,m})$ is connected with both subgraphs $m_l(G_{k,m})$ and $m(G_{k,m})$.

Consider a 4-PPT in $m_r(G_{k,m})$ where the 4-gon \mathfrak{q} has its upper corner in the corner p of $M_{k,m}$ (see Figure 4.24). The points (p, q, r) are now the convex hull of a single chain set with $(k + 3)$ points. Since the flip graph of a single chain set is connected (Theorem 4.3) we can flip into 4-PPTs which lie either in $l(G_{k,m})$ or in $m(G_{k,m})$ (see Figure 4.24). Due to the symmetry of the muffin set the same idea can be used to show that $m_l(G_{k,m})$ is connected with $r(G_{k,m})$ and $m(G_{k,m})$. \square

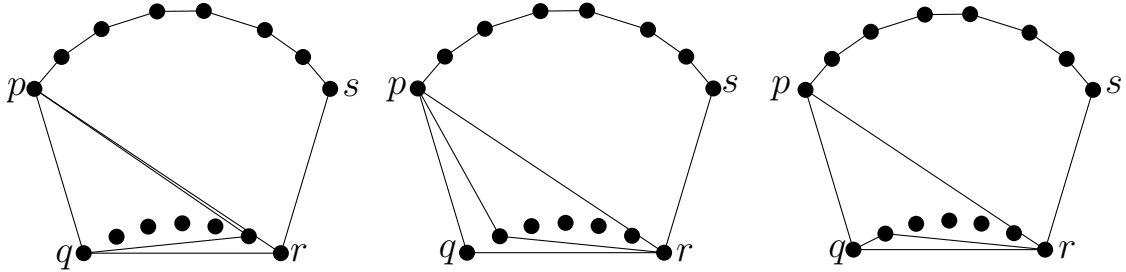


Figure 4.24: Starting with a 4-PPTs in $m_r(G_{5,6})$ (left) and flipping inner edges of a cheerless set leads to 4-PPTs in $l(G_{5,6})$ (middle) and $m(G_{5,6})$.

To finally prove that $G_{k,m}$ is a connected graph, it remains to show that $m(G_{k,m})$ is connected. We will do this by first showing that the subgraphs of $m(G_{k,m})$ where the lower triangle \mathfrak{t} is fixed form a connected graph (Claim 8). Then we present a sequence of flips to change the corner of \mathfrak{t} that lies on the upper chain (Claim 9).

Claim 8. If the lower triangle \mathfrak{t} is fixed, the position of the k 4-gons is defined except for their corners on the upper chain.

Consider the situation in Figure 4.25. The yellow areas represent triangulations of simple convex polygons. Flipping inner edges of this polygons does not change the positions of the 4-gons. In contrast flipping a triangle edge incident to a 4-gon can only effect the position of the upper corner of the 4-gon. If we do not want to change the position of the lower triangle, there is no other flip affecting the other vertices of the 4-gons. \square

From note 8 we can conclude that the subgraphs of $m(G_{k,m})$ where \mathfrak{t} is fixed form a connected graph.

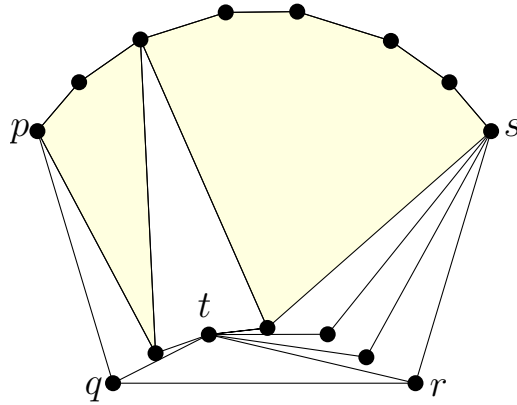


Figure 4.25: Illustration of Claim 8.

Claim 9. Starting with a 4-PPT in $m(G_{k,m})$ there exists a sequence of flips to move the corner t of the triangle \mathfrak{t} on the lower chain.

Consider a 4-PPT \mathcal{P} in $m(G_{k,m})$. W.l.o.g. we assume t is the i -th vertex on the lower chain and we want to move it to any other point on this chain. According to note 8 there exists a sequence of flips of upper triangle edges that results in a 4-PPT \mathcal{P}' that includes a 4-gon with the corners p , t and r . A part \mathcal{P}' is a 4-PPT \mathcal{P}' of a single chain set with $k+3$ points. According to Theorem 4.3 the flip graph of all 4-PPTs of a single chain set is connected. Hence, \mathcal{P}' can be transformed in a way that the corner t of the triangle \mathfrak{t} gets its designated place. \square

Finally, we can conclude that the flip graph of the muffin set $M_{k,m}$ is connected $\forall k, m \in \mathbb{N}$. \square

4.5.1 Counting 4-PPTs of $M_{1,m}$

As we have already counted the number of 4-PPTs of the single chain we shall now describe an approach to obtain the number of 4-PPTs of $M_{1,m}$. A nice property of the set $M_{1,m}$ is that any 4-PPT of this set has only one 4-gon, all other faces are triangles. Let G be the flip graph of $M_{1,m}$, \mathcal{P} a 4-PPT in $r(G)$ and \mathfrak{q} the single 4-gon. In \mathcal{P} the 4-gon separates the 4-PPT of $M_{1,m}$ into either two convex polygons (Figure 4.26 (a)) or in only one case into one convex polygon Figure 4.26 (b)), if \mathfrak{q} is incident to the corner s of the muffin.

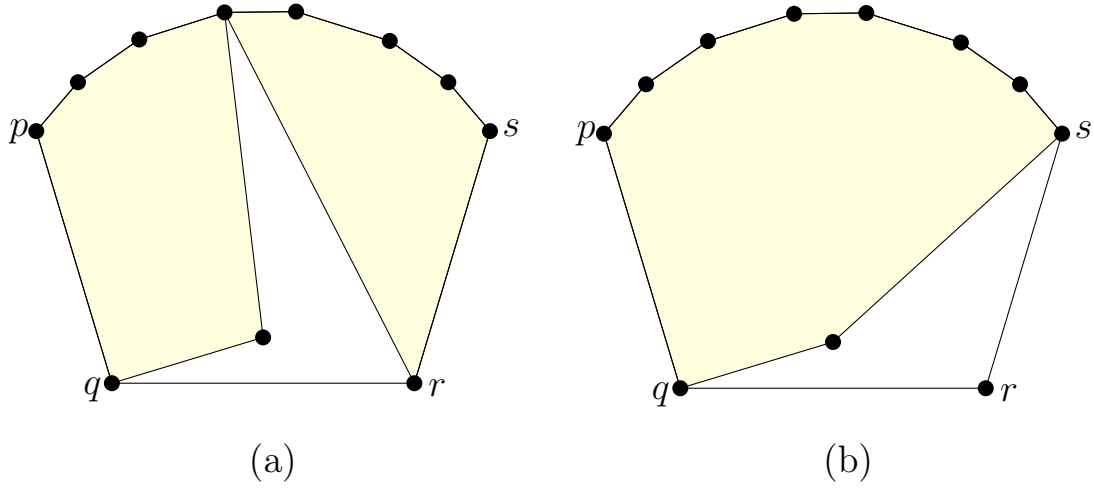


Figure 4.26: The single 4-gon divides the 4-PPT either in one or two convex polygons.

The number of triangulations of a convex polygon with n point is the *Catalan Number* C_{n-2} [25] where the n -th Catalan Number is defined by

$$C_n = \frac{1}{n+1} \binom{2n}{n}, \quad n \geq 0.$$

Let $N_r(M_{1,m})$ and $N_l(M_{1,m})$ be the number of 4-PPTs in $r(G)$ and $l(G)$, respectively. There are $m+2$ possibilities for 4-gon \mathfrak{q} in a 4-PPT in $r(G)$. Counting the number of triangulations of the resulting polygons leads to

$$N_r(M_{1,m}) = \sum_{j=0}^{m+1} C_j \cdot C_{m+2-j} = \sum_{j=0}^{m+2} C_j \cdot C_{m+2-j} - C_{m+2}C_0 = C_{m+3} - C_{m+2}$$

Because of the symmetry, we can obtain $N_l(M_{1,m})$ in exactly the same way.

$$N_l(M_{1,m}) = N_r(M_{1,m}) = C_{m+3} - C_{m+2}$$

Let now $N_{mid}(M_{1,m})$ be the number of 4-PPTs in $m(G)$. As mentioned above,

\mathfrak{q} splits a 4-PPT in $m(G)$ into one or two convex polygons. Due to the possible positions of \mathfrak{q} we derive

$$N_{mid}(M_{1,m}) = \sum_{j=0}^{m+1} C_j \cdot C_{m+1-j} = C_{m+2}$$

All together, the total number $N(M_{1,m})$ of 4-PPTs of the set $M_{1,m}$ is

$$N(M_{1,m}) = 2C_{m+3} - C_{m+2} \approx 4^{m+2} \left(\frac{8}{(m+4)\sqrt{\pi(m+3)}} - \frac{1}{(m+3)\sqrt{\pi(m+2)}} \right)$$

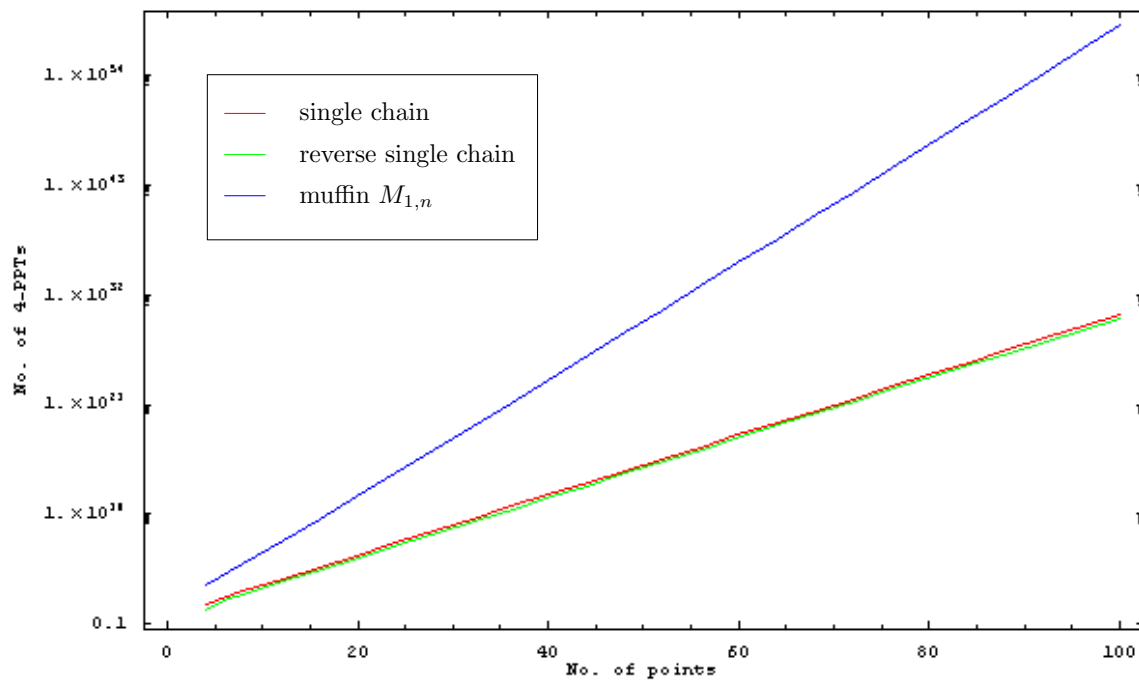


Figure 4.27: The rapidly increasing number of 4-PPTs of three special point sets.

5 A Dual Approach

5.1 Introduction and Definitions

In Chapter 4 we have shown that the flip graph of all 4-PPTs is connected for some special sets. Although it is already proven that the flip graph of all abstract 4-PPTs of any set of points S with $|CH(S)| = 3$ is connected, it is not yet proven that this holds for geometric 4-PPTs as well. This chapter introduces a method for investigating flip sequences in 4-PPTs, especially for moving a triangle along a special path. Therefore the so-called dual graph of a pseudo-triangulation will be introduced (Section 5.1). In terms of the dual graphs a closer look on edge flips will be taken. They will be classified and their effects on the dual graph is studied. Section 5.2 deals with a graphical user interface that allows to perform edge flips in pseudo-triangulations. This software was the outcome of a bachelor project by W. Reisner [31]. A closer look is taken on moving triangles along special alternating dual paths and the flip software was then extended by the implementation of this dual approach (Section 5.3). Finally, experiments with the flip software on different point sets lead to some interesting results, which are discussed in Section 5.3.3.

5.1.1 The Dual Graph

In this section we define the dual graph of a 4-PPT \mathcal{P} of a set S of n points in general position, i.e., we do not allow any three points to be collinear. Let k be the number of points on the convex hull of S . According to Theorem 2.2, \mathcal{P} consists of $(k - 2)$ triangles and $(n - k)$ pseudo-4-gons. Every 4-PPT can be transformed into a triangulation $\mathcal{T}(\mathcal{P})$ by inserting one edge into each pseudo-triangle, connecting the reflex point with its opposite corner. These new edges divide each pseudo-4-gon into two triangles.

Let V be a set of vertices and E a set of edges. We define the *dual graph* $G_{\mathcal{P}}(V, E)$ to be a simple plane graph which has one vertex for each face in $\mathcal{T}(\mathcal{P})$. The outer face of the triangulation can be treated as additional vertex in $G_{\mathcal{P}}$, but in the scope

of this thesis, we consider only vertices corresponding to triangles in $\mathcal{T}(\mathcal{P})$. We will show below in Proposition 5.1 that the number of vertices in the dual graph is $2n - k - 2$. Let $\{t_1, t_2, \dots, t_{2n-k-2}\}$ be the triangles in $\mathcal{T}(\mathcal{P})$ and $v(t_i) \in V$ the vertex in the dual graph that corresponds to the triangle t_i . $G_{\mathcal{P}}(V, E)$ has an edge between two vertices $v(t_i), v(t_j)$ if the corresponding faces t_i, t_j share a common edge in $\mathcal{T}(\mathcal{P})$.

Proposition 5.1 (Properties of the Dual Graph). *Let $G_{\mathcal{P}}(V, E)$ be the dual graph of a 4-PPT \mathcal{P} of a point set S with n points, k of them on the convex hull. The dual graph has the following properties:*

- $G_{\mathcal{P}}(V, E)$ is a connected graph.
- $|V| = 2n - k - 2$
- $|E| = 3n - 2k - 3$
- $G_{\mathcal{P}}(V, E)$ is an at most 3-regular graph.

Proof. Let $d(v)$ be the vertex degree of a vertex v , i.e., the number of edges that have one end point in v . Since a triangulation of a point set is a connected graph and each triangle in such a triangulation has as least one neighbored face, each corresponding vertex $v \in V$ in the dual graph has a vertex degree $d(v) \geq 1$.

As mentioned above a 4-PPT of a point set consists out of $(k-2)$ triangles and $(n-k)$ pseudo-4-gons. Each pseudo-4-gon corresponds to two triangles in the underlying triangulation, hence the number of vertices in the dual graph is $|V| = (k-2) + 2(n-k) = 2n - k - 2$. To count the edges of the dual graph, let h be the number of triangles in \mathcal{P} that are incident to two convex hull edges. The vertices of $G_{\mathcal{P}}$ that correspond to those triangles are incident to one edge. All other $(k-h)$ triangles that are incident to the convex hull correspond to vertices, whose vertex degree equals two. All remaining triangles contribute each the value of three to the sum s of all vertex degrees. Hence,

$$s = \sum_{v \in V} d(v) = h + 2(k-2h) + 3((2n-k-2) - (k-2h) - h) = 6n - 4k - 6$$

Using the Handshake-Lemma, which states that in every graph the sum of all vertex degrees equals two times the number of edges, leads to $|E| = 3n - 2k - 3$.

Let now $\{v_1, \dots, v_{k-h}\}$ be the vertices of the dual graph that corresponds to triangles

incident to the convex hull. These vertices have a vertex degree $1 \leq d(v_i) \leq 2$ for $1 \leq i \leq k - h$, for $i > k - h$ the vertex degree is $d(v_i) = 3$. One can say that for *large* point sets with *few* points on the convex hull the corresponding dual graph is almost 3-regular. \square

Taking a closer look at the edges of $G_{\mathcal{P}}$, we can divide them into two classes. On the one hand, there are edges that correspond to edges that exists in $\mathcal{T}(\mathcal{P})$ as well as in the original 4-PPT \mathcal{P} . On the other hand, $G_{\mathcal{P}}$ has also some edges that correspond to edges that only exists in $\mathcal{T}(\mathcal{P})$, because they were inserted to split a pseudo-4-gon into two triangles. We call the latter *auxiliary edge* and represent them in the following figures with dotted green lines in the pseudo-triangulation and as green edges in the dual graph. See Figure 5.1 for an example of a 4-PPT with $n = 11$ points, four of them on the convex hull and its corresponding dual graph. Note that a vertex of the dual graph which corresponds to one half of a pseudo-4-gon in \mathcal{P} that is not incident to the outer face, is always incident to two edges and one auxiliary edge.

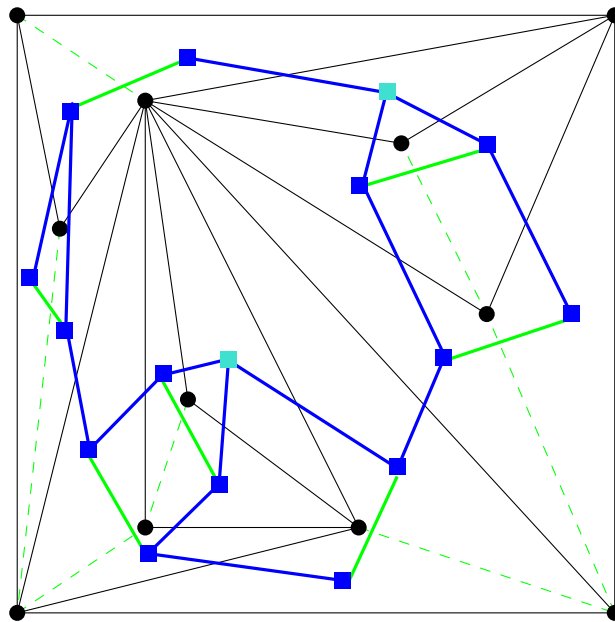


Figure 5.1: A 4-PPT of a set of $n = 11$ points and its corresponding dual graph.

Proposition 5.2. *Let $G(V, E)$ be the dual graph of a 4-PPT \mathcal{P} of a point set S with n points and $|CH(S)| = 3$. $E_a \subset E$ is the set of all auxiliary edges of $G_{\mathcal{P}}(V, E)$.*

The graph $G(V, E \setminus E_a)$ is a tree with one root vertex (corresponding to the one triangle in \mathcal{P}) and three branches.

Proof. The vertex that represents the single triangle in the dual graph is incident to three edges, we let this vertex be the root of the tree. Let $\{v_1, v_2, v_3\}$ be the vertices of the dual graph that correspond to triangles incident to the convex hull. All these vertices v_i with $1 \leq i \leq 3$ have a vertex degree of $d(v_i) = 2$. Since we have only one triangle in the 4-PPT, those dual vertices correspond to half pseudo-4-gons and are adjacent to one auxiliary edge. Removing these auxiliary edges leads to $d(v_i) = 1$ for $1 \leq i \leq 3$. These vertices form the three leaves of the tree. All other vertices are adjacent to three edges, one of them an auxiliary edge. Removing the auxiliary edges remains a vertex degree of two. Therefore, the remaining dual graph is a tree. \square

The dual graph also helps to visualize the three colorability (Theorem 3.1) of 4-PPTs by drawing the dual graph into the 4-PPT in a way such that all points of the point set lie in their corresponding faces in the dual graph. The tree of dual edges omitting the auxiliary edges separates the primal graph into areas, such that all primal vertices lying in the same area can be colored with the same color to obtain a 3-coloring according to the idea of Theorem 3.1 (see Figure 5.2).

In order to identify the effects of an edge flip in \mathcal{P} on its dual graph we introduce a labeling of the faces and vertices of \mathcal{P} , i.e., the vertices in $G_{\mathcal{P}}$. Therefore, we will enumerate the points of our underlying point set S and assign each face a unique letter. In the dual graph every vertex corresponds to a triangle in $\mathcal{T}(\mathcal{P})$. We assign to every vertex of the dual graph a corresponding letter and a 3-dimensional index vector (i, j, k) where i, j and k are the vertices of the corresponding triangle in $\mathcal{T}(\mathcal{P})$ starting with the smallest index i , followed by j, k , in counterclockwise order (Figure 5.3).

5.1.2 Definition and Classification of Flip Operations

To transform one pseudo-triangulation into another, we will use edge flipping. The different types of edge flips were already described in Section 2.3. Considering a 4-PPT \mathcal{P} of a point set S , the deletion flip as well as the insertion flip would no longer result in an 4-PPT. Hence we allow only diagonal flips. To reduce the number of possible flips we take an additional restriction into account: only edges incident to a triangle are allowed to be flipped. Taking a closer look at such a diagonal flip of

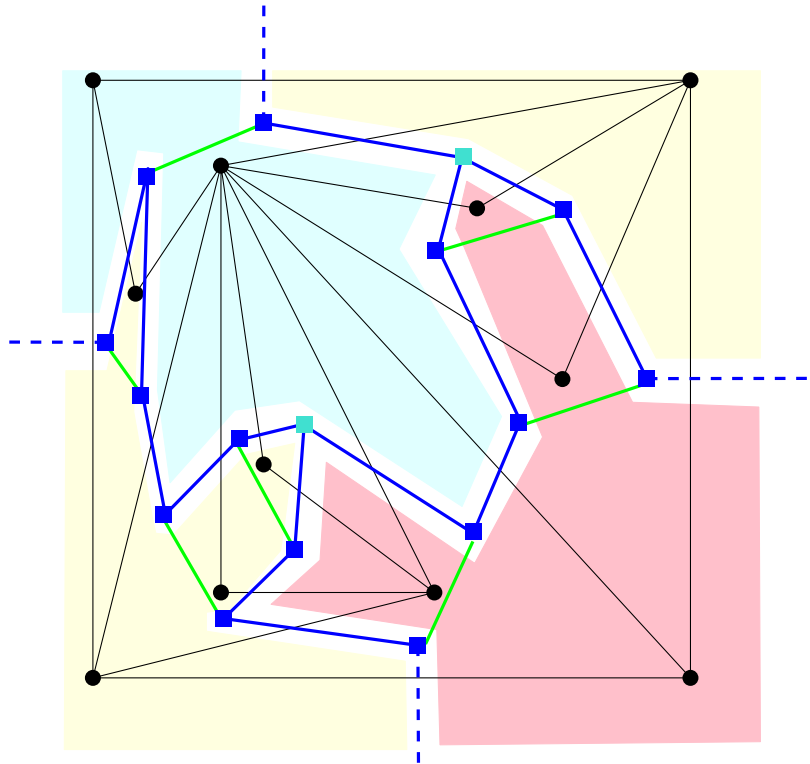


Figure 5.2: Coloring a 4-PPT of a set of $n = 11$ points with the help of the dual graph.

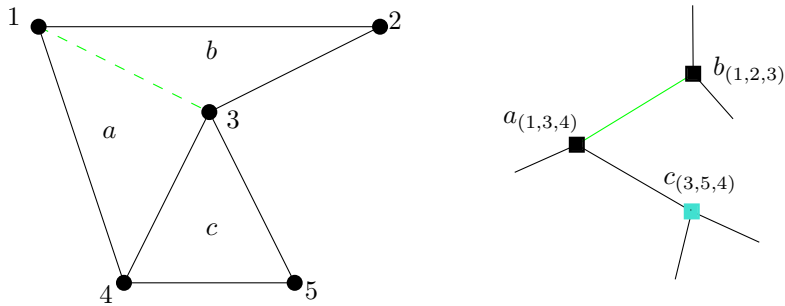


Figure 5.3: Labeling a 4-PPT and the corresponding dual graph.

an edge incident to a triangle, one can classify four types of these flips. We will see that each type has different effects on the dual graph of the 4-PPT. In the following let \mathfrak{q} and \mathfrak{t} be the pseudo-4-gon and the triangle, respectively, that are affected by the flip.

Type Ia

The first two types (Ia and Ib) are so-called *edge sliding flips*, because the removed edge e and the new edge e' share a common point. In Type Ia two edges of the triangle \mathbf{t} are incident to the pseudo-4-gon \mathbf{q} . Flipping one of those edges slides it to the point of \mathbf{q} which was not incident to a triangle edge so far and changes the position of the triangle in the 4-PPT and in the corresponding dual graph. However, it does not change the indices of the effected vertices in the dual graph (Figure 5.4).

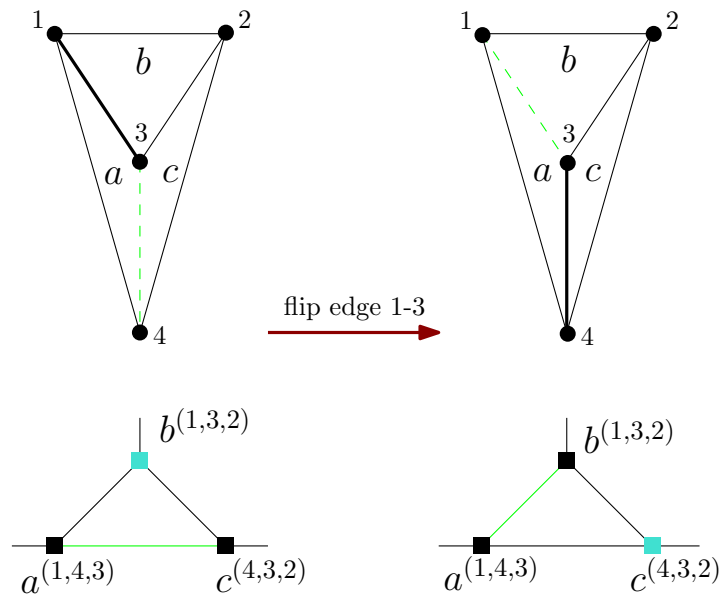


Figure 5.4: Flip type Ia: The corresponding dual graph is shown below the 4-PPT.

Type Ib

In this case the triangle is adjacent to only one edge of the side-chain of \mathbf{q} . The corner of the triangle which is not incident to \mathbf{q} lies inside the angle spanned by the reflex point of \mathbf{q} , its opposite corner and the corner which is not incident to the triangle. The flip of the common edge of \mathbf{t} and \mathbf{q} is again an edge slide to the corner of \mathbf{q} which was not incident to \mathbf{t} and does not change any index in the dual graph.

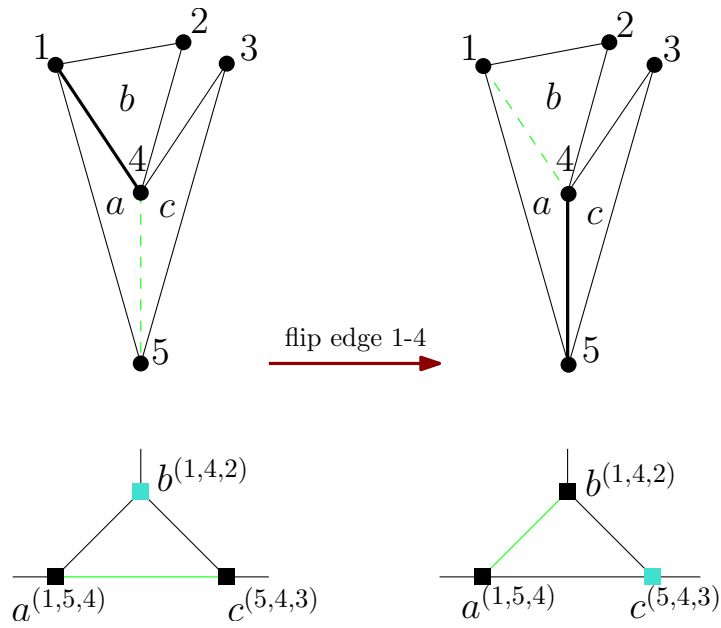


Figure 5.5: Flip type Ib.

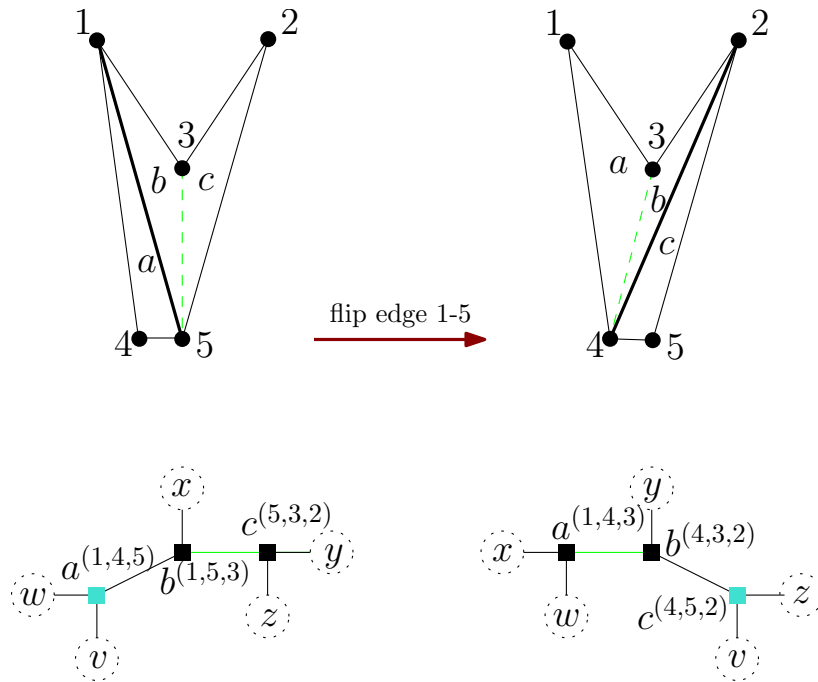


Figure 5.6: Flip type II, the dotted circles represent other components of the graph that gets reallocated.

Type II

Flips of type II and III are called *crossing flips* because the removed edge $e \in \mathcal{P}$ and the new inserted edge $e' \notin \mathcal{P}$ would intersect each other, if they would exist in the same pseudo-triangulation. The edges e and e' do not share a common point.

Type II occurs when the triangle is incident to one edge (but not a pseudo edge) of \mathfrak{q} and its third corner lies in the angle which is spanned by the reflex point of \mathfrak{q} , its corner which is not incident to the triangle and the corner opposite to the reflex point. Flipping the common edge of \mathfrak{q} and \mathfrak{t} means removing it and inserting the diagonal between the corner of the triangle not incident to \mathfrak{q} and the corner of \mathfrak{q} , not incident to the triangle. Note that the indices of all three affected vertices in the dual graph change.

In all three flip types mentioned above, there is a path of length two in the dual graph. This path leads from the vertex where the triangle is before the flip (a in Figure 5.4, 5.5 and 5.6) via an auxiliary edge to the vertex where the triangle is after flipping (c in Figure 5.4, 5.5 and 5.6). These flips can be seen as moving the triangle in the dual graph along this short path. This approach can be very helpful for determining flip directions and will be discussed in greater detail in Section 5.3.

Type III

Flip type III is again a crossing flip. The triangle is adjacent to either one normal edge or one edge of the side-chain of \mathfrak{q} . Its third point lies either in the angle spanned by the reflex point of \mathfrak{q} , its opposite corner and the corner of \mathfrak{q} which is incident to \mathfrak{t} or in the angle spanned by the corner of \mathfrak{q} which is incident to \mathfrak{t} , the reflex point of \mathfrak{q} and its opposite corner. This flip deletes the common edge of \mathfrak{t} and \mathfrak{q} and we connect the point of the triangle which was not incident to \mathfrak{q} and the corner of \mathfrak{q} which was not incident to the triangle with a new edge. If this insertion is not possible without intersecting other edges, we insert the edge such that it becomes part of the geodesic path between the two mentioned points.

Unfortunately, this flip type does not follow the observations from above about moving the triangle along a path of length two ending with an auxiliary edge, so the triangle does not change its position in the dual graph; however the indices of both vertices affected by the flip change.

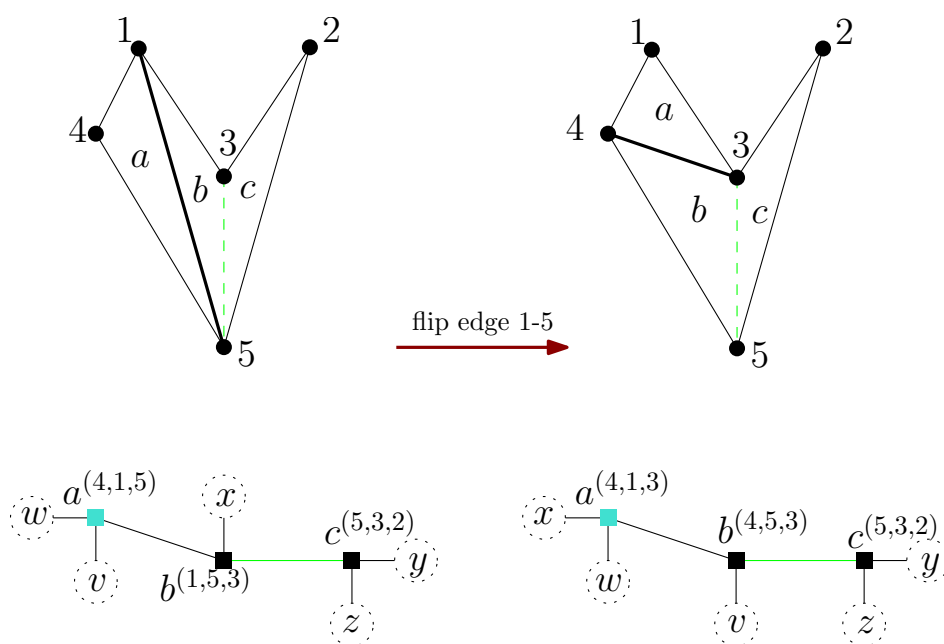


Figure 5.7: Flip type III.

5.2 Implementation of the Dual Graph

In his bachelor project, W. Reisner [31] implemented a software tool to visualize 4-PPTs of point sets and flips in such 4-PPTs.

This tool motivates the conjecture that the triangle in a 4-PPT of a point set S with $|CH(S)| = 3$ can be moved by flipping to any three points whose convex hull do not contain any other point. The idea of moving the triangle in a 4-PPT will be explained in the next section. The implementational preliminary work was to include the dual graph into the software tool.

Therefore we assigned two dual points to each pseudo-4-gon and one dual point to each triangle. The dual points are displayed in the balance point of each half pseudo-4-gon. Each dual point has pointers to its neighbors and is able to differ if a neighbor lies in the same pseudo-4-gon or in a different one. The original tool built up a starting 4-PPT of a point set using the *Super-Easy-Construction* and inserting the inner points sorted by the angles of their polar coordinates. For the implementation of the dual graph, it was necessary to order the inner points of the point set by their x-coordinates and then insert them following the *Super-Easy-Construction*. In the following we shall mark a pseudo-triangulation that was constructed this way with the index X, i.e., \mathcal{P}_X .

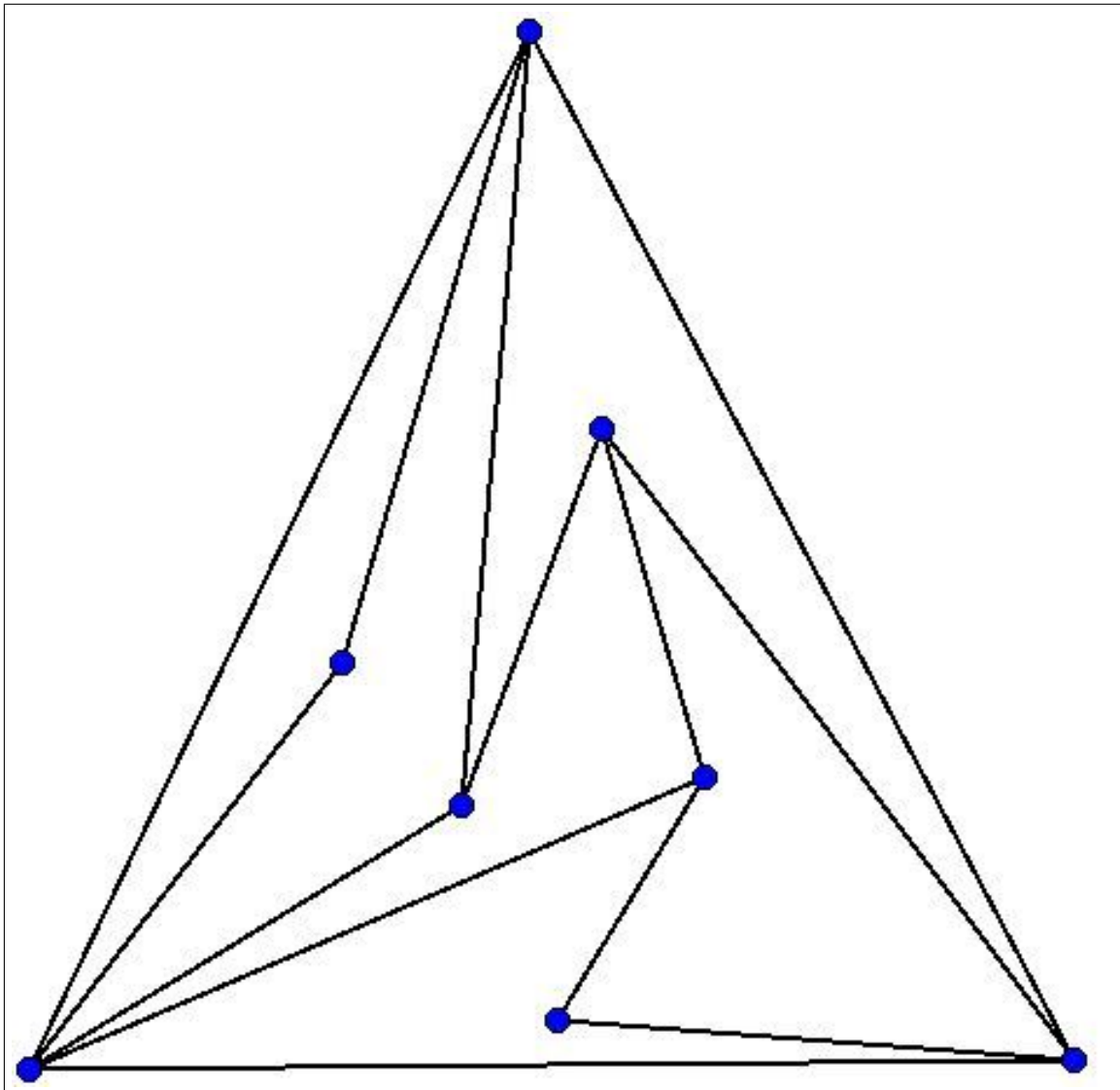


Figure 5.8: The graphical output of Reisner's flip GUI for pointed pseudo-triangulations.

The idea of moving the triangle along so-called alternating paths in the dual graph, described in the next section, was then implemented as well. The extension of the flip software helped to understand the dual graph of special pointed pseudo-triangulations and these results will be discussed later.

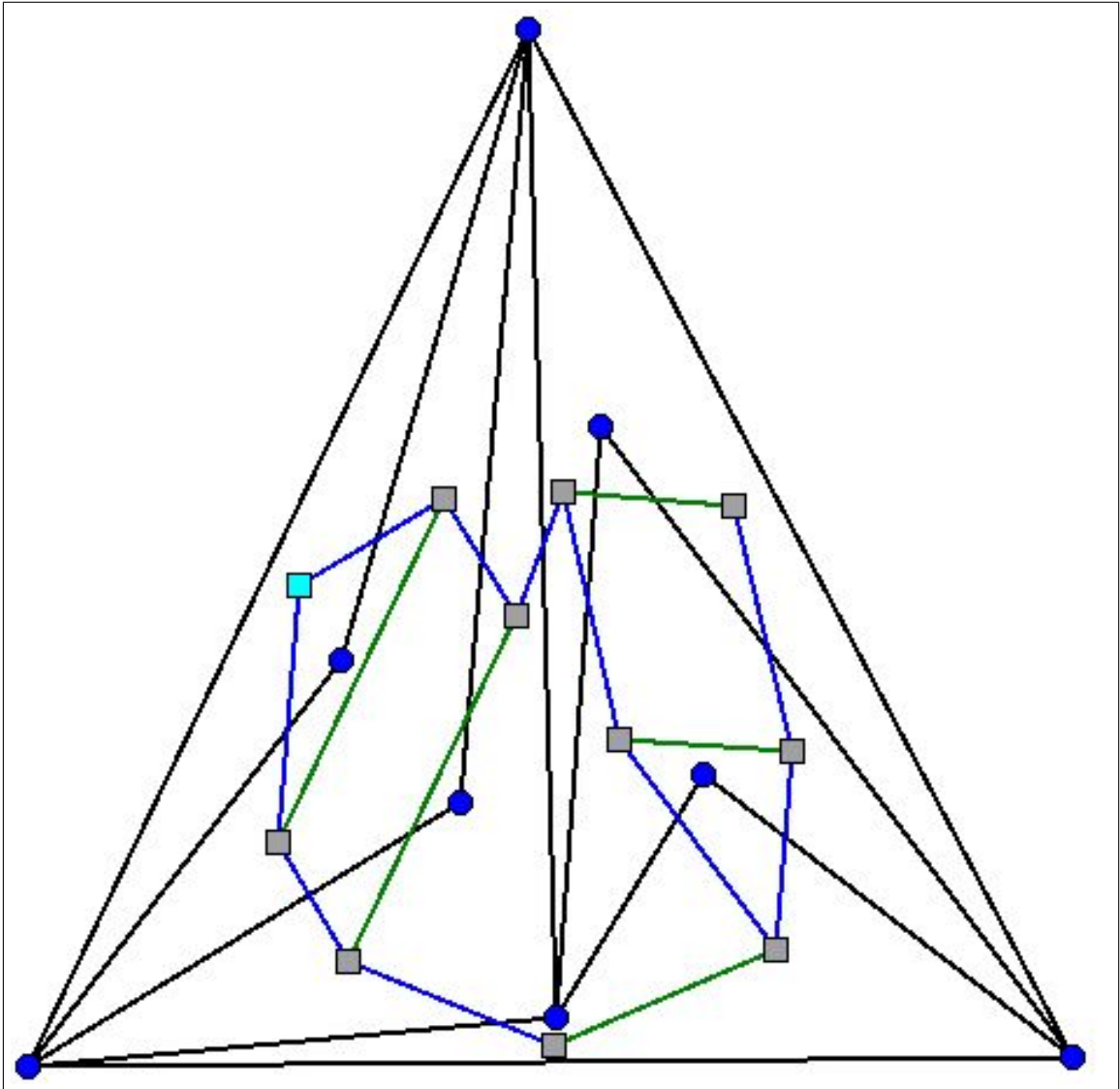


Figure 5.9: The graphical output of the dual extension of Reisner's flip software.

5.3 Moving the Triangle in 4-PPTs

For simplicity we shall deal in this section with point sets in general position and with only three points on the convex hull. This means we have only one triangle in any 4-PPT of such a set, i.e., the maximum number of possible flips in a given 4-PPT is three and there are only two flips possible when one of the triangle edges is part of the convex hull. In this section, the dual extension of the flip software [31] will be described and the results of testing the implemented algorithms on different point sets will be discussed.

5.3.1 Moving the Triangle along Alternating Paths

Consider a set of n points in the plane, a 4-PPT \mathcal{P} of this set and its dual graph $G_{\mathcal{P}}(V, E)$. As shown in Section 5.1.2, every edge flip also changes the dual graph and in three out of four cases, the triangle moves to a different place in the 4-PPT, i.e., to a different vertex in the dual graph. Now the following question arises: Is it possible to find a flip sequence such that we can move the triangle to any vertex of $G_{\mathcal{P}}$ that is not corresponding to the triangle in \mathcal{P} ? To move the triangle to a specific place in the 4-PPT, experiments have shown that it is helpful to follow paths in the dual graph. Therefore we introduce so-called alternating paths. An *alternating path* is a sequence of an even number of consecutive edges $e_i \in E$, $i = 1 \dots m$ where e_i is an auxiliary edge $\forall i$ with $i \equiv 0 \pmod{2}$. Let t be the unique triangle in \mathcal{P} , i.e., t is also a vertex in $G_{\mathcal{P}}$. Using the extended version of the flip tool [31] leads to the assumption that for all vertices $v \neq t$ in $G_{\mathcal{P}}$, there is a dual path starting in t and ending with an auxiliary edge in v . Unfortunately, this is not generally the case, but we can show that for 4-PPTs produced by the x-sorted version of the Super-Easy-Construction, we can find such alternating dual paths except for one special point configuration. We shall now explain this special case and prove that it is the only one. Therefore we take a closer look at the super easy construction, i.e., how the dual graph changes while inserting new inner points. As described in Chapter 3.2, we can either insert a point into the triangle or into a pseudo-4-gon. Depending on the area of the pseudo-4-gon where a point is inserted, we have to differentiate between three cases. The insertion of a new point is a very local operation, hence the changes on the dual graph are very local.

Let \mathcal{P} be a pseudo-triangulation of a set S of ≥ 3 points in the plane with $|CH| = 3$, t the triangle and q a pseudo-4-gon in \mathcal{P} . Further, $G(\mathcal{P})$ is the dual graph of this pseudo-triangulation. Figure 3.3 in Chapter 3.2 shows the three possible areas for inserting a new point.

Proposition 5.3. *Inserting a point into the triangle or into area 2 or 3 of a pseudo-4-gon (Figure 3.3) maintains all alternating dual paths that start in t and have previously existed.*

Proof. In the first case, we insert the new point into the triangle, connect it with two of its three corners and result in the 4-PPT \mathcal{P}' . The new dual graph $G_{\mathcal{P}'}$ has two new vertices adjacent to the vertex that corresponds to the new triangle t' and adjacent to the two vertices that were neighbors of t in $G_{\mathcal{P}}$ (see Figure 5.10). It is

easy to see that in this case, all alternating paths that existed in $G_{\mathcal{P}}$ and started in t were extended by the two new vertices. Additionally, there are two new alternating paths of length two reaching the two new dual vertices.

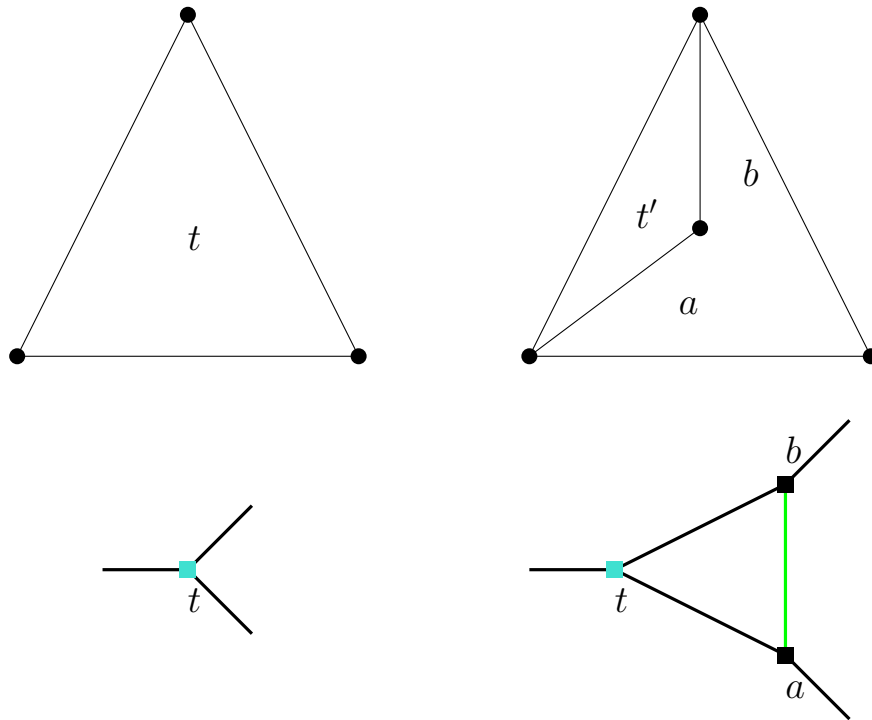


Figure 5.10: Inserting the new point inside the triangle maintains all alternating paths in the dual graph.

Inserting a point in area 2 or 3 of a pseudo-4-gon has the same (symmetric) effect on the dual graph. W.l.o.g. we consider now the case of inserting the point into area 3. Before the insertion of the point, we have four alternating paths segments (h, b, a, e) , (h, b, a, f) , (g, b, a, e) and (g, b, a, f) using the vertices a and b . Every alternating path that involves the vertices a and b includes one of this sequences. W.l.o.g. let the vertex sequence (e, a, b, h) be part of an alternating path in $G_{\mathcal{P}}$ between t and a vertex $v \in G_{\mathcal{P}}$. Inserting the new point into the half pseudo-4-gon b creates two new vertices c, d in the dual graph $G_{\mathcal{P}'}$. The sequence (e, a, b, h) in $G_{\mathcal{P}}$ can now be extended to (e, a, b, d, c, h) and is again part of an alternating path between t and v in $G_{\mathcal{P}}$. Equivalently, inserting the new point into the half pseudo-4-gon a (area 2) leads to the same result. In both cases, the two new faces c and d can also be reached by a dual path in $G_{\mathcal{P}'}$, if b has been reached in $G_{\mathcal{P}}$. \square

Inserting a point in area 1 of a pseudo-4-gon might not necessarily maintain all

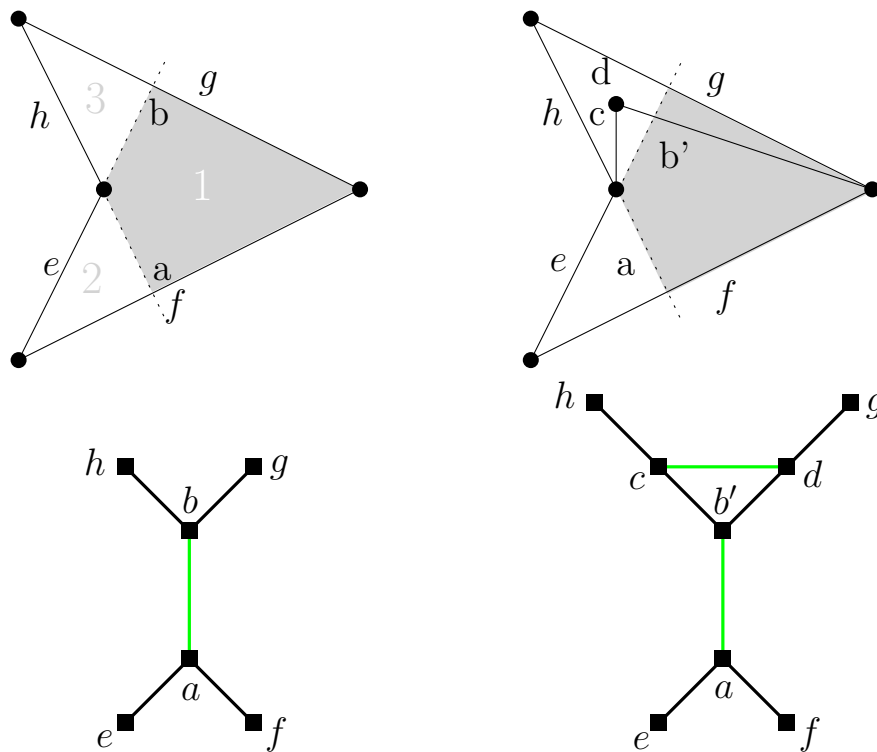


Figure 5.11: One possibility to insert the new point into a pseudo-4-gon.

alternating dual paths. Consider therefore the situation in Figure 5.12. For example, an alternating dual path in $G_{\mathcal{P}}$, starting with the triangle t and ending in a dual vertex v using the sequence (h, b, a, f) no longer exists in $G_{\mathcal{P}'}$. If there is no other alternating path in $G_{\mathcal{P}}$ that is avoiding the mentioned sequence, the vertex v cannot be reached via an alternating path.

If we construct a 4-PPT with the x-sorted version of super easy construction, the triangle will be incident to the leftmost points of the convex hull. During the construction the insertion of a new point into a triangle or area 2 or 3 of a pseudo-4-gon guarantees that in the current dual graph each vertex can be reached by an alternating path starting with the triangle. Only the insertion of a point in area 1 can cause difficulties. The application of the flip software showed that pseudo-triangulation in which not all vertices of the dual graph can be reached by alternating paths have a common structure. We now introduce two geometric gadgets and show that their combined appearance creates a class of 4-PPTs in which not all dual vertices can be reached by alternating paths.

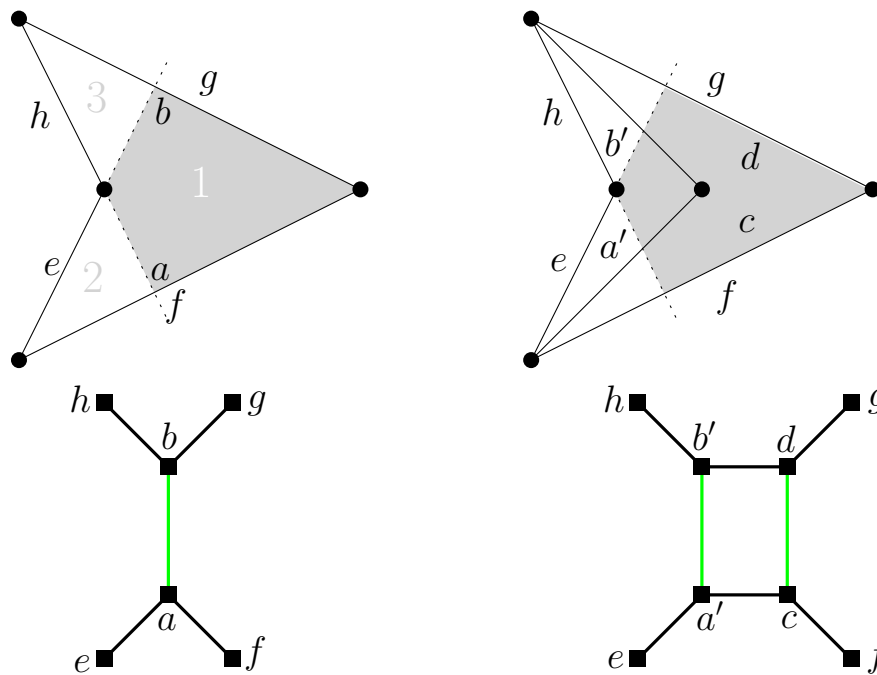


Figure 5.12: Inserting a point into area 1 of a pseudo-4-gon.

5.3.2 Implementation of the Alternating Path Idea and Experimental Results

Reisinger's flip software was not only extended by the dual graph, but also by an automatic flip algorithm. The aim was to test if it is possible to flip the triangle, i.e., the corresponding dual vertex, to any other (already existing) dual vertex in the graph. This leads to two points of interest: if it is possible, can we formulate an algorithm that always delivers a sequence of flips to reach the goal, or if it is not possible, what are the critical situations, counter examples where it does not work? The general idea of an automatic flip algorithm is to choose a target vertex in the dual graph and perform the necessary flips along alternating dual paths to move the triangle to the target. The following algorithm describes this idea. The function $flip(path)$ flips the edge incident to the triangle and the first half pseudo-4-gon in the list of the vertices of path whereas $findAlternatingPath(triangle, target)$ tries, if possible, to avoid that the first flip is of type 3, since this type would not move the triangle along the aimed path. The path search is an adapted version of the depth-first search in graphs. In each step two vertices (corresponding to the two halves of the same pseudo-triangle) are added. If no vertex can be added and the target

Algorithm 2 flipalg(target)

Require: *triangle***Ensure:** *target* \neq *triangle*

```
while triangle  $\neq$  target do  
  path = findAlternatingPath(triangle, target)  
  triangle = flip(path)  
end while
```

was not reached yet, the algorithm tracks back to the last branch and continues the search.

As mentioned in Chapter 5.1.1, the different flip types have different effects on the dual graph. Flips of type 1 and 2 can be interpreted as moving the triangle along an alternating dual path, whereas flips of type 3 do not behave this way. To avoid circling of the algorithm, an edge that was produced by a flip of type 3 gets a special mark. Such marked edges are not allowed to be flipped anymore, unless the mark is removed. If one of the two adjacent halves of pseudo-triangles changes, i.e., at least one of their vertices changes, the edge gets unmarked and is allowed to be flipped again. On the one hand, this avoids flipping the same edge continuously, but on the other hand, the marking can decrease the number of flipable edges strongly. Unfortunately, this leads to situations where the algorithm stopped before the triangle has reached the target. Two ideas were then implemented for first tests, either to choose the shortest alternating path, or the longest. Both concepts were tested on different sets and lead to interesting results. A short overview on some representative results shall be given here. The point set in Figure 5.13 is an example where both algorithms are needed to move the triangle to all dual vertices, always starting with the pseudo-triangulation produced by the x-sorted version of the Super-Easy-Construction. The triangle can be moved to vertex *a* in Figure 5.13 always following the shortest alternating dual path, whereas vertex *b* requires that in each step, the first flip of the longest alternating dual path is done. Following the shortest paths would stop before the target is reached.

An interesting effect was that for some point sets, both algorithms would stop before the target was reached, because there was no flipable edge left. Nevertheless in any of these situations it was possible to solve it by hand, i.e., flipping a marked edge and in some cases ignoring the rule to avoid a Type III flip, if possible. Of course this does not prove anything yet, but it encourages the assumption that the flip graph of 4-PPTs is connected for all point sets in the plane.

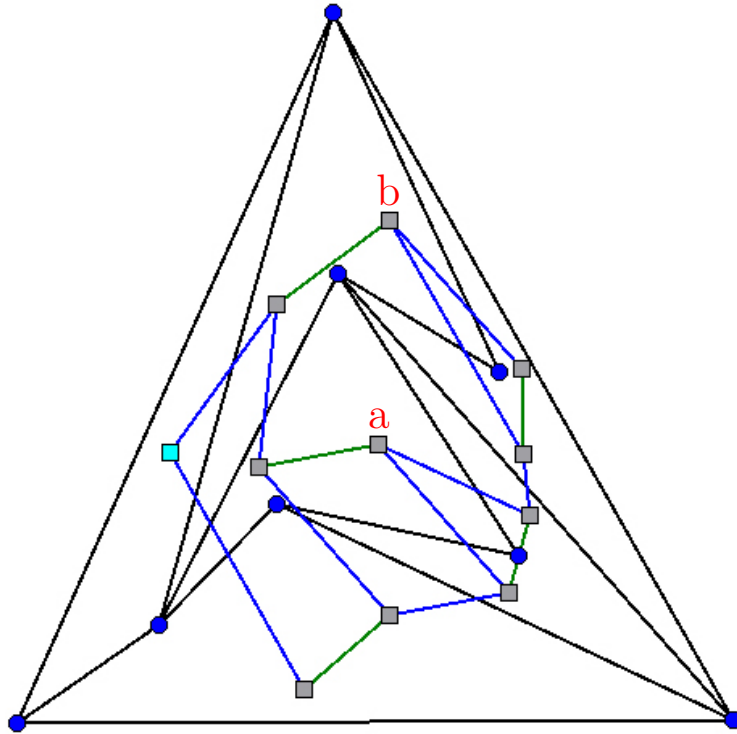


Figure 5.13: A set that claims two different algorithms for moving the triangle.

Another important point is that the mentioned flipping algorithms were always started in a canonical 4-PPT $\mathcal{P}_\mathcal{X}$, i.e., the 4-PPT that results by applying the x-sorted version of the super easy construction. Unfortunately, sets exist where not all vertices of the dual graph of the 4-PPT $\mathcal{P}_\mathcal{X}$ of this set can be reached by alternating dual paths in the first place. The 4-PPTs in this case showed a similar structure. This structure inspired the idea of special geometric gadgets that can be crossed by alternating dual paths in limited ways. A detailed description of these gadgets will be given in the next chapter.

5.3.3 Describing Special Geometric Gadgets

The geometric gadgets we want to introduce, are 4-PPTs of a special pointgon, a four sided pseudo-triangle with inner points. These gadgets might be part of a 4-PPT of a point set and since we are interested in the system of alternating dual paths, we shall study the possibilities to cross such a gadget following the alternating dual path idea [22]. Figure 5.14 shows the hull of such a gadget and a scheme of the six possibilities to cross the gadget with alternating dual paths. Depending on the

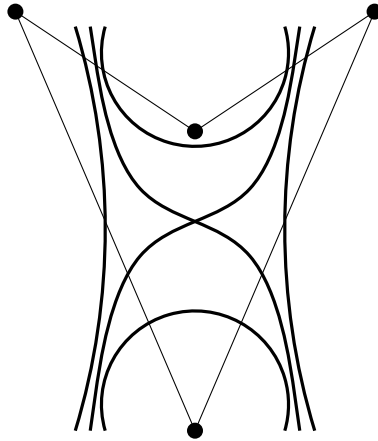


Figure 5.14: Scheme for alternating dual paths that cross the gadget.

4-PPT inside this gadget not all of these options might exist. Two gadgets with only four possible ways to cross are described in the following paragraphs. Remember

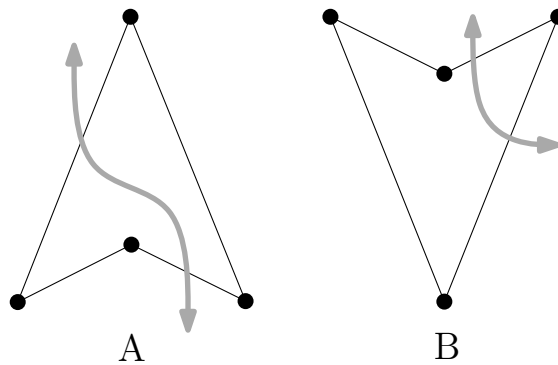


Figure 5.15: Two special gadgets in which, after entering the gadget, the exit is given.

that we deal here with parts of 4-PPTs of a point set in the plane, which has exactly three points on the convex hull. To simplify matters, we consider embeddings of those 4-PPTs where the longest edge of the convex hull lies parallel to the x -axes.

Let gadget A be a four sided pseudo-triangle with a 4-PPT of n_A inner points, such that in its dual graph, entering the gadget in one edge forces us to leave it in the diagonal edge on the side-chain and vice versa (see Figure 5.15 left). The second one, gadget B, is a 4-pseudo-triangle with a 4-PPT of n_B inner points, such that in its dual graph, entering the gadget in one edge forces us to leave it in the opposite edge on the side-chain and vice versa (see Figure 5.15 right). An example

for gadget A would be any 4-pseudo-triangle in which an even number of vertices has been inserted in area one, as an odd number would be an example for gadget B (Figure 5.16).

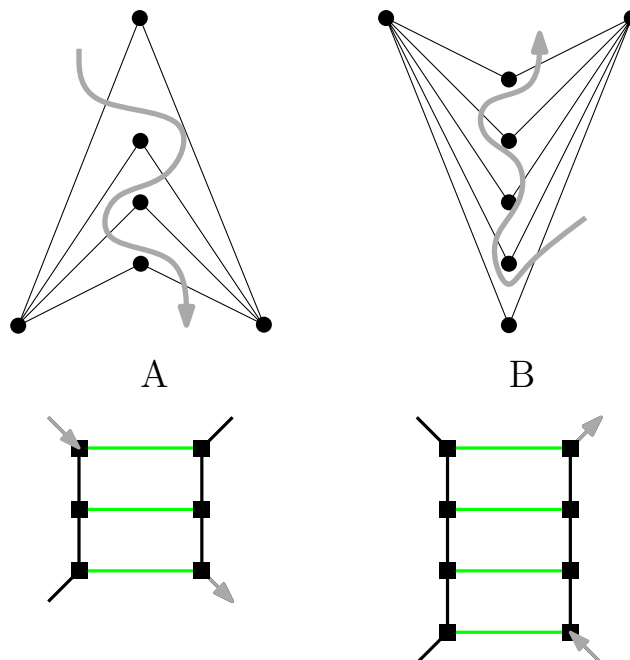


Figure 5.16: Examples for gadget A and gadget B

We define a gadget C as the biggest pointgon that has a 4-pseudo-triangle as its hull and that can be separated into two smaller gadgets C_1 and C_2 such that the reflex point of the hull of gadget C_1 coincides with the corner of the hull of gadget C_2 that comes in clockwise order after the reflex point of C_1 (p_4 in Figure 5.17). The same holds for the reflex point of the hull of gadget C_2 and the corresponding corner of gadget C_1 (p_2 in Figure 5.17). Furthermore, the corner of the hull of gadget C_2 that is opposite its reflex coincides with the second corner of gadget C_1 that is adjacent to the reflex of gadget C_1 (p_5 in Figure 5.17). Now we will see that for gadget $C_1 = A$ and gadget $C_2 = B$ not all points in a 4-PPT might be reached by a dual path. These gadgets can bring up a situation in a 4-PPT \mathcal{P}_χ where no alternating dual paths exist from the dual vertex that corresponds to the triangle to all other vertices when we additionally have the restriction that it is not possible to enter the gadget via the edges p_3p_5 and p_3p_5 . This is, of course, the case if these edges are part of the convex hull. The following proposition shows that this will be the only case where this gadget exists.

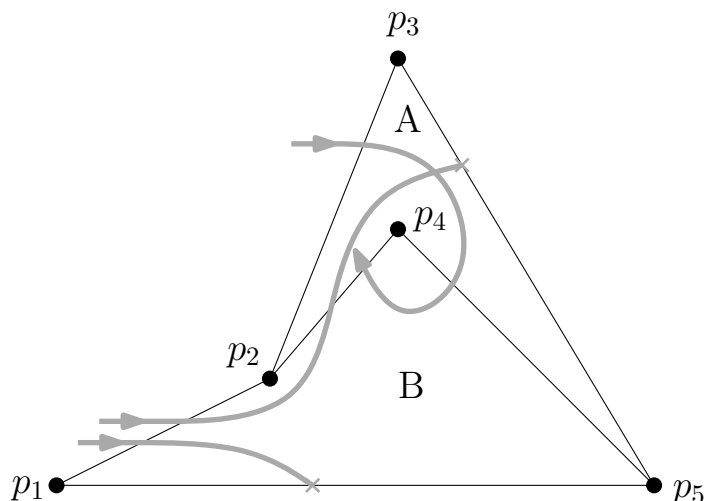


Figure 5.17: The combination of gadgets A and B, and the possible ways to cross those gadgets via alternating dual paths.

Proposition 5.4. *Let $\mathcal{P}_{\mathcal{X}}$ be a pseudo-triangulation of a point set S , that was built with the x -sorted version of the super easy construction. If the special gadget C as defined above consists of the combination of gadget A and gadget B with the additional restriction that it is not possible to enter the gadget via the edges p_3p_5 and p_3p_5 (Figure 5.17), and it appears in $\mathcal{P}_{\mathcal{X}}$, then the three corners of the hull of the gadget are points on the convex hull.*

Proof. For simplicity reasons we do not allow two points to have the same x -coordinate. First we show that either the corner p_3 or the corner p_5 is the rightmost point of the gadget AB. Let $x(p)$ be the x -coordinate of a point p . Since $\mathcal{P}_{\mathcal{X}}$ was constructed by the x -sorted version of the super easy construction, the gadget AB is also built up that way. Note that gadget B has at least one inner point p_i , which has been inserted after p_4 , so $x(p_4) < x(p_i)$.

If p_1 would be the rightmost corner of gadget AB, we get $x(p_3) < x(p_4) < x(p_2)$. The reflex point p_2 cannot be part of the convex hull. Since p_4 was connected with p_5 and p_2 after its insertion, this would mean that $x(p_2) < x(p_4)$ but this is a contradiction to the structure of the gadget. Next we want to show that the corners of the gadget need to be points of the convex hull of our underlying point set. We look first at the case where $x(p_3) < x(p_5)$.

Assume now that p_5 is not part of the convex hull. Since p_5 is the rightmost point of all points of the gadget AB, all points that are incident to p_5 have been inserted

before p_5 . Inserting a point produces only two new edges. Since p_5 is incident to three other vertices that have been inserted before, we can conclude that p_5 has not become part of the gadget via insertion, hence it was already part of the convex hull of S . Assume now that p_1 is not part of the convex hull, hence it was inserted in a way that it became the left corner (the corner next to the reflex point in counter clockwise direction) of a four-sided pseudo-triangle. This is only possible if p_1 was inserted into area 2 of a four sided pseudo-triangle (see Figure 5.18). But this means that p_2 , which cannot be part of the convex hull, has been inserted before, hence $x(p_2) < x(p_1)$. In order to construct the gadget AB, p_4 has to be inserted into area 3 of the pseudo-triangle with the corners p_1 , p_3 and p_5 . A point in area 3 of this pseudo-triangle that has been constructed by inserting p_1 would always have a smaller x-coordinate than p_2 , hence $x(p_4) < x(p_2)$ (Figure 5.18), which cannot be the case if we want to insert p_4 after p_2 . So if p_1 is not part of the convex hull, we cannot construct the gadget AB. Finally, we need to show that p_3 is part of the

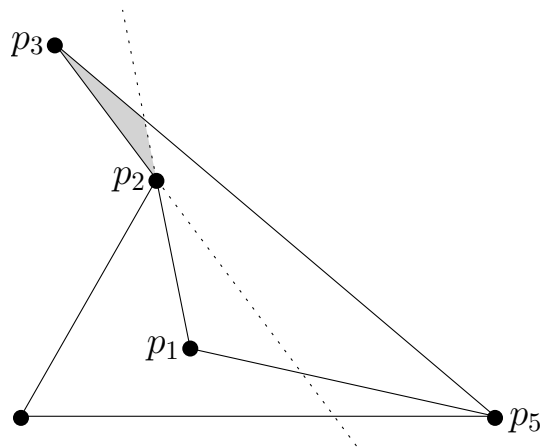


Figure 5.18: If p_1 is not part of the convex hull, the gadget AB cannot be constructed.

The area 3, where p_4 should be inserted is shaded gray.

convex hull. As stated before, $x(p_3) < x(p_5)$. If we assume now that p_3 is not part of the convex hull, but was inserted in the interior, the edge between p_3 and p_5 can only have been created by inserting p_3 , since p_5 is part of the convex hull. First we consider the case that $x(p_3) < x(p_4)$. That p_3 is connected to the rightmost convex hull point means that p_3 was inserted either into area 2 or area 3 of a four sided pseudo-triangle (Figure 5.19). In the first case, we would not get a gadget C as we have defined it above. In the second case, we would get a bigger gadget that has a vertex p'_3 as its corner and consists of two gadgets of type B. If $x(p_4) < x(p_3)$,

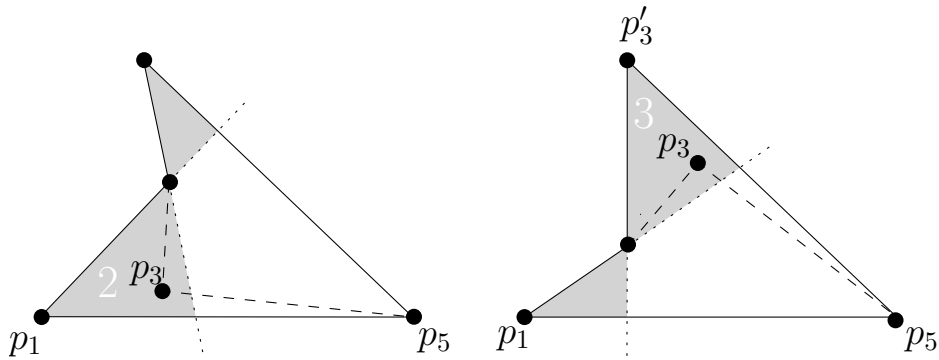


Figure 5.19: If $x(p_3) < x(p_5)$ then p_3 can be inserted in these two ways, since we want to get the edge p_3p_5 .

then p_3 was inserted into area 1 of an pseudo-triangle with p_4 as its reflex point. Then we would get again a bigger gadget that has p'_3 as its corner, and consists of two gadgets of type B. In the case that $x(p_5) < x(p_3)$ (Figure 5.20), we will now show that p_5 will be again a convex hull point. Assume again that p_5 is an inner

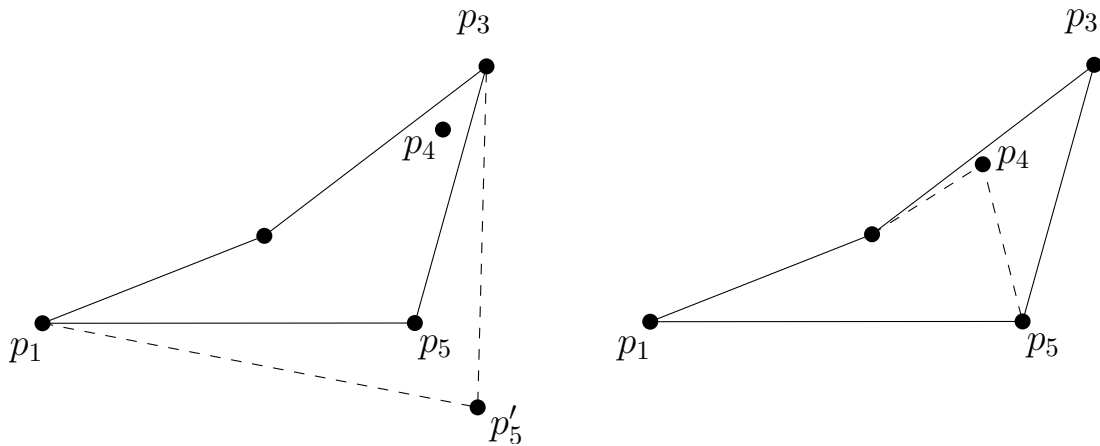


Figure 5.20: The cases $x(p_5) < x(p_4)$ (left) leads to a bigger gadget and in the case $x(p_4) < x(p_5)$ we could not insert p_4 anymore.

point, which was inserted either before or after p_4 . In the first case, this would mean that p_5 was inserted into area 1 of pseudo-triangle with the corners p_1, p_3 and p'_5 . This would result in a bigger gadget, that allows a dual path to leave the original gadget via the edge p_3, p_5 and reenter it via p_1, p_5 , a situation we excluded in the beginning. To construct our gadget, p_4 needs to be inserted after p_5 , hence, the case $x(p_4) < x(p_5)$ would not lead to our gadget. The arguments from above that p_1 and

p_3 must be part of the convex hull of the underlying point set hold also for the case $x(p_5) < x(p_3)$. \square

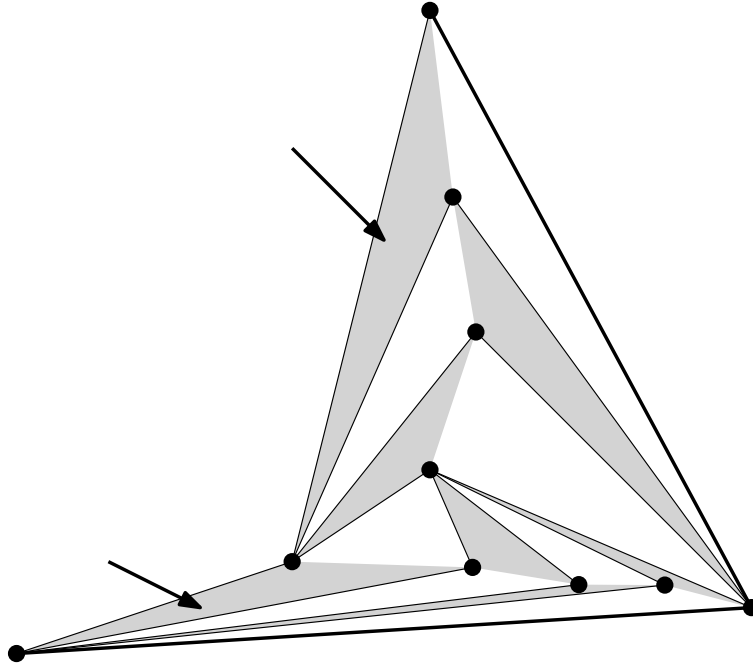


Figure 5.21: Example for an AB gadget. The grey triangles cannot be reached by alternating dual paths.

Figure 5.21 shows an example of an AB gadget. The grey shaded triangles, i.e., their corresponding vertices in the dual graph cannot be reached by alternating dual paths. It is also important to mention that once this special gadget is constructed, the further insertion of points according to the x-sorted version of the Super-Easy-Construction will not change its properties concerning dual paths as long as they are insertions into the areas 2 and 3. Insertions into area 1 of a pseudo-triangle will lead to gadgets that do not fall into the definition of gadget A or B. Proposition 5.4 shows that this unfortunate combination of gadget A and B can only appear in 4-PPTs that were constructed by the x-sorted easy construction algorithm when the gadgets corners are the three convex hull points. So the arguments of the proof will not help to prove the general case. The investigation of the general case, i.e., finding gadgets that prohibit dual paths from the dual vertex that corresponds to the triangle to all other vertices in the dual graph would go beyond the scope of this thesis.

6 Conclusion

6.1 Summary

The aim of this thesis was to investigate the connectedness of flip graphs of pointed pseudo-triangulations with maximum face degree four (4-PPT). We presented a local operation, the edge flip, which allows to transform a pseudo-triangulation into a different one. All pseudo-triangulations of a point set can be represented in a so-called flip graph, whose connectedness was of special interest for this thesis.

In Chapter 3 we pointed out the difference between geometric and abstract pseudo-triangulations. While it was recently achieved to prove the connectedness of the flip graph of all abstract pseudo-triangulations of a set of point, this cannot be shown for geometric ones so far. Nevertheless, focusing on special sets of points simplifies matters. We presented proofs for the connectedness of the flip graph of 4-PPTs on the known single chain set, the reverse single chain set, and the double circle, even if we allowed only to flip edges incident to a triangle. Furthermore, we introduced a new special set, the muffin set, and showed that its flip graph of 4-PPTs is connected, again with the restriction that only edges incident to a triangle were allowed to be flipped. Due to the inductive structure of these proofs, we further were able to derive the number of 4-PPTs of the single chain set, the reverse single chain set, and a special type of the muffin set. It can be seen that the number of 4-PPTs of these sets increases exponentially with the number of vertices.

In parallel to this thesis a flip software tool was developed by W. Reisner [31]. This tool helped greatly to study the behavior of 4-PPTs while flipping edges. To approach a proof of connectedness of the flip graph of all 4-PPTs of general point sets the concept of investigating dual graphs was elaborated. The study of effects of edge flips on the dual graph motivated the concept of alternating dual paths. This approach was intended to automate moving a triangle in a 4-PPT by following a sequence of edge flips. An extension of the flip software by the dual graph idea lead to new experimental results. These results were presented in Chapter 5.2 and led

further to the investigation of special geometric gadgets. To simplify matters, only 4-PPTs with three points on the convex hull were considered. We described how the idea of the dual path can help to move the triangle inside the 4-PPT. Nevertheless, experiments revealed that there are classes of 4-PPTs for which it is not possible to reach every vertex in the dual graph by an alternating dual path that starts in the dual vertex corresponding to the triangle in the 4-PPT.

6.2 Future Research

The thesis showed that for special point sets it is very helpful to use the symmetry in those sets for proving the connectedness of the flip graphs of their 4-PPTs. For the general case, i.e., any arbitrary set of points in the plane this is not that easy. In a 4-PPT of a point set with three points on the convex hull, the dual approach can help to prove that it is possible to move the triangle to any three adequate points of the set. If this is possible, the impact of moving the triangle can be studied to gain statements if and how the movement of the triangle can be used to enforce local changes on the 4-PPT. This could finally prove the conjecture that the flip graph of all 4-PPTs of an arbitrary set of points with three points on the convex hull is connected even if we only allow to flip edges incident to the triangle. When the last requirement is disregarded, the number of flips clearly increases. This might be helpful, especially for the investigation of very local transformations in a 4-PPT. Recently the connectedness of the flip graph of combinatorial 4-PPTs was proven by a group of researchers at a research week on pseudo-triangulations in May 2012 in Alcalá de Henares [6]. The investigation of pseudo-triangulations is a current research topic and many interesting results can be expected in the future.

Glossary

≥ 5 -PPT a pointed pseudo-triangulation with at least one five-sided pseudo-triangle.

37

π -guards guards who have a field of view of π . 21

4-PPT a pointed pseudo-triangulation with a maximum face degree 4. 21

abstract pseudo-triangulation also *combinatorial* pseudo triangulation, a plane graph combined with a special labeling of the angles formed by its edges. 30

alternating path a path of edges in a dual graph that consists of normal edges and auxiliary edges. 74

auxiliary edge specific type of edge in the dual graph of a 4-PPT. 65

bitangent a diagonal, that is a tangent in both its endpoints. 11

combinatorial pseudo-triangulation see *abstract pseudo-triangulation*. 30

convex hull of a point set S is the smallest convex polygon that contains S . 10

convex point of a polygon is a point whose angle outside the border of the polygon is $> \pi$. 10

corner convex point of a pseudo-k-gon. 10

crossing flip a diagonal flip, where the deleted edge and the new inserted edge intersect. 70

deletion flip special type of an edge flip, where the flipped edge is removed and the result is still a valid pseudo-triangulation. 18

diagonal an edge between two vertices of the border of a polygon that crosses the inner area of the polygon. 11

diagonal flip a deletion flip, merging two pseudo-triangles to one pseudo-4-gon, followed by an insertion flip, connecting the corners of the pseudo-4-gon that have not been incident to the deleted edge. 18

double circle a special set of $2m$ points in the plane, m of them on the convex hull, while the other m points are each sufficiently close to one of the convex hull edges. 49

dual graph a graph whose vertices correspond to faces of pseudo-triangulation. 63

edge flip a local operation transforming a pseudo-triangulation into a different one by deleting and/or inserting one edge. 18

edge sliding flip a special type of a diagonal flip, where the removed and the inserted edge have one endpoint in common. 68

face degree number of edges that bound the face. 12

flip graph a graph whose vertices represents a unique pseudo-triangulation of a point set and two vertices are connected if there exists an edge flip that transforms the two corresponding pseudo-triangulations into each other. 20

general position a pointset S is in g.p. if no three points of S are collinear. 10

geodesic path the shortest path between two points of a polygon. 11

geodesic triangulation alternative (old) term for pseudo-triangulation. 11

geometric gadget specified pseudo-triangulation of special pointgons. 79

Henneberg-Construction an algorithm for constructing minimal rigid graphs. 16

insertion flip special type of an edge flip, where an additional edge is inserted. 18

lense shutter a specific 4-PPT of the double circle set. 49

minimum pseudo-triangulation other term for pointed pseudo-triangulation. 13

muffin set a set of points in the plane, very similar to the single chain set, but with more points on the convex hull. 53

pointed pseudo-triangulation pseudo-triangulation whose points are pointed. 13

pointgon a polygon with additional points inside the interior face. 10

polygon a geometric figure whose non-crossing edges connect n vertices to a closed path. 10

pseudo-k-gon a polygon with exactly k convex points. 10

pseudo-triangle a pseudo-3-gon. 10

pseudo-triangulation partition of a region into pseudo-triangles. 12

reflex points that have an outer angle $< \pi$. 10

reverse single chain a set of n points in the plane, such that $|CH(S')| = 3$ and $n - 3$ interior points together with one convex hull point t form a convex polygon and all points of this polygon are visible by the two other convex hull points p and q .. 39

shutter edge a specific edge in the lense shutter. 49

side-chain a geodesic path with ≥ 2 edges between two consecutive corners of a polygon. 11

simple polygon polygon with exactly one inner face that is bounded by the closed path. 10

single chain a set with $n > 3$ points in the plane, such that $|CH(S)| = 3$, $n - 1$ points form a convex polygon and one point t , outside the polygon, sees all edges of the polygon but one.. 38

Super-Easy-Construction an algorithm to construct a 4-PPT of a point set. 71

tangent a special diagonal of a polygon. 11

triangle a convex simple polygon with 3 corners. 12

triangulation partition of a region into triangles. 12

List of Figures

2.1	Introducing pseudo-triangles.	11
2.2	Defining tangents, bitangents and geodesic paths.	12
2.3	pseudo-triangulations of a simple polygo, a pointgon and a set of points. 13	
2.4	A pointed pseudo-triangulation of a set of points.	14
2.5	Insertion step for constructing a pointed pseudo-triangulation.	17
2.6	Insertion and deletion edge flip.	18
2.7	Two diagonal edge flips.	19
3.1	Pointset enforcing vertex degree 5 for any PPT.	28
3.2	Constructing 4-PPTs: insert point in triangle.	29
3.3	Constructing 4-PPTs: insert point into 4-gon 1.	29
3.4	Constructing 4-PPTs: insert point into 4-gon 2.	30
3.5	A CPT, its embedding and a non-stretchable CPT.	31
3.6	Possible edge flips in an abstract pointed pseudo-triangulation.	32
3.7	Edge-flips in CPTs that effect embeddings.	32
3.8	Merging step in 3-coloring algorithm for 4-PPTs.	34
3.9	Example for 3-coloring of 4-PPT.	34
4.1	Singletons in flip graph of 4-PPTs of simple polygon with 10 points.	37
4.2	Counterexample for connectedness of flip graph of ≥ 5 -PPTs.	37
4.3	Eight ways to draw a five sided pseudo-triangle for a counterexample.	38
4.4	Example for a single chain and a reverse single chain set.	39
4.5	Flip graph for the single chain with $n = 4$	40
4.6	Sub-flip-graphs of the single chain set are connected among each other.	40
4.7	Flip graph of the single chain set for $n = 6$	41
4.8	$r(G)$ of the reverse single chain is connected.	42
4.9	Connected sub-flip-graphs of reverse single chain set.	43
4.10	Fragments of the flip graph of a reverse single chains set.	44
4.11	Omitted corners of the base triangle.	47

4.12	Example of a 4-PPT of the double circle with $n = 16$ points.	48
4.13	The clockwise and counterclockwise lense shutter.	49
4.14	Flip sequence to change the orientation of the shutter lense.	50
4.15	Flip sequence to change the orientation of the shutter lense.	52
4.16	Creating inner polygon edges for lense shutter.	52
4.17	The special set $M_{5,6}$	53
4.18	The flip graph of $M_{0,0}$ is connected.	54
4.19	The flip graph of $M_{1,0}$ is connected.	55
4.20	Vertices of sub-flip-graphs of $M_{1,5}$	55
4.21	Sub-flip-graph of $M_{1,5}$	56
4.22	Scheme of representative 4-PPTs of $m(G_{5,6})$, $m_r(G_{5,6})$ and $r(G_{5,6})$	57
4.23	Illustration of Claim 5.	58
4.24	Sub-flip-graphs of $M_{k,m}$ are conected among each other.	59
4.25	Illustration of Claim 8.	60
4.26	Counting 4-PPTs of the muffin set.	61
4.27	Number of 4-PPTs of special sets	62
5.1	Dual graph of a 4-PPT of a set of $n = 11$ points.	65
5.2	Coloring of 4-PPT with dual graph.	67
5.3	Labeling a 4-PPT and the corresponding dual graph.	67
5.4	Edge flip type Ia.	68
5.5	Edge flip type Ib.	69
5.6	Edge flip type II.	69
5.7	Edge flip type III.	71
5.8	GUI of the flip software.	72
5.9	Dual extension of the flip software.	73
5.10	Effects of point insertion in triangle on dual graph.	75
5.11	Effects of point insertion in pseudo-4-gon on dual graph.	76
5.12	Effects of point insertion in area 1 of a pseudo-4-gon on dual graph.	77
5.13	Point set that claims two different algorithms for moving the triangle.	79
5.14	Scheme for alternating dual paths that cross the gadget.	80
5.15	Two special gadgets in which the exit is given.	80
5.16	Examples for gadget A and gadget B	81
5.17	Combination of gadgets A and B.	82
5.18	Corner $p1$ of gadget aB is a convex hull point.	83
5.19	Corner $p3$ of gadget aB is a convex hull point.	84

5.20	Corner p_5 of gadget aB is a convex hull point.	84
5.21	Example for an AB gadget.	85

Bibliography

- [1] P. K. Agarwal, J. Basch, L. J. Guibas, J. Hershberger, and L. Zhang. Deformable free space tilings for kinetic collision detection. *International Journal of Robotics Research*, 21:179–797, 2002.
- [2] O. Aichholzer. Counting Triangulations - Olympics.
<http://www.ist.tugraz.at/aichholzer/research/rp/triangulations/counting/>, June 2011.
- [3] O. Aichholzer, F. Aurenhammer, T. Hackl, C. Huemer, A. Pilz, and B. Vogtenhuber. 3-Colorability of Pseudo-Triangulations. In *26th European Workshop on Computational Geometry EuroCG '10*, pages 21–24, 2010.
- [4] O. Aichholzer, F. Aurenhammer, and H. Krasser. Enumerating order types for small point sets with applications. *Order*, 19:265–281, 2002.
- [5] O. Aichholzer, F. Aurenhammer, H. Krasser, and B. Speckmann. Convexity minimizes pseudo-triangulations. *Computational Geometry: Theory and Applications*, 28:3–10, 2004.
- [6] O. Aichholzer, T. Hackl, D. Orden, A. Pilz, M. Saumell, and B. Vogtenhuber. Manuscript on results of the Pseudo-Triangulation-Week in Alcalá de Henares. May 2012.
- [7] O. Aichholzer, T. Hackl, D. Orden, P. Ramos, G. Rote, A. Schulz, and B. Speckmann. Flip graphs of bounded-degree triangulations. In *Electronic Notes in Discrete Mathematics 34: Proc. European Conference on Combinatorics, Graph theory and Applications (EuroComb 2009)*, pages 509–513, 2009. Journal version to appear.
- [8] O. Aichholzer, F. Hurtado, and M. Noy. A lower bound on the number of triangulations of planar point sets. *Computational Geometry: Theory and Applications*, 29(2):135–145, 2004.

- [9] O. Aichholzer, D. Orden, F. Santos, and B. Speckmann. On the number of pseudo-triangulations of certain point sets. *Journal of Combinatorial Theory*, 115:254–278, 2008.
- [10] O. Aichholzer, B. Vogtenhuber, T. Hackl, and A. Pilz. Manuscript on results of the 7th European Research Week on Geometric Graphs and Pseudo-Triangulations, Castelldefels, Spain. 2010.
- [11] American Mathematical Society. Monthly essays on mathematical topics: sneak preview on carpenter’s ruler problems. <http://www.ams.org/samplings/feature-column/fcarc-linkages5>, June 2012.
- [12] S. Bereg. Transforming pseudo-triangulations. *Information Processing Letters*, 90:141–145, 2004.
- [13] S. Bereg. Enumerating Pseudo-Triangulations in the Plane. *Computational Geometry*, 30/3:207–222, 2005.
- [14] H. Brönnimann, L. Kettner, M. Pochiola, and J. Snoeyink. Counting and enumerating pseudo-triangulations with the greedy flip algorithm. In *SIAM Journal on Computing*, 2001.
- [15] V. Brumberg, S. Ramswami, and D. Souvaine. Experimental results on upper bounds for vertex π -lights. In *11th Annual Fall Workshop Computational Geometry*, 2001.
- [16] V. Chvátal. A combinatorial theorem in plane geometry. *Journal of Combinatorial Theory, Series B*, 18:39–41, 1975.
- [17] B. Cloitre. The On-Line Encyclopedia of Integer Sequences. <http://oeis.org/A079583>, Jan. 2003.
- [18] R. Connelly, E. D. Demaine, and G. Rote. Straightening polygonal arcs and convexifying polygonal cycles. *Discrete and Computational Geometry*, 30(2):205–239, 2003.
- [19] S. Fisk. A short proof of chvátal’s watchman theorem. *Journal of Combinatorial Theory, Series B*, 24:374, 1978.

- [20] R. Haas, D. Orden, G. Rote, F. Santos, B. Servatius, H. Servatius, D. Souvaine, I. Streinu, and W. Whiteley. Planar minimally rigid graphs and pseudo-triangulations. *Comput. Geom. Theory Appl.*, 31(1-2):31–614, 2005.
- [21] T. Hackl. *Relaxing and lifting triangulations*. PhD thesis, Graz University of Technology, 2010.
- [22] T. Hackl and O. Aichholzer. Personal communication. 2011.
- [23] T. Hackl and A. Pilz. Personal communication. 2011.
- [24] L. Henneberg. *Die graphische Statik der starren Systeme*. Johnson Reprint Corp, 1968., New York, 1911. in German.
- [25] F. Hurtado and M. Noy. Counting triangulations of almost-convex polygons. *Ars Combinatoria*, 45:169–179, 1997.
- [26] F. Hurtado and M. Noy. Graph of triangulations of a convex polygon and tree of triangulations. *Comput. Geom. Theory Appl.*, 13:179–188, 1999.
- [27] L. Kettner, D. Kirjpatrick, A. Mantler, J. Snoeyink, B. Speckmann, and F. Takeuchi. Tight degree bounds for pseudo-triangulations of points. *Comput. Geom. Theory Appl.*, 25:3–12, 2003.
- [28] D. Orden, F. Santos, B. Servatius, and H. Servatius. Combinatorial pseudo-triangulations. *Discrete Mathematics*, 307:554–566, 2007.
- [29] M. Pocchiola and G. Vegter. The visibility complex. *9th Annual Symposium Computational Geometry*, pages 328–337, 1993.
- [30] M. Pocchiola and G. Vegter. Topologically sweeping visibility complexes via pseudo-triangulations. *Discrete and Computational Geometry*, 16:419–453, 1996.
- [31] W. Reisner. Ein Programm zur Veranschaulichung von Kantenflips in pointed Pseudo-Triangulierungen. Bachelor Thesis, in German, Graz University of Technology, 2012.
- [32] G. Rote, F. Santos, and I. Streinu. Pseudo-triangulations – a survey. In *Surveys on discrete and computational geometry*, volume 453 of *Contemp. Math.*, pages 343–410. Amer. Math. Soc., Providence, RI, 2008.

- [33] F. Santos and R. Seidel. A better upper bound on the number of triangulations of a planar point set. *Journal of Combinatorial Theory*, 102:186–193, 2003.
- [34] V. K. Singh and S. Mehta. Flip graph of pseudo triangulation with a fixed set of pointed vertices. Technical report, Indian Institute of Technology, Kanpur, India, 2004.
- [35] B. Speckmann and C. D. Tóth. Allocating vertex π -guards in simple polygons via pseudotriangulations. *Discrete and Computational Geometry*, 33:345–364, 2005.
- [36] I. Streinu. Pseudo-triangulations, rigidity and motion planning. *Discrete and Computational Geometry*, 34:587–635, 2005.
- [37] C. D. Tóth. Art gallery problem with guards whose range of vision is 180° . *Comput. Geom. Theory Appl.*, 17:121–134, 2000.